

## Article

# Revealing the Stygobiotic and Crenobiotic Molluscan Diversity in the Caucasus: Part IV – Crenobiotic Belgrandiellinae Radoman, 1983 (Mollusca, Hydrobiidae) from Georgia †

Elizaveta Chertoprud <sup>1,2,3</sup> , Jozef Grego <sup>4,\*</sup> , Levan Mumladze <sup>5</sup> , Sebastian Hofman <sup>6</sup> , Dmitry Palatov <sup>2,3</sup>, Artur Osikowski <sup>7</sup> , Aleksandra Jaszczyńska <sup>8,9</sup>  and Andrzej Falniowski <sup>8</sup> 

- <sup>1</sup> Department of Invertebrate Zoology, Biological Faculty, Lomonosov Moscow State University, 1, Leninskie Gory, 119991 Moscow, Russia
- <sup>2</sup> Laboratory of Macroecology & Biogeography of Invertebrates, St. Petersburg State University, 7/9 Universitetskaya Emb., 199034 Saint Petersburg, Russia
- <sup>3</sup> A.N. Severtzov Institute of Ecology and Evolution, 33, Leninsky Prospect, 117071 Moscow, Russia
- <sup>4</sup> Department of Biology, SubBioLab, Biotechnical Faculty, University of Ljubljana, Jamnikarjeva 101, SI-1000 Ljubljana, Slovenia
- <sup>5</sup> Institute of Zoology, Ilia State University, Tbilisi, Kakutsa Cholokashvili Ave. 3/5, Tbilisi 0162, Georgia
- <sup>6</sup> Department of Comparative Anatomy, Institute of Zoology and Biomedical Research, Jagiellonian University, Gronostajowa 9, 30-387 Kraków, Poland
- <sup>7</sup> Department of Animal Reproduction, Anatomy and Genomics, University of Agriculture in Krakow, Mickiewicza 24/28, 30-059 Kraków, Poland
- <sup>8</sup> Department of Malacology, Institute of Zoology and Biomedical Research, Jagiellonian University, Gronostajowa 9, 30-387 Kraków, Poland
- <sup>9</sup> Department of Invertebrate Evolution, Institute of Zoology and Biomedical Research, Jagiellonian University, Gronostajowa 9, 30-387 Kraków, Poland
- \* Correspondence: jozef.grego@gmail.com
- † LSIDurn:lsid:zoobank.org:act:EE474F38-7C58-447B-B978-AA15E2D7FB61; LSIDurn:lsid:zoobank.org:act:DB4ED2C2-3149-4C69-9DC6-9470F408C38; LSIDurn:lsid:zoobank.org:act:44AE0561-C4EE-41AC-87CD-B9896AA827F3; LSIDurn:lsid:zoobank.org:act:5DD19D22-B2B8-401E-B282-B78C8D4CE6EE; LSIDurn:lsid:zoobank.org:act:31A039DA-36BC-470B-ACBF-1CFD1CF1BD34; LSIDurn:lsid:zoobank.org:act:1729E817-AEE4-4922-9A0E-B79755897819; LSIDurn:lsid:zoobank.org:act:BE784866-0790-43FE-9D28-725096B2CB51; LSIDurn:lsid:zoobank.org:act:263F3855-8DBB-4028-8632-F653DBA7F3F7; LSIDurn:lsid:zoobank.org:act:B3CD32D0-41C2-4E24-8F96-5459B50BFFA4; LSIDurn:lsid:zoobank.org:act:706E6847-5231-4D3E-9AFA-DE4A7AAF4F7D.



**Citation:** Chertoprud, E.; Grego, J.; Mumladze, L.; Hofman, S.; Palatov, D.; Osikowski, A.; Jaszczyńska, A.; Falniowski, A. Revealing the Stygobiotic and Crenobiotic Molluscan Diversity in the Caucasus: Part IV – Crenobiotic Belgrandiellinae Radoman, 1983 (Mollusca, Hydrobiidae) from Georgia. *Diversity* **2023**, *15*, 450. <https://doi.org/10.3390/d15030450>

Academic Editors: Michael Wink, Michel Baguette and Luc Legal

Received: 29 December 2022

Revised: 8 March 2023

Accepted: 11 March 2023

Published: 17 March 2023



**Copyright:** © 2023 by the authors. Licensee MDPI, Basel, Switzerland. This article is an open access article distributed under the terms and conditions of the Creative Commons Attribution (CC BY) license (<https://creativecommons.org/licenses/by/4.0/>).

**Abstract:** Since 2020, the south-western Caucasus has been recognized as a hotspot of stygobiotic Mollusca diversity after revealing a large number of new, range-restricted species within the spring snail family Hydrobiidae, subfamily Sadlerianinae *sensu* Szarowska. Meantime, based on extensive material collected in the south-western Caucasus during the last decades, we studied members of another spring snail subfamily Belgrandiellinae Radoman, 1983. Modern integrative taxonomic work revealed hitherto unknown diversity within this subfamily in the region and further proved the importance of the south-western Caucasus as a hotspot of stygobiotic life. In particular, the subterranean environment and springs of Georgia were known to be inhabited by the genus *Tschernomorica* Vinarski and Palatov, 2019 with four nominal species. Our research, based on a morpho-anatomical study and genetic investigation of COI/H3 mitochondrial/nuclear markers, revealed additionally seven species and three genera new to science—*Colchiella lugella* gen. et sp. nov., *C. nazodelavo* gen. et sp. nov., *C. shiksa* gen. et sp. nov., *C. dadiani* gen. et sp. nov., *Sataplia cavernicola* gen. et sp. nov., *Aetis starobogotovi* gen. et sp. nov., and *Tschernomorica kopidophora* sp. nov. —to inhabit the Georgian part of south-western Caucasus. The full taxonomic description of each new taxa, along with the review of habitat characteristics and conservation status, is provided. Molecular genetics suggests that the ancestors of Caucasian Belgrandiellinae have migrated from south-western Europe, probably more than once during the late Messinian and early Pliocene. Later, Plio-Pleistocene

climate oscillations, particularly the repeated rise and fall of the Black Sea water level, resulted in the isolation and radiation of various lineages within the Caucasus and Crimea.

**Keywords:** biodiversity; cave; freshwater; interstitial; DNA; molecular taxonomy; spring; subterranean

## 1. Introduction

The south-western Great Caucasus hosts a remarkable diversity of stygobiotic and crenobiotic molluscan species [1–12]. Lindholm [1] described *Bythinella adsharica* (= *Tschernomorica adsharica*) from the Adjara region near the Turkish border (western Lesser Caucasus) as the first Caucasian member of the Belgrandiellinae Radoman, 1983 (Gastropoda; Hydrobiidae). Later, the first specimens in the south-western Great Caucasus were collected by Tzvetkov (1940), Birstein (1959–1960) and Lyovuschkin (1961), which were then described by Starobogatov [5] as *Belgrandiella caucasica* (= *Tschernomorica caucasica*) and *Belgrandiella abchasica* (= *Tschernomorica caucasica*). All of these Caucasian species share the shell morphology (ovate-conical shell with an ovate aperture), and habitat preference (stygobiotic and crenobiotic habitats) with the genus *Belgrandiella* Wagner, 1928, which is reported from southern Europe: from the Iberian Peninsula [13,14], the Alps [15,16], the Balkans [17–19], Turkey and Lebanon [6,18,20]; hence, the Caucasian species have been assigned to that genus [5]. Since then, the Caucasian Belgrandiellinae has been long considered under the genus *Belgrandiella* by Bole and Velkovrh [21], Kantor et al. [22], Barjadze et al. [23], and Vinarski and Kantor [24]. However, recent molecular investigations of the Belgrandiellinae from Georgia by Grego et al. [25] revealed their closer relationship to the genus *Agrafia* Szarowska and Falniowski, 2011 from Greece, which questioned the generic assignment of these species. Nevertheless, due to limited taxon sampling and genetic data, it was impossible to see the broader phylogeny and clearly separate the Caucasian taxa from their relatives. Later, Vinarski and Palatov [9] revised the Caucasian/Crimean members of *Belgrandiella* based on the anatomy of the reproductive system and the shell morphological features and again recognized the uniqueness of this group. As a result, they erected a new genus, *Tschernomorica* Vinarski and Palatov, 2019 with five nominal species, including two new species *T. inconspicua* Vinarski and Palatov, 2019 and *T. lindholmi* Vinarski and Palatov, 2019. The genus is reported to be distributed all over the western Caucasus and Crimea. Despite this later work, the phylogenetic links of *Tschernomorica* are still unknown, as well as the true species diversity within the genus in the region, due to the lack of sampling coverage.

In the present work, we provide the results of our recent field and laboratory work in the south-western Great Caucasus and western Lesser Caucasus, which revealed a remarkable diversity of the Belgrandiellinae fauna. Based on conchological, anatomical and genetic investigations, we here describe three new genera and seven new species within the subfamily Belgrandiellinae Radoman, 1983, and provide their diagnostic features and distribution data. Members of the subfamily discussed in this paper are crenobiotic or troglophilic species that live in small spring localities, sometimes a single known one, and sometimes scattered across a larger area. The assemblage of such tiny localities is very vulnerable to negative anthropogenic impact as well as to human-driven climatic changes, such as droughts or floods.

## 2. Materials and Methods

### 2.1. Sample Collection

The hydrobiid snails and shells were collected during field trips in the Samegrelo, Imereti, Racha, and Guria regions of western Georgia in 2014–2022. Large numbers of caves, spring outflows and karst springs were sampled (Figures 1 and 2; Table 1). Altogether 93 samples were collected from 63 localities. Microhabitat preference and sampling

methods were used as described by Grego et al. [26]. Samples of fine sand were freshly wet-screened under a stereomicroscope to retrieve live animals. Then, the samples were dried and screened again using the flotation method for shells that might have been overlooked during the wet screening.

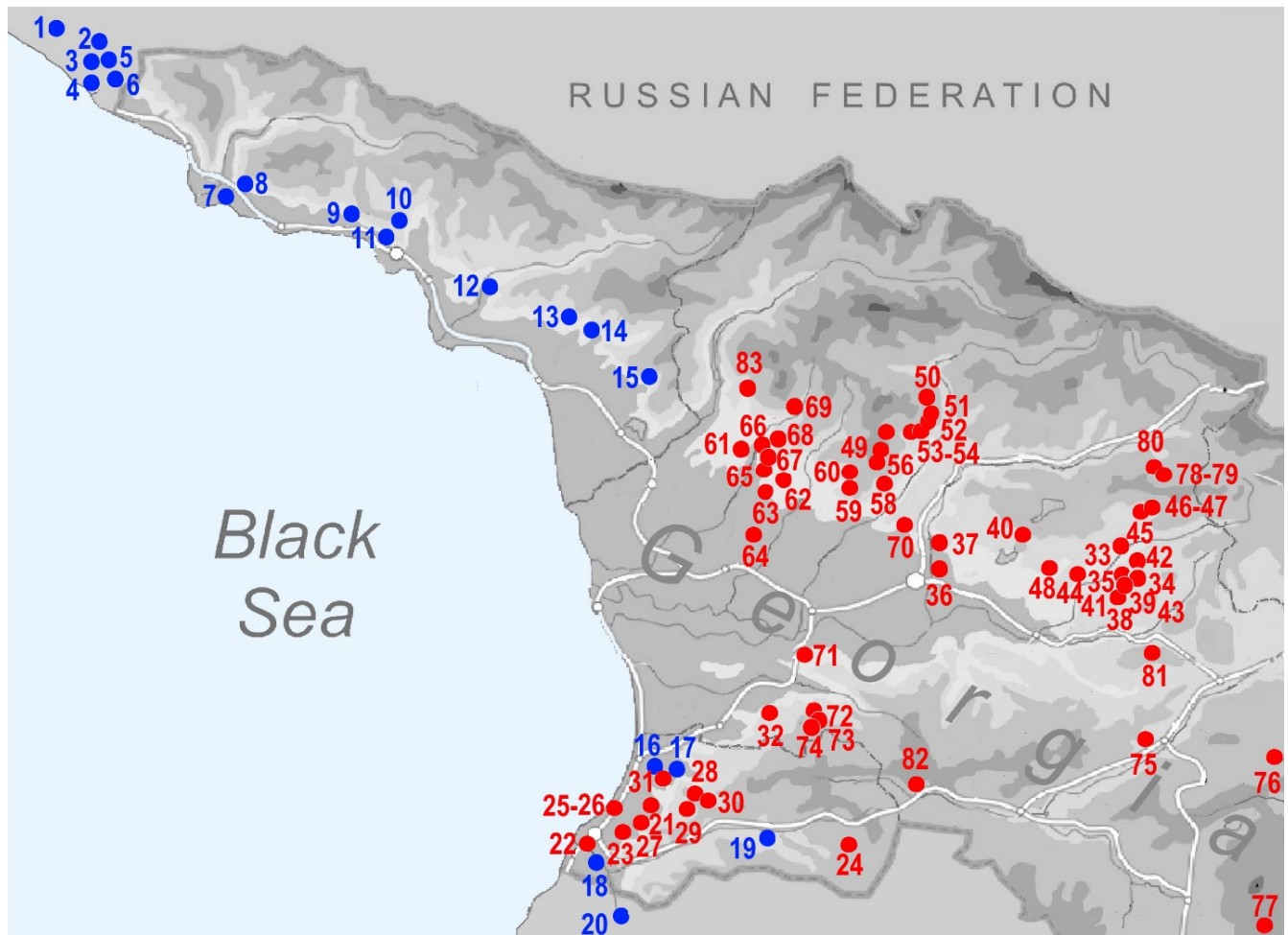


**Figure 1.** Distribution of the crenobiotic *Belgrandiellinae* in western Caucasus: 1–20; Blue dots—Hitherto studied localities: Vinarski et al., 2019 [9]; 21–83; Red dots—localities studied in present work. (Numbering of the localities according to Table 1.)



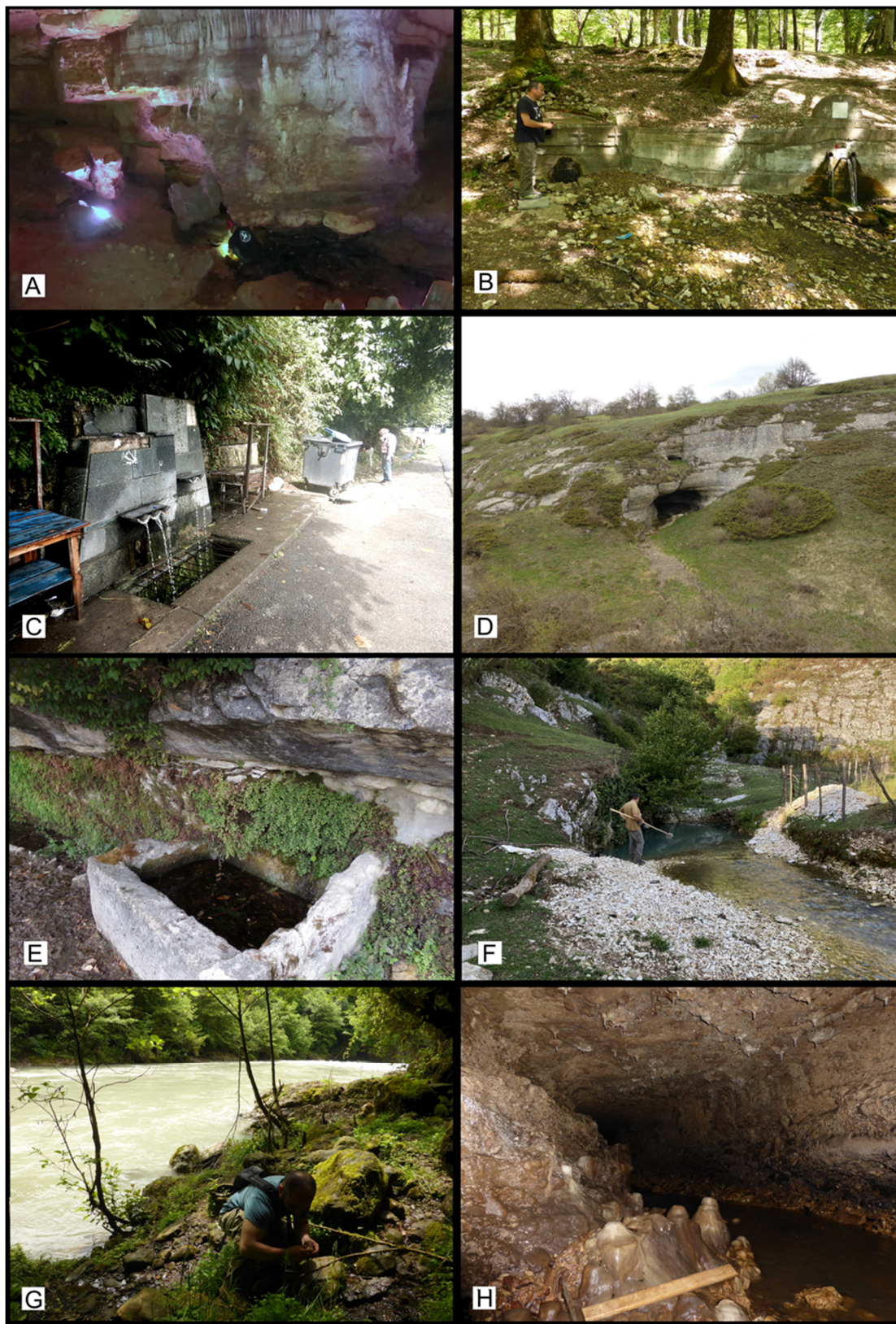


**Figure 2.** Photos from selected studied localities: (A) Banoja, Sataplia Cave LT. of *Sataplia cavernicola* sp. nov.; (B) Spring in Dadiani Forest Park, LT of *Colchiella dadiani* sp. nov.; (C) Spring Berdnis Tskaro in Zemo Nogha, LT. of *Aetis starobogatovi* sp. nov.; (D) Shkmeri Cave, *Tschernomorica* sp. indet; (E) Skindori spring, *Tschernomorica* cf. *kopidophora* sp. nov.; (F) Mukhuri, Shiksha Spring, LT of *Colchiella shiksha* sp. nov.; (G) Khobistskhali Valley, spring above Lugella spring, LT of *Colchiella lugella* sp. nov.; (H) Nazodelavo Cave, LT of *Colchiella nazodelavo* sp. nov.



**Table 1.** List of sampled localities in western Georgia. Numbers corresponds with the numbers on the presented maps (Figure 1 and Figure 20); Regions: I—Imereti, S—Samegrelo, R—Racha, G—Guria, A—Adjara; Leg. by: B—George Bananashvili, C—Elizaveta M. Chertoprud, G—Jozef Grego, M—Levan Mumladze, O—Mário Olšovský, S—Miklós Szekeres.

No Map	Genus	Species	Region	Georgia: Locality	Latitude	Longitude	Altitude (m)	Leg.	Date
21	" <i>Tschernomorica</i> "	<i>adsharica</i> Lindholm, 1913	A	Chakvistavi	41.676890°	41.859046°	348	M	19.09.2017.
22	" <i>Tschernomorica</i> "	<i>adsharica</i> Lindholm, 1913	A	Charnali	41.555460°	41.608890°	92	M	12.07.2014.
23a	" <i>Tschernomorica</i> "	<i>adsharica</i> Lindholm, 1913	A	Korolistavi, small stream 1	41.638380°	41.745750°	152	M	03.08.2019.
23b	" <i>Tschernomorica</i> "	<i>adsharica</i> Lindholm, 1913	A	Korolistavi, small stream 2	41.641870°	41.758510°	394	M	03.08.2019.
23c	" <i>Tschernomorica</i> "	<i>adsharica</i> Lindholm, 1913	A	Korolistavi, rivulet	41.652680°	41.762480°	542	M	17.09.2017.
24	" <i>Tschernomorica</i> "	<i>adsharica</i> Lindholm, 1913	A	Kveda Chkhutuneti, near Karimana Waterfall	41.499270°	41.839810°	411	M	22.09.2017.
25	" <i>Tschernomorica</i> "	<i>adsharica</i> Lindholm, 1913	A	Makhinjauri, Batumi, left side of the Shua Street	41.675487°	41.706926°	34	G	17.08.2017.
26	" <i>Tschernomorica</i> "	<i>adsharica</i> Lindholm, 1913	A	Makhinjauri, Batumi Botanical Garden	41.698350°	41.717801°	94	M	18.09.2017.
27	" <i>Tschernomorica</i> "	<i>adsharica</i> Lindholm, 1913	A	Mtirala Nat. Park, small stream	41.680917°	41.860360°	276	M	19.09.2017.
28	" <i>Tschernomorica</i> "	<i>adsharica</i> Lindholm, 1913	A	Mtirala National Park, (mt11)	41.679162°	41.886043°	440	M	02.03.2014.
29	" <i>Tschernomorica</i> "	<i>adsharica</i> Lindholm, 1913	A	Mtirala National Park, Georgia (mt3)	41.669210°	41.853620°	746	M	02.03.2014.
30	" <i>Tschernomorica</i> "	<i>adsharica</i> Lindholm, 1913	A	Mtirala National Park, Georgia (mt9)	41.679703°	41.888040°	436	M	02.03.2014.
31	" <i>Tschernomorica</i> "	cf. <i>adsharica</i> Lindholm, 1913	I	Vakijvari, right tributary rivulet of Natanebi River,	41.906740°	42.162170°	470	M	22.08.2014.
32	" <i>Tschernomorica</i> "	cf. <i>adsharica</i> Lindholm, 1913	A	Sameba, Georgia	41.799500°	41.863570°	47	M	19.09.2016.
33	<i>Tschernomorica</i>	<i>kopidophora</i> sp. nov.	I	Chiatura region, Ghrodo Cave and spring	42.307671°	43.327316°	433	M	21.10.2021.
34	<i>Tschernomorica</i>	<i>kopidophora</i> sp. nov.	I	Chiatura region, Mandaeti, Unnamed Spring,	42.164197°	43.317441°	794	M	22.10.2021.
35a	<i>Tschernomorica</i>	<i>kopidophora</i> sp. nov.	I	Chiatura region, Skindori, karst spring,	42.241431°	43.258988°	545	M	21.10.2021.
35b	<i>Tschernomorica</i>	<i>kopidophora</i> sp. nov.	I	Chiatura region, Skindori, karst spring,	42.241431°	43.258988°	545	C, G, O	13.09.2022.
36	<i>Tschernomorica</i>	<i>kopidophora</i> sp. nov.	I	Kuatisi, Iazoni Cave, right bank of river Tskalsitela	42.271811°	42.734153°	132	G, M, O	01.05.2018.
36	<i>Tschernomorica</i>	<i>kopidophora</i> sp. nov.	I	Kuatisi, Iazoni Cave, right bank of river Tskalsitela	42.271811°	42.734153°	132	G, M	13.10.2019.
37	<i>Tschernomorica</i>	<i>kopidophora</i> sp. nov.	I	Mostsameta, Gelati spring above road to Monastery	42.297183°	42.770364°	387	G, S	21.10.2021.
38	<i>Tschernomorica</i>	<i>kopidophora</i> sp. nov.	I	Sareki W, cave spring on the left bank of Jruchula river	42.325356°	43.267953°	443	C	27.08.2021.
39	<i>Tschernomorica</i>	<i>kopidophora</i> sp. nov.	I	Shvilobisa Cave between Bunikauri and Tabagrebi	42.325356°	43.267953°	628	C	29.08.2021.
40a	<i>Tschernomorica</i>	<i>kopidophora</i> sp. nov.	I	spring under Nakerala pass above road, travaertine fall	42.382927°	43.012168°	953	M	14.08.2016.
40b	<i>Tschernomorica</i>	<i>kopidophora</i> sp. nov.	I	spring under Nakerala pass above road, travaertine fall	42.382927°	43.012168°	953	M	28.07.2017.
40c	<i>Tschernomorica</i>	<i>kopidophora</i> sp. nov.	I	spring under Nakerala pass above road, travaertine fall	42.382927°	43.012168°	953	G, M, O	04.05.2018
40d	<i>Tschernomorica</i>	<i>kopidophora</i> sp. nov.	I	spring under Nakerala pass above road, travaertine fall	42.382927°	43.012168°	953	C, G, O	10.09.2022.
41	<i>Tschernomorica</i>	<i>kopidophora</i> sp. nov.	I	Sveri village, spring near the road	42.23574°	43311485°	551	C, G, O	13.09.2022.
42a	<i>Tschernomorica</i>	cf. <i>kopidophora</i> sp. nov.	I	Chiatura region, Itkhvisi village. karst spring.	42.289192°	43.350163°	671	M	21.10.2021.
42b	<i>Tschernomorica</i>	cf. <i>kopidophora</i> sp. nov.	I	Chiatura region, Itkhvisi village. karst spring.	42.289192°	43.350163°	671	C, G, O	13.09.2022.

Table 1. Cont.

No Map	Genus	Species	Region	Georgia: Locality	Latitude	Longitude	Altitude (m)	Leg.	Date
43	<i>Tschernomorica</i>	cf. <i>kopidophora</i> sp. nov.	I	Chiatura region, Skindori, in cave	42.241454°	43.258937°	548	C, G, O	13.09.2022.
44	<i>Tschernomorica</i>	cf. <i>kopidophora</i> sp. nov.	I	Mukhura, 6km E of Tkibuli, ssmall stream in Mukhura	42.325160°	43.065930°	687	M	28.07.2017.
45	<i>Tschernomorica</i>	cf. <i>kopidophora</i> sp. nov.	I	right triburaty spring o Jurchula river, near Kvemo Khevi	42.390500°	43.359820°	553	M	26.07.2017.
46	<i>Tschernomorica</i>	cf. <i>kopidophora</i> sp. nov.	I	stream Jurchula N of Kvemo Khevi at Jurchi Monastery	42.394964°	43.364591°	544	M	26.07.2017.
47	<i>Tschernomorica</i>	cf. <i>kopidophora</i> sp. nov.	I	Tsushkvati, Tsutskhvati cave (Maghara)	42.272718°	42.852900°	392	C, G, O	10.09.2022.
48	<i>Tschernomorica</i>	cf. <i>kopidophora</i> sp. nov.	I	Chiatura region, Skindori III, spring fom cave with pipes	42.250153°	43.273786°	557	C, G, O	13.09.2022.
78	<i>Tschernomorica</i>	cf. <i>kopidophora</i> sp. nov.	R	Skhmeri Plateau, Kheuri seepage and spring	42.484475°	43.429302°	1732	C, G, O	11.09.2022.
79	<i>Tschernomorica</i>	cf. <i>kopidophora</i> sp. nov.	R	Skhmeri Plateau, Kheuri seepage and spring	42.486177°	43.426250°	1704	C, G, O	11.09.2022.
80	<i>Tschernomorica</i>	cf. <i>kopidophora</i> sp. nov.	R	Skhmeri, Shkhrimeri Cave at left tributary of Kheuri	42.489233°	43.401644°	1662	G, M	05.05.2018.
49	<i>Colchiella</i>	<i>dadiani</i> sp. nov.	I	Imereti, Turchu Gamosadivari Basin, Nakriduri 3 spring	42.478030°	42.512797°	875	G, M, O	03.05.2018.
50	<i>Colchiella</i>	<i>dadiani</i> sp. nov.	I	Kinchkaperd iabout 1,5 km NE of the Kinchkha Waterfall	42.513206°	42.558801°	923	G, S	15.10.2021.
50a	<i>Colchiella</i>	<i>dadiani</i> sp. nov.	I	Kinchkaperdi about 1,8 km NE of the Kinchkha Waterfall	42.517252°	42.559959°	978	G, S	15.10.2021.
50b	<i>Colchiella</i>	<i>dadiani</i> sp. nov.	I	Kinchkaperdi about 2 km NE of the Kinchkha Waterfall	42.518485°	42.557299°	960	G, S	15.10.2021.
51	<i>Colchiella</i>	<i>dadiani</i> sp. nov.	I	Kinchkaperdi, Spring at right tributary of Saskitsvilo River	42.519975°	42.556215°	976	G, S	15.10.2021.
52a	<i>Colchiella</i>	<i>dadiani</i> sp. nov.	I	Kinchkaperdi, about 1 km NE of the Kinchkha Waterfall	42.502183°	42.559525°	874	G, M, O	02.05.2018.
52b	<i>Colchiella</i>	<i>dadiani</i> sp. nov.	I	Kinchkaperdi, about 1 km NE of the Kinchkha Waterfall	42.502183°	42.559525°	874	G, S	15.10.2021.
53	<i>Colchiella</i>	<i>dadiani</i> sp. nov.	I	Kinchkaperdi, about 1,1 km NE of the Kinchkha Waterfall	42.502265°	42.559821°	874	G	26.07.2017
54	<i>Colchiella</i>	<i>dadiani</i> sp. nov.	I	Saskitsvilo, Thurchismtha, spring of Okatse and Cave	42.497017°	42.547122°	1044	G, M, O	02.05.2018.
55	<i>Colchiella</i>	<i>dadiani</i> sp. nov.	I	Turchu Gamosadivar Basin, Nakriduri 2 spring ford	42.477581°	42.512194°	866	G, M, O	03.05.2018.
56	<i>Colchiella</i>	<i>dadiani</i> sp. nov.	I	Turchu Gamosadivar Basin, Upskhero spring lake	42.463150°	42.500967°	886	G, M, O	03.05.2018.
57	<i>Colchiella</i>	<i>dadiani</i> sp. nov.	I	Turchu Gamosadivari Basin, Nakriduri 4 travertine spring	42.478030°	42.512797°	875	G, M, O	03.05.2018.
58	<i>Colchiella</i>	<i>dadiani</i> sp. nov.	I	Zeda Gordi, spring in Dadiani Forest Park in Okatse OkatseCanyon	42.456286°	42.529152°	642	G	11.08.2017.
58	<i>Colchiella</i>	<i>dadiani</i> sp. nov.	I	Zeda Gordi, spring in Dadiani Forest Park in Okatse OkatseCanyon	42.456286°	42.529152°	642	G, M, O	01.05.2018.
58	<i>Colchiella</i>	<i>dadiani</i> sp. nov.	I	Zeda Gordi, spring in Dadiani Forest Park in Okatse OkatseCanyon	42.456286°	42.529152°	642	G, S	15.10.2021.
59	<i>Colchiella</i>	cf. <i>dadiani</i> sp. nov.	S	Pirveli Balda, spring at bank of Toba River near waterfall	42.476505°	42.458445°	677	G	14.10.2019.
60	<i>Colchiella</i>	cf. <i>dadiani</i> sp. nov.	S	Pirveli Balda, spring in village above road	42.484039°	42.398128°	296	G, M, O	09.05.2018.
62	<i>Colchiella</i>	<i>nazodelavo</i> sp. nov.	S	Chkhorotsku, Nazodelavo Cave	42.505189°	42.220847°	277	G, M, O	11.05.2018.
64	<i>Colchiella</i>	<i>nazodelavo</i> sp. nov.	S	Kotianteti, Nakhuri stream	42.322830°	42.154000°	73	M	05.08.2019.

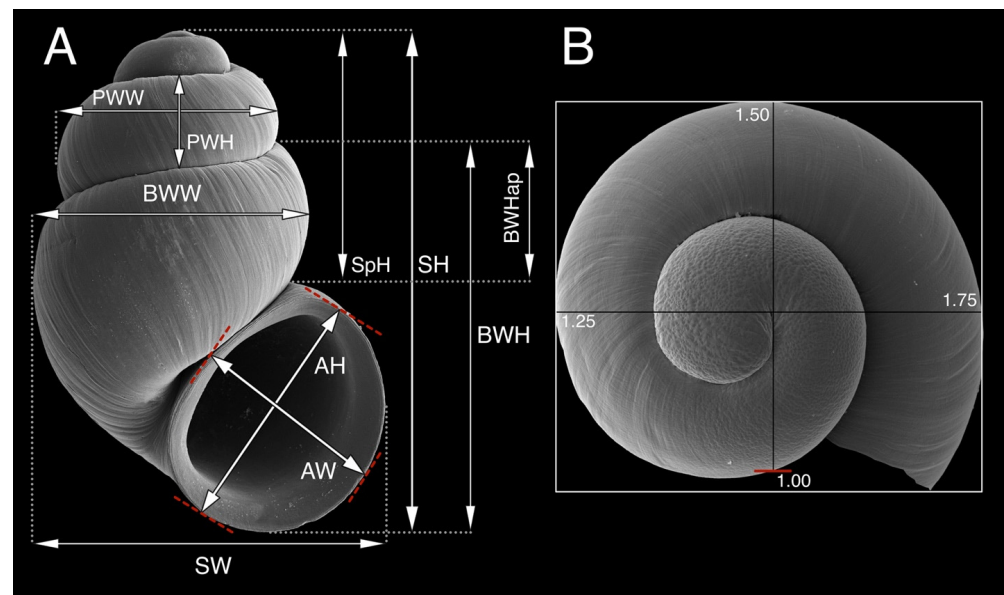


Table 1. Cont.

No Map	Genus	Species	Region	Georgia: Locality	Latitude	Longitude	Altitude (m)	Leg.	Date
83a	<i>Colchiella</i>	<i>nazodelavo</i> sp. nov.	S	Chkvaleri, Kvatskalara spring	42.721250°	42.091639°	383	G, S	19.10.2021.
83b	<i>Colchiella</i>	<i>nazodelavo</i> sp. nov.	S	Chkvaleri, Kvatskalara spring	42.721250°	42.091639°	383	G, S	19.10.2021.
61	<i>Colchiella</i>	cf. <i>nazodelavo</i> sp. nov.	S	Chkhorotsku, Letsurtsume, Letsurtsume Cave, conglomerates	42.539228°	42.113400°	176	G, M, O	10.05.2018.
63	<i>Colchiella</i>	cf. <i>nazodelavo</i> sp. nov.	S	Garakha, Garakha Cave, comnglomerates	42.177567°	42.529869°	56	G, S	17.09.2021.
65	<i>Colchiella</i>	cf. <i>nazodelavo</i> sp. nov.	S	Nakiani, spring near road to Abano Cave, conglomerates	42.518472°	42.202833°	216	G, S	18.10.2021.
67	<i>Colchiella</i>	cf. <i>nazodelavo</i> p. nov.	S	Small cave Hupina with the spring and reservoir	42.554095°	42.036681°	232	C, G, O	17.09.2022.
66	<i>Colchiella</i>	<i>kopidophora</i> sp. nov.	S	Cave Onzile and spring at left bank of Chanitskali River	42.529654°	42.046006°	180	C, G, O	17.09.2022.
68a	<i>Colchiella</i>	<i>shiksha</i> sp. nov.	S	Mukhuri, Shiksha spring	42.629811°	42.190467°	233	G, M, O	10.05.2018.
68b	<i>Colchiella</i>	<i>shiksha</i> sp. nov.	S	Mukhuri, Shiksha spring	42.629811°	42.190467°	233	G, M B	12.10.2019.
68c	<i>Colchiella</i>	<i>shiksha</i> sp. nov.	S	Mukhuri, Shiksha spring	42.629811°	42.190467°	233	C, G, O	16.09.2022.
69	<i>Colchiella</i>	<i>lugella</i> sp. nov.	S	Mukhuri, spring Lugella at bank of Khobsitskali River	42.654430°	42.224117°	321	G	13.08.2017.
69	<i>Colchiella</i>	<i>lugella</i> sp. nov.	S	Mukhuri, spring Lugella at bank of Khobsitskali River	42.654430°	42.224117°	321	C, G, O	10.05.2018.
69	<i>Colchiella</i>	<i>lugella</i> sp. nov.	S	Mukhuri, spring Lugella at bank of Khobsitskali River	42.654430°	42.224117°	321	C, G, O	16.09.2022.
70a	<i>Sataplia</i>	<i>cavernicola</i> sp. nov.	I	Banoja, Sataplia Cave, well in cave with water inlet	42.311641°	42.675151°	467	G, M, O	01.05.2018.
70b	<i>Sataplia</i>	<i>cavernicola</i> sp. nov.	I	Banoja, Sataplia Cave, rivulet in the end of cave	42.311641°	42.675151°	467	M	23.03.2014.
70c	<i>Sataplia</i>	<i>cavernicola</i> sp. nov.	I	Banoja, Sataplia Cave, rivulet in the end of cave	42.311641°	42.675151°	467	M	23.03.2014.
70d	<i>Sataplia</i>	<i>cavernicola</i> sp. nov.	I	Banoja, Sataplia Cave, water inlet at the end of cave	42.311641°	42.675151°	467	G, M, O	01.05.2018.
70e	<i>Sataplia</i>	cf. <i>cavernicola</i> sp. nov.	I	Banoja, rivulet above the spring in the village	42.280479°	42.665173°	168	G, M, O	01.05.2018.
70d	<i>Sataplia</i>	cf. <i>cavernicola</i> sp. nov.	I	Kumistavi, Prometheus Cave	42.600860°	42.376636°	174	G, M, O	01.05.2018.
71	<i>Aetis</i>	<i>starobogatovi</i> sp. nov.	I	Khevistskali river, south to the village Kvemo Nogha	42.063440°	42.269450°	53	M	01.09.2017.
72a	<i>Aetis</i>	<i>starobogatovi</i> sp. nov.	G	Kvabghi spring,	41.925174°	42.387773°	477	C, G, O	14.09.2022.
72b	<i>Aetis</i>	<i>starobogatovi</i> sp. nov.	G	Kvabghi, at Chokhatauri-Bakhmaro road, above Gubazuli	41.924991°	42.387607°	458	M	01.09.2017.
32a	<i>Aetis</i>	<i>starobogatovi</i> sp. nov.	G	Small stream near village Chkhakoura,	41.909827°	42.387033°	945	M	30.08.2017.
32b	<i>Aetis</i>	<i>starobogatovi</i> sp. nov.	G	Small stream near village Chkhakoura,	41.947869°	41.947869°	46	M	24.05.2017.
74a	<i>Aetis</i>	<i>starobogatovi</i> sp. nov.	G	Spring Berdnis Tskharo near Zemo Nogha, pipe+ stream	42.063471°	42.269417°	50	C, G, O	14.09.2022.
74b	<i>Aetis</i>	cf. <i>starobogatovi</i> sp. nov.	G	spring by side of the Chokhatauri-Bakhmaro road	41.891203°	42.371960°	1368	C, G, O	14.09.2022.
74c	<i>Aetis</i>	cf. <i>starobogatovi</i> sp. nov.	G	spring by side of the Chokhatauri-Bakhmaro road	41.909662°	42.386778°	945	C, G, O	14.09.2022.
75	<i>Tschernomorica</i>	sp.1 indet.	J	Kvabiskhevi, junct.of Khitakhevi and Gura Riv. to Mtsvane	41.802557°	43.318725°	46	M	24.09.2017.
76	<i>Tschernomorica</i>	sp.2 indet.	K	River Khrami near Nakhiduri village,	41.478612°	44.696655°	412	M	25.06.2017.
77	<i>Tschernomorica</i>	sp.3 indet.	K	Rivulet 5 km south from the village Sapparlo	41.275130°	44.312940°	1049	M	21.06.2017.
81	<i>Tschernomorica</i>	sp.5 indet.	I	Small stream in the village Vardzia 10km S of Zestafoni	42.014699°	43.091673°	555	M	27.07.2017.
82	<i>Tschernomorica</i>	sp.6 indet.	A	stream near the Zvare; Right tributary of Ajarischkali River	41.62721°	41.976750°	232	M	22.09.2017.

## 2.2. Morphological Study

The frontal view of the shells was captured by a Carton SPZT50 microscope equipped with a TOUPCAM U3CMOS camera. ImageJ image analysis software [27] was used to measure the specimens. The shell morphology features were followed by Davis et al. [28] and Hershler and Ponder [29]. Ten linear measurements were made from each shell (Table 2 following the standard scheme (Figure 3A). The whorl number was also counted (Figure 3B). Eight morphometric indices in Figure 3 characterizing the shell shape and proportions were calculated (Table 2). An analysis of morphometric characters was carried out for populations from the type localities. Scanning electron microscopy (SEM) images of the shells, protoconchs, opercula, and radulae were made in the PIN RAS, Moscow, using a Vega 3 Tescan microscope. The adult reproductive anatomy of males was studied with a LeicaM165C stereomicroscope and photographed with a Leica DFC420 (5.0MP) digital camera at the WSBS MSU. The detailed structure of the male copulatory apparatus was examined on temporary total preparations under Micromed MC-5 ZOOM LED microscopy equipped with the ToupCam 14 MP camera.



**Figure 3.** A scheme of shell (A) and whorl number (B) measurements applied in this paper. Abbreviations: SH—shell height, SW—shell width, SpH—spire height, BWH—body whorl height, BWW—body whorl width, AH—aperture height, AW—aperture width, BWHap—body whorl height measured above aperture, PWH—penultimate whorl height, PWW—penultimate whorl width.



**Table 2.** Morphometric characteristics of shells of the species discussed in this paper. Above the line—limits of variation (min–max), below the lines—the mean value ± standard deviation.

Character/Index	Species							
	<i>Tschernomorica</i>	<i>Tschernomorica</i>	<i>Colchiella</i>	<i>Colchiella</i>	<i>Colchiella</i>	<i>Colchiella</i>	<i>Aetis</i>	<i>Sataplia</i>
	<i>kimmeria</i> (n = 25)	<i>kopidophora</i> (n = 31)	<i>dadiani</i> (n = 32)	<i>shiksha</i> (n = 51)	<i>nazodelavo</i> (n = 11)	<i>lugella</i> (n = 29)	<i>starobogatovi</i> (n = 37)	<i>cavernicola</i> (n = 20)
Whorl number (WhN)	3.10–3.75 3.58 ± 0.19	3.9–4.25 4.04 ± 0.10	3.30–4.00 3.74 ± 0.20	3.75–4.20 3.73 ± 0.21	3.45–3.80 3.62 ± 0.14	3.60–4.10 3.90 ± 0.13	3.75–4.25 3.90 ± 0.15	3.80–4.25 4.05 ± 0.13
Shell height, mm (SH)	1.34–1.93 1.52 ± 0.15	1.61–1.91 1.76 ± 0.08	1.48–1.84 1.65 ± 0.10	1.46–2.00 1.71 ± 0.14	1.34–1.60 1.50 ± 0.08	1.37–1.74 1.59 ± 0.09	1.43–1.76 1.60 ± 0.07	1.60–1.79 1.69 ± 0.06
Shell width, mm (SW)	0.86–1.21 1.01 ± 0.08	0.86–1.03 0.95 ± 0.04	1.00–1.26 1.13 ± 0.07	0.98–1.36 1.16 ± 0.09	0.88–1.00 0.96 ± 0.04	0.90–1.14 1.01 ± 0.05	0.84–1.02 0.94 ± 0.04	0.93–1.05 1.00 ± 0.04
Body whorl height, mm (BWH)	1.04–1.50 1.18 ± 0.10	1.22–1.40 1.29 ± 0.05	1.20–1.45 1.31 ± 0.06	1.19–1.56 1.35 ± 0.09	1.07–1.26 1.19 ± 0.07	1.07–1.31 1.20 ± 0.06	1.15–1.40 1.26 ± 0.06	1.10–1.39 1.27 ± 0.06
Body whorl width, mm (BWW)	0.73–0.94 0.82 ± 0.05	0.80–0.92 0.87 ± 0.03	0.82–1.04 0.94 ± 0.06	0.82–1.09 0.98 ± 0.07	0.75–0.88 0.83 ± 0.04	0.78–0.94 0.87 ± 0.05	0.75–0.93 0.83 ± 0.04	0.82–0.96 0.90 ± 0.03
Body whorl height above aperture, mm (BWHap)	0.35–0.59 0.44 ± 0.05	0.50–0.60 0.55 ± 0.02	0.45–0.58 0.50 ± 0.04	0.44–0.60 0.53 ± 0.05	0.38–0.53 0.47 ± 0.05	0.37–0.57 0.47 ± 0.04	0.45–0.55 0.51 ± 0.03	0.43–0.60 0.52 ± 0.04
Spire height, mm (SpH)	0.66–1.01 0.78 ± 0.09	0.92–1.14 1.02 ± 0.06	0.72–1.00 0.84 ± 0.08	0.74–1.07 0.89 ± 0.09	0.67–0.90 0.77 ± 0.07	0.69–1.00 0.86 ± 0.07	0.74–0.92 0.84 ± 0.04	0.85–1.10 0.94 ± 0.06
Penultimate whorl height, mm (PWH)	0.22–0.42 0.29 ± 0.05	0.23–0.38 0.34 ± 0.03	0.23–0.36 0.29 ± 0.03	0.22–0.40 0.30 ± 0.04	0.23–0.30 0.26 ± 0.02	0.25–0.37 0.31 ± 0.02	0.23–0.35 0.29 ± 0.03	0.25–0.35 0.32 ± 0.03
Penultimate whorl width, mm (PWW)	0.58–0.79 0.66 ± 0.05	0.66–0.78 0.72 ± 0.03	0.64–0.83 0.72 ± 0.05	0.64–0.89 0.74 ± 0.06	0.58–0.70 0.64 ± 0.04	0.61–0.80 0.70 ± 0.04	0.59–0.72 0.64 ± 0.03	0.69–0.79 0.73 ± 0.03
Aperture height, mm (AH)	0.63–0.82 0.71 ± 0.04	0.66–0.80 0.73 ± 0.04	0.74–0.90 0.81 ± 0.04	0.70–0.92 0.81 ± 0.06	0.65–0.76 0.72 ± 0.03	0.65–0.80 0.74 ± 0.05	0.62–0.82 0.72 ± 0.05	0.70–0.82 0.76 ± 0.03
Aperture width, mm (AW)	0.53–0.69 0.59 ± 0.04	0.51–0.62 0.56 ± 0.03	0.60–0.72 0.67 ± 0.03	0.57–0.74 0.65 ± 0.04	0.53–0.60 0.57 ± 0.02	0.5–0.64 0.57 ± 0.04	0.48–0.67 0.55 ± 0.04	0.50–0.63 0.58 ± 0.03
SW/SH	0.62–0.73 0.67 ± 0.03	0.51–0.58 0.54 ± 0.02	0.62–0.74 0.68 ± 0.03	0.59–0.73 0.68 ± 0.03	0.61–0.67 0.64 ± 0.02	0.60–0.68 0.64 ± 0.02	0.56–0.63 0.59 ± 0.01	0.52–0.66 0.59 ± 0.03
BWH/SH	0.73–0.84 0.78 ± 0.02	0.70–0.78 0.74 ± 0.02	0.75–0.85 0.80 ± 0.02	0.76–0.85 0.79 ± 0.02	0.77–0.83 0.80 ± 0.02	0.70–0.79 0.75 ± 0.02	0.75–0.85 0.79 ± 0.02	0.69–0.80 0.76 ± 0.03
SpH/SH	0.44–0.56 0.51 ± 0.03	0.55–0.62 0.58 ± 0.02	0.46–0.56 0.51 ± 0.02	0.48–0.56 0.52 ± 0.02	0.48–0.56 0.51 ± 0.02	0.50–0.59 0.54 ± 0.02	0.50–0.56 0.53 ± 0.01	0.53–0.61 0.56 ± 0.02
AH/SH	0.42–0.51 0.47 ± 0.02	0.38–0.45 0.41 ± 0.02	0.46–0.53 0.49 ± 0.02	0.43–0.52 0.48 ± 0.02	0.45–0.52 0.48 ± 0.02	0.40–0.50 0.46 ± 0.02	0.42–0.50 0.45 ± 0.02	0.42–0.47 0.45 ± 0.01
AH/AW	1.14–1.28 1.22 ± 0.04	1.21–1.41 1.29 ± 0.05	1.14–1.33 1.22 ± 0.04	1.14–1.32 1.25 ± 0.04	1.19–1.34 1.26 ± 0.04	1.05–1.38 1.29 ± 0.07	1.12–1.48 1.32 ± 0.06	1.17–1.42 1.30 ± 0.06
PWH/SH	0.15–0.23 0.19 ± 0.02	0.14–0.22 0.19 ± 0.01	0.15–0.20 0.17 ± 0.01	0.15–0.21 0.17 ± 0.01	0.16–0.19 0.18 ± 0.01	0.16–0.22 0.20 ± 0.01	0.15–0.21 0.18 ± 0.01	0.16–0.20 0.19 ± 0.01
PWH/BWH	0.19–0.30 0.25 ± 0.03	0.18–0.30 0.26 ± 0.02	0.18–0.26 0.22 ± 0.02	0.18–0.26 0.22 ± 0.02	0.19–0.25 0.22 ± 0.02	0.21–0.30 0.26 ± 0.02	0.17–0.28 0.23 ± 0.02	0.21–0.29 0.25 ± 0.02
PWW/BWW	0.68–0.90 0.80 ± 0.05	0.79–0.87 0.83 ± 0.02	0.72–0.90 0.77 ± 0.03	0.70–1.00 0.76 ± 0.04	0.74–0.80 0.77 ± 0.02	0.71–0.87 0.81 ± 0.04	0.71–0.97 0.81 ± 0.06	0.78–0.87 0.81 ± 0.02

### 2.3. Statistical Analysis

Linear measurements of shells were analyzed using standard methods of univariate (Pearson correlation analysis) and multivariate ordination (the linear discriminant analysis, LDA) methods using the PAST 4.11 statistical software [30]. The non-parametric Mann–Whitney test was used to assess the univariate differences. The conchological differences between species and sexes were assessed using a permutational multivariate analysis of variance (PERMANOVA) implemented in PRIMER 7 [31,32]. The PERMANOVA analysis was based on a Euclidean distance calculated using either raw values of 11 conchological variables or size-standardized values; in both cases, all variables were normalized prior to analysis by subtracting the mean and then dividing by the standard deviation. Elliott’s allometric standardization [33], implemented in PAST software, was performed to eliminate or reduce the influence of shell size on its other dimensional features. For this “size-free” analysis, the shell height (SH) was used as a reference measurement, i.e., the raw SH values were used, while the other conchological variables were standardized to the SH. The Type 3 sums of squares (partial) and permutation of residuals according to the reduced model (999 permutations) were used in PERMANOVA. The sexual dimorphism in shell traits was studied exclusively on the type samples of the following species: *C. dadi-ani* sp. nov. (28 specimens: 14 females and 14 males), *C. shiksha* sp. nov. (42 specimens: 23 females and 19 males), *A. starobogatovi* sp. nov. (36 specimens: 17 females and 19 males) and *T. kopidophora* sp. nov. (25 specimens: 8 females and 17 males), for which the gender was undoubtedly determined by means of anatomical dissection.

### 2.4. Molecular Phylogenetic Methods

Specimens for molecular analysis were fixed in 80% ethanol. DNA was extracted from whole specimens; tissues were hydrated in TE buffer (3 × 10 min); then total genomic DNA was extracted with the Sherlock extraction kit (A&A Biotechnology), and the final product was dissolved in 20 µL of tris-EDTA (TE) buffer. The extracted DNA was stored at −80 °C at the Department of Malacology, Institute of Zoology and Biomedical Research, Jagiellonian University in Kraków (Poland).

Mitochondrial cytochrome oxidase subunit I (COI) and nuclear histone 3 (H3) loci were sequenced. Details of PCR conditions, primers used, and sequencing were given in Szarowska et al. [34]. In the phylogenetic analysis, additional sequences from GenBank were used as references (Table 3). Sequences were initially aligned in the MUSCLE [35] Programme in MEGA 7 [36] and then checked in Bioedit 7.1.3.0 [37]. Uncorrected p-distances were calculated in MEGA 7. The estimation of the proportion of invariant sites and the saturation test for entire data sets [38,39] were performed using DAMBE [40]. The data were analyzed using approaches based on Bayesian inference (BI) and maximum likelihood (ml). For RAxML analysis, the jModelTest2 via the CIPRES Science Gateway [41] was used to find the best-fitting model for each gene. For COI and H3 sequences, the models TPM2uf+I+G and TIM2ef+G were used, respectively. The ML analysis was conducted in RAxML-NG v. 0.8.0 [42] via web service available at <https://raxml-ng.vital-it.ch/>, accessed on 24 November 2022 with 10 random and 10 parsimony starting trees. In the BI analysis, the K81+G and SYM+G models of nucleotide substitution were applied in tree reconstruction for COI and H3. Models were selected using MrModelTest 2.4 [43]; for concatenated sequences, the model parameters were estimated for each partition separately. The analyses were run using MRBAYES v. 3.2.7a [44] with defaults of most priors. Two simultaneous analyses were performed, each with 10,000,000 generations, with one cold chain and three heated chains, starting from random trees and sampling the trees every 1000 generations. The first 25% of the trees were discarded as burn-in. The analyses were summarized as a 50% majority-rule consensus tree. Convergence was checked in TRACER v.1.7.1 [45], in all cases, the effective sample size exceeded 200. FigTree v. 1.4.4 [46] was used to visualize the trees. Two species delimitation methods were performed: Poisson tree processes (PTP) [47] and automatic barcode gap discovery (ABGD) [48]. The PTP approach was run using the web server <https://species.h-its.org/ptp/>, accessed on 14 December 2022



with 100,000 MCMC generations, 100 thinning, and 0.1 burn-in. We used the RAXML output phylogenetic tree. The ABGD approach used the web server (<https://bioinfo.mnhn.fr/abi/public/abgd/abgdweb.html>, accessed on 14 December 2022) with the default parameters. The Fastchar application [49] was used to distinguish particular species from another species, based on COI and H3 sequences, by determining the molecular diagnostic characters (MDCs). Two types of characters were accepted: at binary positions (the character state in the query group is different from the uniform character state in the reference group) and at asymmetric positions (the character state in the query group is different from the non-uniform character state in the reference group). To calibrate the molecular clock, the sequences of two hydrobiids, *Peringia ulvae* (Pennant, 1777) and *Salenthydrobia ferreri* Wilke, 2003, were used as outgroups [50–52]. In order to infer the temporal scenario of the diversification of Georgian genera, we reconstructed a time tree in BEAST 2 ver. 2.7.3 [53] based on COI. The analysis in BEAST was set up using BEAUTi. Two independent analyses were run under a strict molecular clock and calibrated Yule model tree prior. Site and clock models were unlinked across partitions. Analyses were run for 10 million generations, sampled every 10,000 generations. Convergences of both runs and ESS were verified as in BI. Log and tree files were combined using LogCombiner 2.7.3. The maximum credibility tree was constructed in TreeAnnotator 2.7.3.

**Table 3.** Taxa used for phylogenetic analyses with their GenBank accession numbers and references.

Species	COI/H3 GB Numbers	References
<i>Aetis starobogatovi</i> Chertoprud, Grego & Mumladze, sp. nov.	OQ396620-30/OQ401670-80	present study
<i>Agrafia wiktora</i> Szarowska et Falniowski, 2011	JF906762	Szarowska & Falniowski, 2011 [54]
<i>Alzoniella finalina</i> Giusti & Bodon, 1984	AF367650	Wilke et al., 2001 [55]
<i>Avenionia brevis berenguieri</i> (Draparnaud, 1805)	AF367638	Wilke et al., 2001 [55]
<i>Belgrandiella</i> cf. <i>kuesteri</i> (Boeters, 1970)	MG551325/MG551366	Osikowski et al., 2018 [56]
<i>Belgrandiella</i> cf. <i>robusta</i> Radoman, 1975	MG551331	Osikowski et al., 2018 [56]
<i>Caucasogeyeria gloeri</i> Grego & Mumladze, 2020	MT406097/MT410523	Grego et al., 2020 [10]
<i>Caucasopsis letsurtsume</i> Grego & Mumladze, 2020	MT406082/MT410510	Grego et al., 2020 [10]
<i>Colchiella dadiani</i> Chertoprud, Grego & Mumladze, sp. nov.	OQ396613-19/OQ401663-69	present study
<i>Colchiella lugella</i> Chertoprud, Grego & Mumladze, sp. nov.	MG543150-51/MG543153-54	Grego et al., 2017 [25]
<i>Colchiella nazodelavo</i> Chertoprud, Grego & Mumladze, sp. nov.	OQ396608-12/OQ401658-62	present study
<i>Colchiella shiksha</i> Chertoprud, Grego & Mumladze, sp. nov.	OQ396606-07/OQ401656-57	present study
<i>Dalmatinella fluviatilis</i> Radoman, 1973	KC344541	Falniowski & Szarowska, 2013 [57]
<i>Daphniola louisi</i> Falniowski & Szarowska, 2000	KM887915/MZ265364	Szarowska et al., 2014 [58]/Hofman et al., 2021 [59]
<i>Ecrobia maritima</i> (Milaschewitsch, 1916)	KX355830/MG551322	Osikowski et al., 2016 [60]/Grego et al., 2017 [25]
<i>Fissuria boui</i> Boeters, 1981	AF367654	Wilke et al., 2001 [55]
<i>Graecoarganiella parnassiana</i> Falniowski & Szarowska, 2011	JN202352/MZ265362	Falniowski & Szarowska, 2011 [61]/Hofman et al., 2021 [59]
<i>Graziana alpestris</i> (Frauenfeld, 1863)	AF367641	Wilke et al., 2001 [55]
<i>Grossuana angeltsekovi</i> Glöer & Georgiev, 2009	KU201090	Falniowski et al., 2016 [62]
<i>Hauffenia michleri</i> Kuščer, 1932	KY087865/KY087878	Rysiewska et al., 2017 [63]
<i>Hausdorfenia pseudohauffenia</i> Grego & Mumladze, 2020	MT406102/MT410528	Grego et al., 2020 [10]
<i>Horatia klecakiana</i> Bourguignat 1887	KJ159128	Szarowska & Falniowski, 2014 [64]
<i>Iglica</i> cf. <i>gracilis</i> (Clessin, 1882)	MH720988	Hofman et al., 2018 [65]
<i>Imeretiopsis gorgoleti</i> Grego & Mumladze, 2020	MT406092/MT410520	Grego et al., 2020 [10]
<i>Islamia zermanica</i> (Radoman, 1973)	KU662362/MG551320	Beran et al., 2016 [66]/Grego et al., 2017 [25]
<i>Kartvelobia sinuata</i> Grego & Mumladze, 2020	MT406091/MT410517	Grego et al., 2020 [10]
<i>Montenegrospeum bogici</i> (Pešić & Glöer, 2012)	KM875510/MG880218	Falniowski et al., 2014 [67]/Grego et al., 2018 [68]
<i>Paladilhopsia grobbeni</i> Kuscer, 1928	MH720991	Hofman et al., 2018 [65]
<i>Peringia ulvae</i> (Pennant, 1777)	AF118302	Wilke and Davis, 2000 [51]
<i>Pontobelgrandiella</i> sp. Radoman, 1978	KU497012	Rysiewska et al., 2016 [69]
<i>Pontohoratia pichkhaiai</i> Grego & Mumladze, 2020	MT406087/MT410513	Grego et al., 2020 [10]
<i>Sadleriana fluminensis</i> (Küster, 1853)	KF193067	Szarowska & Falniowski, 2013 [70]
<i>Salenthydrobia ferrerii</i> Wilke, 2003	AF449213	Wilke, 2003 [50]
<i>Sarajana apfelbecki</i> (Brancsik, 1888)	MN031432	Hofman et al., 2019 [71]
<i>Satapia cavernicola</i> Chertoprud, Grego & Mumladze, sp. nov.	OQ396631-32/OQ401681-82	present study
<i>Terranigra kosovica</i> Radoman, 1978	xxx	Jaszczynska et al. in press [72]
<i>“Tschernomorica” adsharica</i> (Lindholm, 1913)	OQ396633-38/OQ401683-88	present study
<i>Tschernomorica kimmeria</i> Vinarski & Palatov, 2019	OQ396600-05/OQ401650-55	present study
<i>Tschernomorica kopidophora</i> Chertoprud, Grego & Mumladze, sp. nov.	OQ396576-99/OQ401626-49	present study

## 2.5. Species Conservation Status

To facilitate the future conservation of the newly described species, we suggest that the conservation status for each species is based on the categories and criteria of the Inter-

national Union for Conservation of Nature (IUCN 2012 v-3.1./2) and the recommendations provided by [73].

## 2.6. Abbreviations Used in the Text

ANSP	Academy of Natural Sciences of Drexel University, Philadelphia, USA
AOO	Area of occupancy
EOO	Extent of occurrence
IEE	A.N. Severtzov Institute of Ecology and Evolution
ISU	Iliia State University, Tbilisi, Georgia
JGS	collection Jozef Grego, Banská Bystrica, Slovakia
FLMNH-UF	The Florida Museum of Natural History, Gainesville, Florida
LDA	Linear Discriminant Analysis
MNHN	Muséum national d'Histoire naturelle, Paris, France
MSU	Lomonosov Moscow State University
NHMUK	Natural History Museum London, UK
NHMW	Naturhistorisches Museum Wien, Austria
NMBE	Naturhistorisches Museum Bern, Switzerland
PIN	Yu. A. Orlov Paleontological Museum of the Paleontological Institute
RAS	Russian Academy of Sciences
WSBS	White Sea Biological Station
ZMH	Zoological Museum University Hamburg
<i>Abbreviations related to the shell morphology</i>	
AH	Aperture height
AW	Aperture width
BWH	Body whorl height
BWHap	Body whorl height above aperture
BWW	Body whorl width
PWH	Penultimate whorl height
PWW	Penultimate whorl width
SH	Shell height
SW	Shell width
SpH	Spire height

## 3. Results

### 3.1. Molecular Phylogeny

We obtained 63 new sequences of COI (457 bp, GenBank accession numbers OQ396576–OQ396638) and 63 of H3 (310 bp, GenBank accession numbers OQ401626–OQ401688). The test for the substitution saturation analysis [39] showed an ISS (0.74 for COI; 0.45 for H3) significantly smaller than the critical ISS value (ISSC: 0.96 for COI; 0.63 for H3), indicating that sequences are not saturated and thus useful in phylogenetic reconstruction. In all analyses, the topologies of the resulting phylograms were identical in both the ML and BI phylogram analyses; thus, we present the phylogram computed with RAXML.

The COI and H3 phylograms (Figures 4–6) clearly show all the new Georgian sequences as a distinct, highly supported group closely related to Belgrandiellinae snails. However, this group is very different from other Belgrandiellinae; the p-distance between them is 0.14 and 0.05 for COI and H3, respectively. Among the Gregorian group, sequences formed nine distinct mOTUs, with high support for COI and joined COI and H3 sequences (Figures 4 and 6); for H3 sequences, most mOTUs were also clearly distinct (Figure 5). The p-distances between mOTUs are given in Table 4. According to p-distances and species delimitation results, all mOTUs were assigned to distinct species. Distinct genera were defined based on the topography of the phylogram, p-distance, and morphological differences. All mOTUs formed three distinct lineages: *Tschernomorica*, *Colchiella*, and the third, including three other genera (Figure 6). The divergence time of all Georgian groups was estimated at  $3.75 \pm 0.89$  Ma (Figure 7). The most diverse appeared in the third line, which included three mOTUs, probably separate genera, with p-distances 0.096–0.106 (Table 4). The second line, containing four mOTUs, was moderately diverse, with p-distances 0.021–0.048, so it may represent one genus with four species. The p-distance between two species belonging to the first line is 0.015.

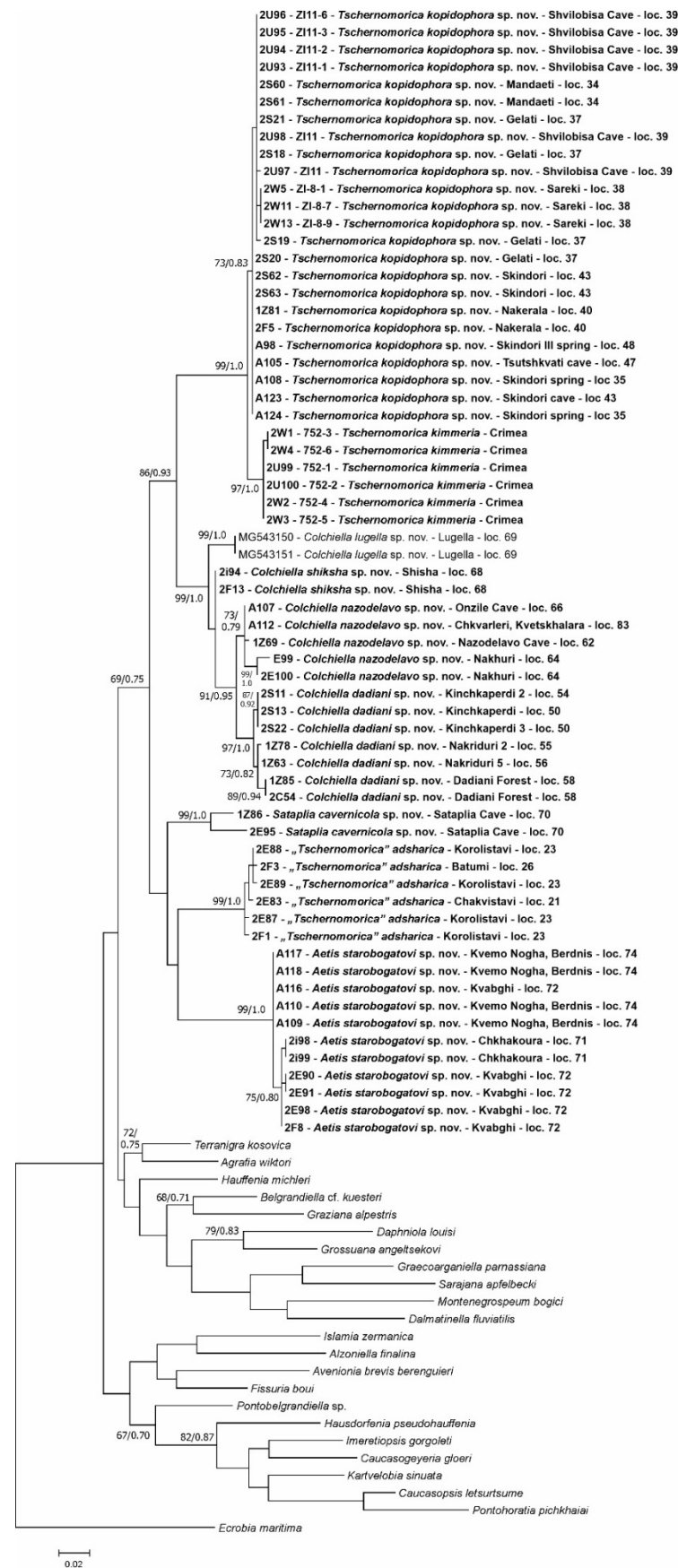


**Figure 4.** Maximum likelihood tree inferred from mitochondrial COI. Bootstrap supports and Bayesian probabilities are given. Newly obtained sequences are in bold.

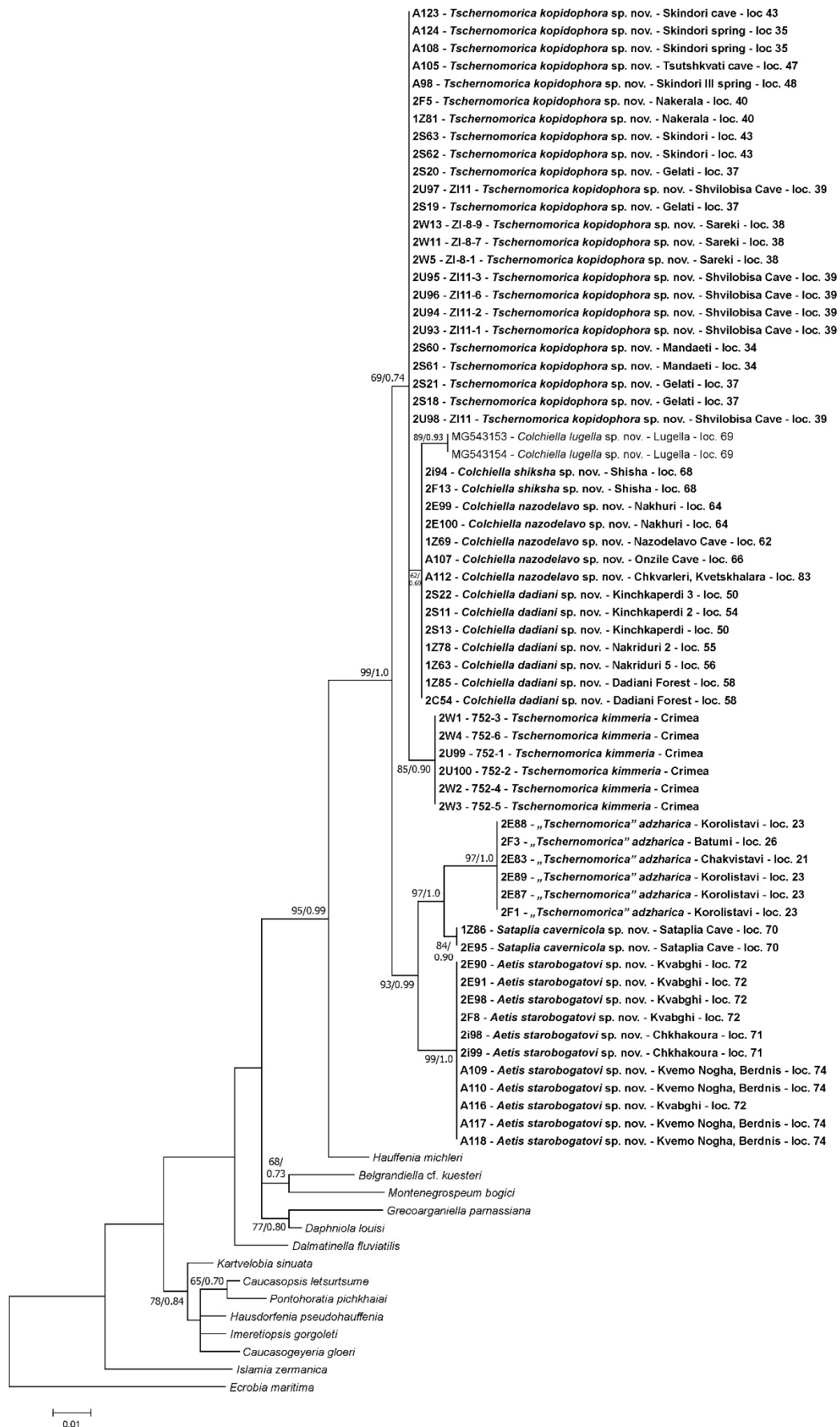


**Figure 5.** Maximum likelihood tree inferred from nuclear H3. Bootstrap supports (if >65%) and Bayesian probabilities are given. Newly obtained sequences are in bold.



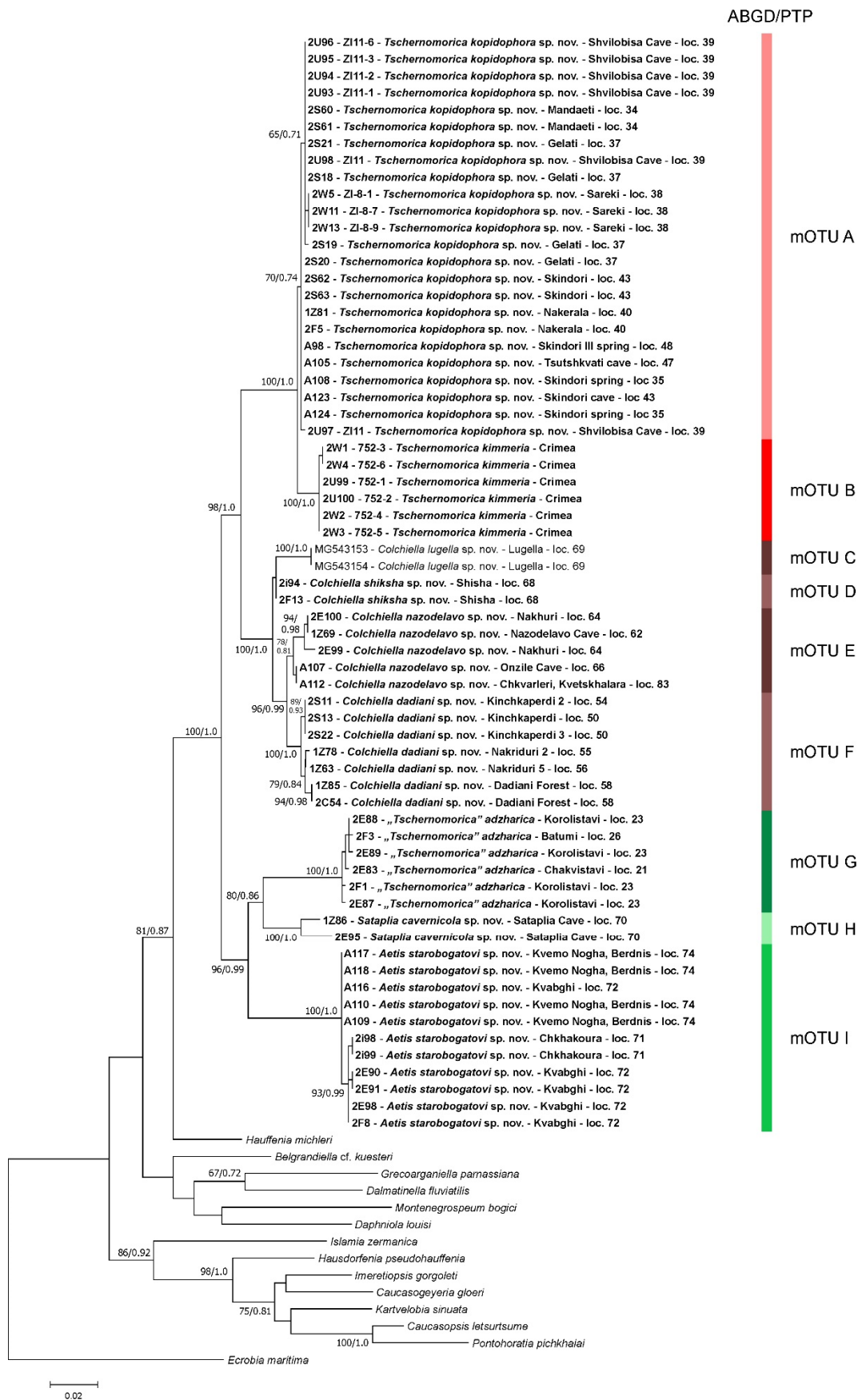


**Figure 6.** Maximum likelihood tree inferred from COI + H3. Bootstrap supports (if >65%) and Bayesian probabilities are given. Red, brown, and green bars indicate results from the ABGD and PTP methods, respectively. Newly obtained sequences are in bold.

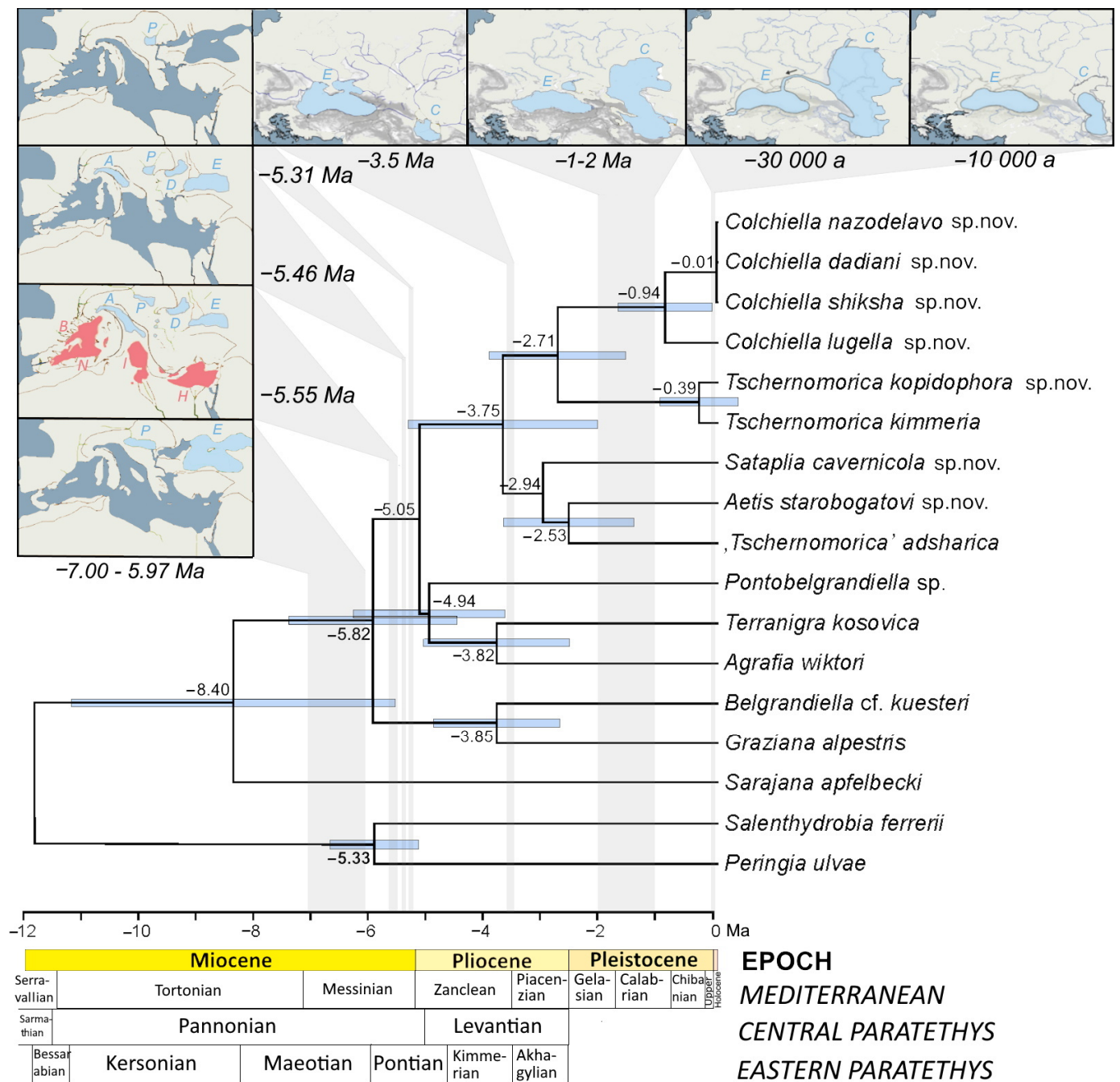


**Figure 7.** Bayesian time phylograms for COI gene. Posterior probabilities and the highest posterior density intervals at nodes are shown. Scale bar in substitutions per site; timeline on the bottom in Ma before present [74,75]. The saline sea environment is highlighted by dark blue color; Brackish or freshwater lakes by light blue color: A—Apennine Foredeep, C—Caspian Lake, D—Dacic Lake, E—Euxine Lake, P—Pannonian Lake; Hyper-salinated lakes by dark pink color: B—Balearic Basin, I—Ionian Basin, H—Herodotus Basin, N—North Algerian Basin.

**Table 4.** p-distances between *Tschernomorica* mOTUs for COI (below diagonal, blue) and H3 (above diagonal, green). p-distances within mOTUs for COI are also indicated (diagonal, bold, italic).

	A	B	C	D	E	F	G	H	I
A	<b>0.002</b>	0.007	0.010	0.003	0.003	0.003	0.020	0.020	0.031
B	0.015	<b>0.001</b>	0.017	0.010	0.010	0.010	0.027	0.027	0.038
C	0.078	0.085	<b>0.000</b>	0.007	0.007	0.007	0.031	0.031	0.041
D	0.069	0.075	0.021	<b>0.000</b>	0.000	0.000	0.024	0.024	0.034
E	0.084	0.092	0.047	0.029	<b>0.016</b>	0.000	0.024	0.024	0.034
F	0.092	0.096	0.048	0.027	0.028	<b>0.006</b>	0.024	0.024	0.034
G	0.106	0.113	0.100	0.092	0.109	0.114	<b>0.003</b>	0.020	0.031
H	0.104	0.106	0.097	0.092	0.104	0.108	0.106	<b>0.043</b>	0.017
I	0.104	0.109	0.099	0.090	0.103	0.108	0.102	0.096	<b>0.010</b>

### 3.2. Morphological Analysis

In order to test whether the species in question could be reliably distinguished by conchology, we performed the PERMANOVA analysis. In general, the interspecific differences account for a considerable part of overall individual variations (Table 5). Pairwise comparisons showed that almost all species were significantly different from each other, with  $p$ -values not exceeding 0.001 (Supplementary Table S2). The only exceptions were the pairs of *C. dadiani* vs. *C. shiksha* ( $p = 0.011$ ) and *C. nazodelavo* vs. *T. kimmeria* ( $p = 0.049$ ); their  $p$  values are still  $< 0.05$ ; however, they are closer to the threshold.

The results of linear discriminant analysis (LDA) to group individuals based on linear shell measurements are presented in Table 6 and Figure 8. The first three axes explained more than 90% of the total variation, the individuals being correctly classified by species in 83.5% of cases (Supplementary Table S1). The first axis explained 70.4% of the variance; it included the relative number of shell whorls (WhN) and spire height (SpH) set against the main shell width measurements (SW, BWW, AW) and can be interpreted as the integral characteristic of slenderness or elongation of the shell. Both the second and third axes (11.0% and 9.2%, respectively, of the total variance) combined most of all variables (all with positive loadings) and may be interpreted as a generalized measure of shell size.

The scatter plot in the two first discriminant axes illustrated the arrangement of the studied species in a “shell morphology” space. For example, *C. dadiani* sp. nov. and *C. shiksha* sp. nov. have the wide, barrel-shaped shell, which distinguishes them from *A. starobogatovi* sp. nov., *S. cavernicola* sp. nov., and *T. kopidophora* sp. nov. with slenderer, tower-shaped shells and a greater number of whorls. The 95% concentration ellipses of these two species groups were separated and almost did not overlap. At the same time, such species as *C. lugella* sp. nov., *C. nazodelavo* sp. nov. and *T. kimmeria* occupied an intermediate position; the scatter plots of their populations were widely overlapped, so 25–50% of individuals of these species could not be classified correctly. It is worth noting that *T. kimmeria* turns out to be conchologically closer to the representatives of genus *Colchiella* gen. nov. than to its congener *T. kopidophora* sp. nov.

**Table 5.** Results of PERMANOVA test with species identity (SPECIES) as grouping variable.  $p$  values are significant levels estimated by permutations of residuals ( $p < 0.05$  are given in bold).

Source of Variation	df	SS	MS	Pseudo-F	$p$	Unique Perms	Variance Component (%)
SPECIES	7	2121.8	303.11	29.473	<b>0.001</b>	998	49.6
Residual variation	228	2344.9	10.284				50.4

**Table 6.** Factor loadings for the first three axes of a LDA based on ten linear measurements and whorl numbers (WhN). Characteristics with highest scores are shown in bold.

Character	Axis 1	Axis 2	Axis 3
SH	0.004	<b>0.025</b>	<b>0.076</b>
SW	<b>−0.029</b>	<b>0.016</b>	<b>0.035</b>
BWH	−0.006	<b>0.038</b>	<b>0.040</b>
BWHap	0.004	<b>0.018</b>	0.024
SpH	<b>0.015</b>	0.005	<b>0.062</b>
PWW	−0.005	0.000	<b>0.036</b>
PWH	0.004	−0.006	0.016
BWW	<b>−0.014</b>	<b>0.020</b>	<b>0.040</b>
AH	−0.012	<b>0.016</b>	0.021
AW	<b>−0.015</b>	0.007	0.017
WhN	<b>0.050</b>	<b>0.020</b>	<b>0.062</b>

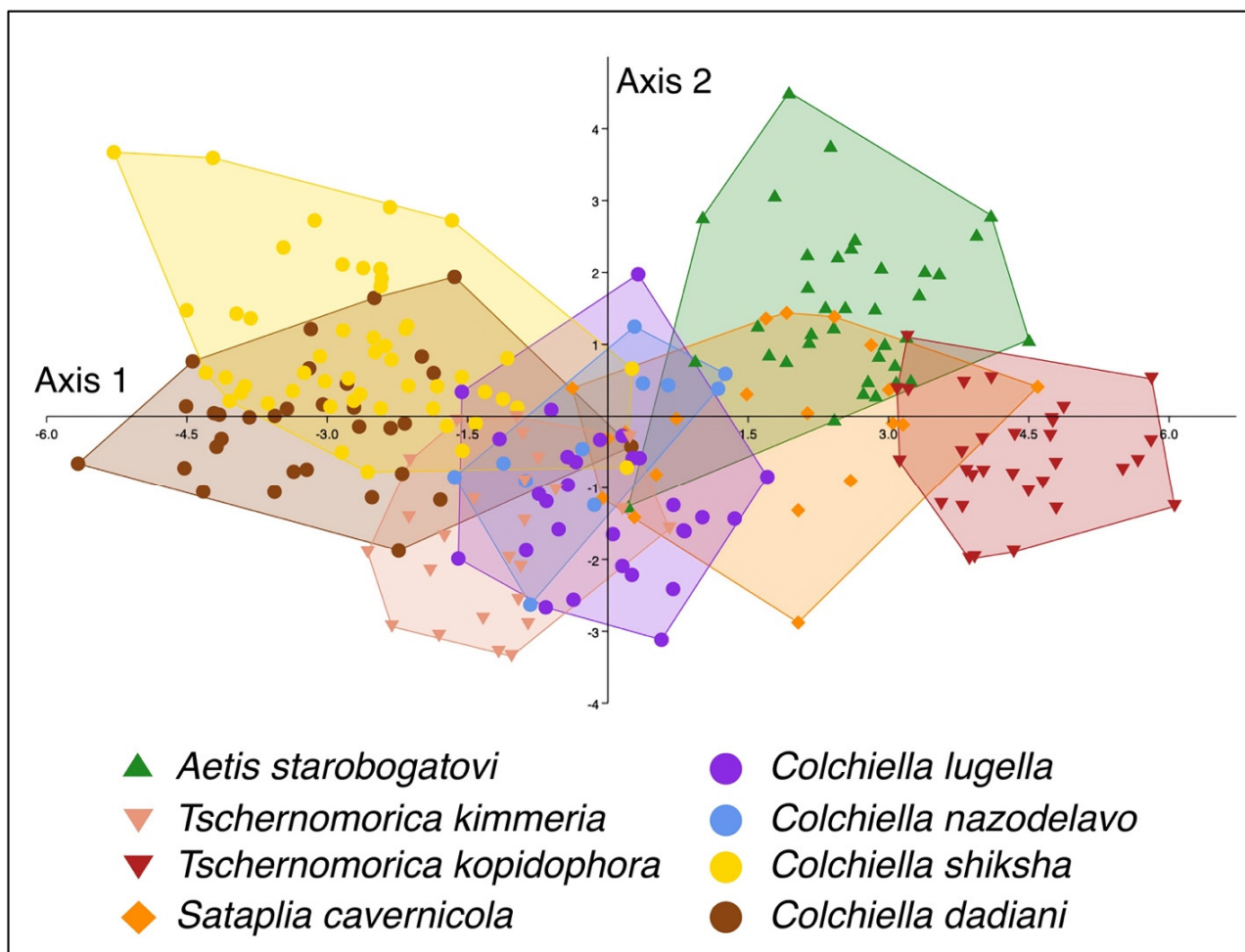


**Figure 8.** The results of the linear discriminant analysis (LDA) of shell measurements of eight Belgrandiellinae species. A scatter plot of individuals in the plane of the first two axes. The two first axes explained 81.4% of the variation (Axis 1—70.4%; Axis 2—11.0%).

### 3.3. Taxonomic Accounts

Class: GASTROPODA Cuvier, 1795

Subclass: Caenogastropoda Cox, 1960

Clade: Hypsgastropoda Ponder & Lindberg, 1997

Order: Littorinimorpha Golikov and Starobogatov, 1975



Superfamily: Truncatelloidea Gray, 1840  
 Family: Hydrobiidae Stimpson, 1865  
 Subfamily: Belgrandiellinae Radoman, 1983  
 Figures 9–19.

### 3.4. Genus *Tschernomorica* Vinarski & Palatov, 2019

**Type species:** *Tschernomorica kimmeria* Vinarski & Palatov, 2019.

**Species assigned to the genus:** *Tschernomorica kimmeria* Vinarski & Palatov, 2019, *Belgrandiella caucasica* Starobogatov 1962, *Tschernomorica lindholmi* Vinarski & Palatov, 2019, *Tschernomorica inconspicua* Vinarski & Palatov, 2019, *Bythinella adsharica* Lindholm, 1913 (provisional assignment), and *Tschernomorica kopidophora* Chertoprud, Grego & Mumladze, sp. nov.

#### 3.4.1. Diagnosis

The shell small, elongate, ovoid to barrel-shaped, with a relatively high spire and rounded whorls. Eyes present. The penis large, elongated, more or less curved, tapered distally with a thin, delicate tip. The penis usually with a small left lateral outgrowth or a simple shape (without outgrowth). The outgrowth located in the medial part of the penis or displaced to the distal part, small, delicate, and in some cases in the form of a small protrusion on the edge of the penis or tucked under it. In a number of populations, the outgrowth more or less reduced to complete absence but never large and pulpy. Sometimes there with a second, more distal, underdeveloped outgrowth. Weakly developed lateral penial outgrowth distinguishes *Tschernomorica* from other conchologically close genera—*Belgrandiella*, *Pontobelgrandiella*, *Colchiella* gen. nov., *Aetis* gen. nov., and *Sataplia* gen. nov. We did not find any visible taxonomically relevant differences on the female reproductive organ morphology during our study.

COI sequences OQ396576–OQ39659; H3 sequences: OQ401626–OQ401649. MDCs for *Tschernomorica* in comparison with other Georgian genera: COI: 135: G; 195: A; 222: C; 237: G; 255: T; 285: G; 309: C; 342: C; 360: T.

#### 3.4.2. Distribution

At present, the genus is found along the Black Sea Coast from Crimea to Turkey, as well as in the southern foothills of the western Greater Caucasus from the Black Sea coast to Zemo Imereti.

#### 3.4.3. Habitat

The genus *Tschernomorica* can be classified as crenobiotic to stygophilic. The habitats they occur are identical to those occupied by the Balkan *Belgrandiella* Wagner, 1928, and in Greece by *Agrafia* Szarowska and Falniowski, 2011. Live specimens are found throughout the whole spring zone, frequently in the stream emerging from the spring and sometimes in fast, well-aerated cold streams. They inhabit the spring head, at the border of the stygobiotic and crenobiotic habitats as well as in the primary spring sedimentation zone, and are also likely inhabiting the shallow stygobiotic habitat. In many cases, populations can be found inside the caves. Even unpigmented cave populations still have eyespots indicating that they are not fully troglomorphic.

#### 3.4.4. Remarks

The genus displays relatively low variability of the investigated molecular markers (COI and H3), which does not reflect the diversification in the penial morphology observed in the populations from Imereti.

### 3.5. *Tschernomorica kimmeria* Vinarski & Palatov, 2019.

Figure 9(2a–2l), Figure 10, Figure 18D, Figure 19(D1).

**Material examined.** CRIMEA • 9♂♂, 16♀♀; Crimean Peninsula, Belogorsky District, springs of the Zuya River valley; 44.924067° N, 34.368822° E; alt. 623 m; 03.04.2022; D.M. Palatov leg.

### 3.5.1. Molecular Diagnosis

COI sequences: OQ396600-OQ396605; H3 sequences: OQ401650-OQ401655. MDCs for *T. kimmeria* in comparison with *T. kopidophora*: **COI**: 66: A; 102: C; 138: G; 177: G; 348: A; **H3**: 18: A; 150: G.

**Description:** for the morphological description, we refer to the original publication [9]. Here we only give complementary data and comments for the penial morphology and the radula.

**Penial morphology:** the original description of the penial morphology [9] seems to be based on an immature or aberrant specimen. The authors described the penis as small in size and simple in shape. However, we found that the predominant pattern of penial shape in the population is different. The penis is usually large, flattened, folded in the proximal part, and blade-shaped (Figure 10H–J). The penial base lies behind the right eye (Figure 10G); the proximal part is relatively dilated. The penis is extended medially and may bear a tiny and very delicate outgrowth on its left side, although the presence of a lateral outgrowth is not a stable feature. The distal part of the penis is medium in length (about 150 µm), rather triangular in shape, and curved upwards, giving it the saber shape. The penial tip is pointed. The vas deferens is slightly curved and runs approximately through the center of the penis. In contrast, Figure 5a, provided by [9] Palatov and Vinarski (2019), apparently shows a deviant form of the penis, most probably underdeveloped or castrated by parasites. A small proportion (two out of nine) of males with a similar copulatory apparatus was found in the type population (Figure 10E,F). According to our assumption, this type of penis cannot be considered functional due to its dimensional characteristics (150 µm average).

**Radula:** Rachis with two basal cusps and four cusps on each side of the median cusp. The median cusp is longer than adjacent ones, and cusps are relatively long and narrow. Lateral tooth bears four cusps on each side of the median cusp, all cusps only broader and rather slightly longer than those of the rachis (Figure 18D).

### 3.5.2. Distribution

The species is known from a few localities over the eastern part of the Crimean Peninsula in the Belogorsky district.

### 3.5.3. Conservation Status

The number of known locations is no more than five, and its EOO is smaller than 20 km<sup>2</sup>. There is no reason to suppose that the AOO, EOO, the number of locations, the number of subpopulations, or the number of mature individuals is declining. However, due to its extremely small EOO and the fact that some of the localities and their surrounding habitats are under continuous anthropogenic pressure, we assessed the species as Vulnerable (VU) D2.

### 3.6. “*Tschernomorica*” *adsharica* (Lindholm, 1913)

*Tschernomorica adsharica* Vinarski & Palatov, 2019 [9]

*Agrafia adsharica* Grego et al., 2017 [25]

*Belgrandiella adsharica* Vinarski & Kantor, 2016 [24]

*Belgrandiella adsharica* Barjadze et al., 2015 [23]

*Belgrandiella adsharica* Kantor et al., 2010 [22]

*Belgrandiella adsharica* Bole & Velkovrh, 1983 [21]

*Belgrandiella adsharica* Schütt & Şeşen, 1993 [6]

*Bythinella adsharica* Lindholm, 1913 [1]

**Description:** for the morphological and anatomical description, we refer to the publication [9] (Plaltov & Vinarski 2019).

### 3.6.1. Material Examined

We examined the material collected in SW Georgia, Adjara autonomous region, from localities: GEORGIA • 3 wet and 1 dry specimens; Adjara (აჭარა), Chakvistavi (ჩაკვისთავი); 41.676890° N, 41.859046° E; alt. 348 m.; L. Mumladze leg.; 19.09.2017. Adjara (აჭარა), Charnali (ჭარნალი); 41.555460° N, 41.608890° E; alt. 92 m; L. Mumladze leg.; 12.07.2014. GEORGIA • 2 wet and 2 dry specimens; Adjara (აჭარა), Korolistavi (კორლისთავი), small stream; 41.638380° N, 41.745750° E; alt. 152 m; L. Mumladze leg.; 03.08.2019. • 3 wet and 1 dry specimens; same data as for preceding; 41.641870° N, 41.758510° E; alt. 394 m; L. Mumladze leg.; 03.08.2019. 22 dry specimens; same data as for preceding; 41.652680° N, 41.762480° E; alt. 542 m; L. Mumladze leg.; 17.09.2017. GEORGIA • 3 dry specimens; Adjara (აჭარა), Kveda Chkhutuneti (ქვედა ჩხუტუნეთი), near Karimana (კარიმანა) Waterfall; 41.499270° N, 41.839810° E; alt. 411 m; L. Mumladze leg.; 22.09.2017. GEORGIA • 3 wet and 12 dry specimens; Adjara (აჭარა), Makhinjauri (მახინჯაური), Batumi, left side of the Shua (შუა) Street; 1.675487° N, 41.706926° E; alt. 34 m; J. Grego leg.; 17.08.2017. GEORGIA • 4 wet specimens; Adjara (აჭარა), Makhinjauri (მახინჯაური), Batumi Botanical Garden; 41.698350° N, 41.717801° E; alt. 94 m; L. Mumladze leg.; 18.09.2017. GEORGIA • 18 wet and 2 dry specimens; Adjara (აჭარა), Mtirala Nat. Park. Small stream; 41.680917° N, 41.860360° E; alt. 276 m; L. Mumladze leg.; 19.09.2017; GEORGIA • 6 wet specimens; Adjara (აჭარა), Mtirala Nat. Park. Small stream (mt11); 41.679162° N, 41.886043° E; alt. 440 m; L. Mumladze leg.; 02.03.2014. • 4 wet specimens; data as for preceding (mt3); 41.669210° N, 41.853620° E; alt. 746 m; L. Mumladze leg.; 02.03.2014; 10 wet specimens; same data as for preceding (mt9); 41.679703° N, 41.888040° E; alt. 436 m; L. Mumladze leg.; 02.03.2014. (Table 1).

### 3.6.2. Molecular Diagnosis

COI sequences: OQ396633-OQ396638; H3 sequences: OQ401683-OQ401688. MDCs for "*Tschernomorica*" *adsharica* in comparison with two other *Tschernomorica* species: **COI**: 72: G; 78: G; 99: G; 111: A; 120: C; 126: G; 135: A; 144: A; 168: C; 180: C; 183: G; 195: T; 198: A; 204: C; 216: C; 222: T; 228: A; 234: C; 237: A; 240: T; 246: C; 252: A; 255: A; 258: C; 268: T; 285: A; 306: G; 309: T; 315: G; 324: T; 342: T; 360: G; 378: G; 429: A; **H3**: 6: T; 48: A; 78: G; 81: G; 89: T; 108: A; 201: C; 205: A; 258: A.

### 3.6.3. Distribution

The species is distributed at the westernmost part of the Lesser Caucasus from the vicinity of Khobuleti through Batumi to Keda surroundings, at altitudes of 20–540 m. Apart from the few localities reported from Turkey, its southernmost distribution limits remain unknown.

### 3.6.4. Conservation Status

The "*T*". *adsharica* is known from about a dozen locations along the Lesser Caucasus foothills along the Black Sea. The EOO exceeds 600 km<sup>2</sup>. The population is fragmented over its EOO, while the AOO is represented by several known springs and seepages, with a much smaller total area compared to the EOO. The EOO hosts a large number of suitable habitats, so it is likely that many more populations could be detected during future field investigations. Each AOO is very fragile to anthropogenic and climatic impacts, such as excavation work, live-stock farming, or drought. However, there is no reason to suppose that the AOO, EOO, or the number of mature individuals/population size is declining, and we suggest defining its conservation status as being of Least Concern (LC).

### 3.6.5. Remarks

The COI and H3 phylograms (Figures 4–6) and 34 MDCs for this taxon, in comparison with the other two *Tschernomorica* species, suggest an independent generic position of this species. However, the variability of anatomical data is still under study, and samples from more localities in Adjara and Turkey would be needed to clarify its taxonomic position. We opted, for the time being, to maintain the species tentatively under the genus “*Tschernomorica*” and to publish the results after the data collection is complete as the subject of a further study.

### 3.7. *Tschernomorica kopidophora* Chertoprud, Grego & Mumladze, sp. nov.

LSIDurn:lsid:zoobank.org:act:706E6847-5231-4D3E-9AFA-DE4A7AAF4F7D

Figure 9(1a–1l), Figure 11, Figure 18C, Figure 19(E1).

**Type material:** Holotype (Figure 9(1a)) 1 adult, alcohol specimen from type locality, 21.10.2021, collected by J. Grego & M. Szekeres, ISU FM-T024-H. Paratypes 3 adult ♂, alcohol specimen, same data as for holotype ISU FM-T024-P1/1, ISU FM-T024-P2/1, ISU FM-T024-P3/1; 1 adult ♀, alcohol specimen, same data as for holotype, ISU FM-T024-P4/1; 3 dry shells, same data as for holotype, ISU FM-T024-P5/4; 6 alcohol specimens, same data as for holotype, ISU FM-T024-P6/6; 315 wet specimens, same data as for holotype, ISU FM-T024-P7/10; 10 wet specimens, same as from holotype, NHMW-MO-113732; 10 wet specimens, same data as for holotype NMBE 577008; 10 wet specimens, same data as for holotype, MNHN-IM-2012-25412; 10 wet specimens, same data as for holotype, NHMUK 20220456; 10 wet specimens, same data as for holotype, UF-580902; 10 wet specimens, same data as for holotype, ZMH 141460; 10 wet specimens, same data as for holotype, ANSP 493826; 300 wet and 45 dry specimens, same data as for holotype, JGS F1977.

#### 3.7.1. Material Examined

GEORGIA • 17♂♂, 8♀♀, 615 wet and 106 dry shells; Imereti (იმერეთი), Motsameta (მოწამეთა), Gelati spring (გელათის წყარო); 42.297183° N, 42.770364° E; 21.10.2021; J. Grego & M. Szekeres leg.

GEORGIA • 1♂♂, 4♀♀, 31 wet and 4 dry specimens; Imereti, Tkibuli-Nikortsminda road (ტყიბული-ნიკორწმინდას გზა) left side, spring with travertine waterfall and small cave; 42.382927° N, 43.012168° E; alt. 953 m; 10.09.2022; J. Grego, M. Olšavský, E. Chertoprud leg.; • 28 wet and 25 dry specimens; same data as for preceding; 04.05.2018; J. Grego, M. Olšavský & L. Mumladze leg.; • 5 wet specimens; same data as for preceding; L. Mumladze leg.; 14.08.2016; • 8 wet specimens; same data as for preceding; 28.07.2017; L. Mumladze leg.; GEORGIA • 3♂♂, 1♀, 4 wet and 10 empty shells; Racha (რაჭა), Kharitsvali (ხარისთვალი), small spring at the right bank of Kheuri river (მდინარე ხეურის მარჯვენა შენაკადი); 42.489233° N, 43.401644° E; alt. 1704 m; 11.09.2022; J. Grego & E. Chertoprud leg.; • 1 wet and 3 dry specimens; same data as for preceding; 05.05.2018; J. Grego & L. Mumladze leg.; GEORGIA • 3 dry specimens, Shkmeri (შქმერი), Shkhrimeri Cave at the left tributary of Kheuri River (შქმერის მღვიმე, ხეურას მარცხენა შანაკდათან); 42.489233° N, 43.401644° E; alt. 1662 m; 05.05.2018; J. Grego, M. Olšavský and L. Mumladze; GEORGIA • 5♂♂, 14♀♀, 2 empty shells; Zemo Imereti (ზემო იმერეთი), Chiatura Municipality (ჭიათურა), Skindori (სკინდორი), Sakodra spring (სკინდორის წყარო); 42.241538° N, 43.258842° E; alt. 545 m; 21.10.2021; L. Mumladze leg.; • 22 wet specimens; same data as for preceding; 13.09.2022; J. Grego & E. Chertoprud leg.; GEORGIA • 8♂♂, 3♀♀, 13 empty shells; Zemo Imereti (ზემო იმერეთი), Chiatura Municipality (ჭიათურა), a small cave spring on the left bank of Jruchula river, western outskirts of the Sareki village (მდინარე ჯრუჭულას მარცხენა სანაპირო სოფელ სარეკის მიმდებარედ); 42.334053° N; 43.350199° E; alt. 443 m; 27.08.2021; E. Chertoprud leg.; GEORGIA • 8♂♂, 3♀♀, 13 empty shells; Zemo Imereti (ზემო იმერეთი) Chiatura Municipality (ჭიათურა), Shvilobisa cave between Bunikauri and Tabagrebi villages (შვილობისას მღვიმე); 42.325356° N, 43.267953° E; alt. 628 m; 29.08.2021; E. Chertoprud leg.; GEORGIA • 4 wet and 2 dry specimens; Imereti (იმერეთი), Chiatura region (ჭიათურა), Ghrudo cave and spring; 42.307671°, 43.327316°;



alt. 433 m; 21.10.2021; L. Mumladze leg.; GEORGIA • 3 wet and 2 dry specimens; Imereti (იმერეთი), Chiatura region (ჭიათურა), Mandaeti (მანდაეთი), Unnamed Spring; 42.164197° N, 43.317441° E; alt. 794 m; 22.10.2021; L. Mumladze leg.; GEORGIA • 2 dry specimens; Imereti (იმერეთი), Kuatisi (კუთასი), Iazoni Cave (იაზონის მღვიმე), the right bank of river Tskalsitela (მდინარე წყალწითელას მარჯვენა შენაკადი); 42.271811° N, 42.734153° E; alt. 132 m; 01.05.2018; J. Grego, L. Mumladze, M. Olšavský leg.; • 3 dry specimens; same data as for preceding; 42.271811° N, 42.734153° E; alt. 132 m; 13.10.2019; J. Grego, L. Mumladze leg.; GEORGIA • 312 wet and 10 dry specimens; Imereti (იმერეთი), Sveri (სვერი), spring nearby road; 42.23574N°, 43.311485°; alt. 551 m; 13.09.2022; E. Chertoprud, L. Mumladze, J. Grego, M. Olšavský leg.; GEORGIA • 47 dry specimens; Imereti (იმერეთი), Chiatura region (ჭიათურა), Itkhvisi village (სოფელი ითხვისი), karst spring; 42.289192° N, 43.350163° E; alt. 671 m; 21.10.2021; L. Mumladze leg.; 125 dry specimens; same data as for preceding; 42.289193° N, 43.350121° E; alt. 661 m; 13.09.2022; E. Chertoprud, J. Grego, M. Olšavský leg.; GEORGIA • 2 wet and 6 dry specimens; Imereti (იმერეთი), Chiatura region (ჭიათურა), Skindori (სკინდორი), in cave; 42.241454° N, 43.258937° E; alt. 548 m; 13.09.2022; E. Chertoprud, L. Mumladze, J. Grego, M. Olšavský leg.; GEORGIA • 3 wet specimens Imereti (იმერეთი), Mukhura (მუხურა), 6 km E of Tkibuli (ტყიბული), a small stream in Mukhura village; 42.325160° N, 43.065930° E; alt. 687 m; 28.07.2017; L. Mumladze leg.; GEORGIA • 7 wet specimens; Imereti (იმერეთი), the right tributary spring of Jurchula river (მდინარე ჯრუჭულა), near Kvemo Khevi (ქვემო ხევი); 42.390500° N, 43.359820° E; alt. 553 m; 26.07.2017; L. Mumladze leg.; GEORGIA • 1 wet specimen; Imereti (იმერეთი), a small tributary of river Jurchula N of Kvemo Khevi (ქვემო ხევი) near Jurchi (ჯრუჭი) Monastery; 42.394964° N; 43.364591° E, alt. 544 m; 26.07.2017; L. Mumladze leg.; GEORGIA • 3 wet and 5 dry specimens; Imereti (იმერეთი), Tsutskhvati (ცუცხვათი), Tsutskhvati (Maghara) cave (ცუცხვათის (მაღარას) მღვიმე); 42.272718° N, 42.852900° E; alt. 392 m; 10.09.2022; E. Chertoprud, J. Grego, L. Mumladze, M. Olšavský leg.; GEORGIA • 6 dry specimens; Imereti (იმერეთი), Chiatura region (ჭიათურა), Skindori (სკინდორი) III, spring from a cave with pipes; 42.250153° N, 43.273786° E; alt. 557 m; 13.09.2022; E. Chertoprud, J. Grego, L. Mumladze, M. Olšavský leg.

**Type locality.** GEORGIA • Imereti (იმერეთი), Mostsameta vicinities, Gelati spring (მოწამეთა, გელათის წყარო); 42.297183° N, 42.770364° E; 388 m alt.

### 3.7.2. Diagnosis

The new species differs from geographically close representatives of the genus *T. caucasica*, *T. lindholmi*, *T. inconspicua*, and *T. adsharica*, by a characteristic saber-shaped penis with a small left lateral outgrowth. In a number of populations, there is some degree of reduction up to complete absence, but it is never large in size. From the geographically distant species *T. kimmeria*, *T. kopidophora* sp. nov. differs in the proportions of its shell, which is higher and slender, and also in the shape of the penis. COI sequences: OQ396576–OQ396599; H3 sequences: OQ401626–OQ401649. MDCs for *T. kimmeria* in comparison with *T. kopidophora*: COI: 66: A; 102: C; 138: G; 177: G; 348: A; H3: 18: A; 150: G.

### 3.7.3. Description

**Shell:** thin-walled, elongate ovoid, quite high, on average constitutes 1.76 mm varied from 1.61 to 1.91 mm (Figure 11A–C). Spire high, constituting about 0.55–0.62 of SH. Whorls moderately inflated with noticeable sutures, their number not exceeding 4.25.

Umbilicus closed. Shell surface smooth or with irregular growth lines, whitish, translucent. Shell relatively narrow (SW/SH ratio 0.51–0.58). Aperture ovoid, parietal margin tightly adjoined to the body's whorl wall. Body whorl high and oblong, slightly inflated, about 0.74 of SH. Protoconch relatively large, dome-like, covered by a net of pits and wrinkles (Figure 11D–G). The border between protoconch and teleoconch indistinguishable.

**Sexual dimorphism.** There is no pronounced sexual dimorphism in the shell shape of the *Tschernomorica kopidophora* sp. nov. within the type population. According to non-

parametric multivariate statistical analysis of the shell variables, the differences between the sexes account for only 2.8% of all differences (PERMANOVA,  $p > 0.05$ ).

**Operculum:** irregularly-ovoid, relatively thin, paucispiral with a submarginal nucleus, generally orange or yellowish. Outer surface flat with axial growth lines. Inner surface with roughly sculpted rounded thickening in the nucleus area (Figure 11H).

**Soft parts:** white with well-developed eyes.

**Holotype measurements:** SH-1.78 mm; SW-1.03 mm; SpH-1.00 mm; BWH-1.32 mm; BWHap-0.55 mm; BWW-0.84 mm; PWH-0.36 mm; PWW-0.71 mm; AH-0.72 mm; AW-0.57 mm.

**Penial morphology:** Penis quite large (about 600  $\mu\text{m}$  long), flattened and folded, elongate triangular, gradually tapering towards the end. Its base lies behind the right eye; the proximal part quite dilated. The saber-shaped penis usually with one to two characteristic curves in medial and distal parts. Penis with single media-lateral outgrowth on its left side (Figure 19(E1)). Outgrowth usually small, about 25  $\mu\text{m}$  in length, gentle, in some cases bent under the penis. The distal penial part, continuing beyond medial outgrowths, long (about 250–300  $\mu\text{m}$ ), consisted of a slightly dilated proximal part and a long, thin, delicate, saber-curved part with a pointed tip. Vas deferens almost straight, with smooth curves within the penis, running approximately along the axis of the penis, in the distal part closer to the left penial edge (Figure 11I,J).

**Radula:** Rhachis with two basal cusps and four cusps on each side of the median cusp. Median cusp only longer than adjacent ones, cusps relatively long and narrow. Lateral tooth bears five cusps on the outer side of the largest cusp and three on the inner side, all cusps only broader than those of the rhachis. The inner marginal tooth with 28 cusps, outer marginal tooth with 21 cusps (Figure 18C).

#### 3.7.4. Variation

Currently, *T. kopidophora* sp. nov. is represented by six populations united by a common pattern of penial structure (Figure 11I–M). However, a number of traits vary considerably both between and within populations. The presence of the lateral outgrowth of the penis is a characteristic but not an always present trait. One of the patterns replacing or supplementing the presence of the outgrowth is the dilation of the corresponding penial part. In this case, the distal part becomes arrow-shaped (Figure 11M).

#### 3.7.5. Etymology

The name “kopidophora” is literally translated from Greek (κοπιδοφόρα) as «carrying a kopis (anc. gr. κόπις)», a special type of saber with a forward-curved blade. This type of cutting weapon was widely distributed on the territory of the ancient Kartli kingdom, and its curved shape resembles the shape of the male copulatory apparatus of this species (Figure 11J).

#### 3.7.6. Distribution

Western south Caucasus: known from Eastern Imereti (Zemo Imereti), karstic areas between Kutaisi to Chiatura, up to the Shkmeri Plateau in Racha, where it is detected in the following localities: Gelati, Nakerarala Pass, Skindori, Jurchula, Mandaeti, Kutaisi, Sareki, Shvilobisa Cave, Sveri, Mukhura, Ghrudo, Itkhvisi, Shkmeri, and Kharistvali.

#### 3.7.7. Habitat

Crenobiotic species inhabiting small karst springs and water outlets, occurring on stones, under fallen leaves, among sand grains, and partly in underground cavities associated with springs. Some of the numerous crenobiotic populations are not invading the adjacent cave (Skindori), while other populations look to be troglomorphic, and in the spring, heads appear as just fresh dead shells (for instance, in Itkhvisi). However, maybe the latter is a result of the groundwater circulation destruction by Manganese mining in the Chiatura region. The type locality is a permanent roadside spring frequently visited by travelers to

Gelati Monastery; the snails inhabit the outlet channel from the stone collector basin. Over the distribution area, the species can be found at altitudes between 130 and 1730 m. The water parameters over Imeretian habitats vary in the range of 10.7–13 °C, pH 7.5–8.1, and conductivity 371–887 µS., while the high alpine habitats in Racha region ranges 5.8–6.2 °C., pH 8.3–8.5, and conductivity 287–300 µS.

#### 3.7.8. Conservation Status

The species *T. kopidophora* sp. nov. is known from six locations stretching nearly all over the Imereti region of Western Georgia and with three locations in Southern Racha. The EOO exceeds 230 km<sup>2</sup>, and the distribution area contains several different unconnected basins/Karst massifs. The population is fragmented over EOO, while the AOO is represented by only several known spring zones and water seepages with a much smaller total area compared to the EOO. Each AOO is very fragile to anthropogenic and climate impacts. Many roadside springs are exposed to pollution (plastic, fuel, oil, organic) or could easily vanish during road extensions and excavations and lose water supply due to mining activities and droughts induced by climate changes. At this moment, however, there is no reason to suppose that the AOO, EOO, or the number of mature individuals/population sizes is declining significantly, and we suggest defining its conservation status as being of Least Concern (LC).

#### 3.7.9. Remarks

Penial and shell morphology of populations over Zemo Imereti indicate that particular populations could display autapomorphies. However, the COI and H3 data of the whole group are not significantly differentiated and not supporting the elevation of the autapomorphies into well-defined taxa. The wide variability of penial morphology within the *T. kopidophora* populations is not convincing enough for the taxonomic separation of local populations without significant differences in the molecular markers.

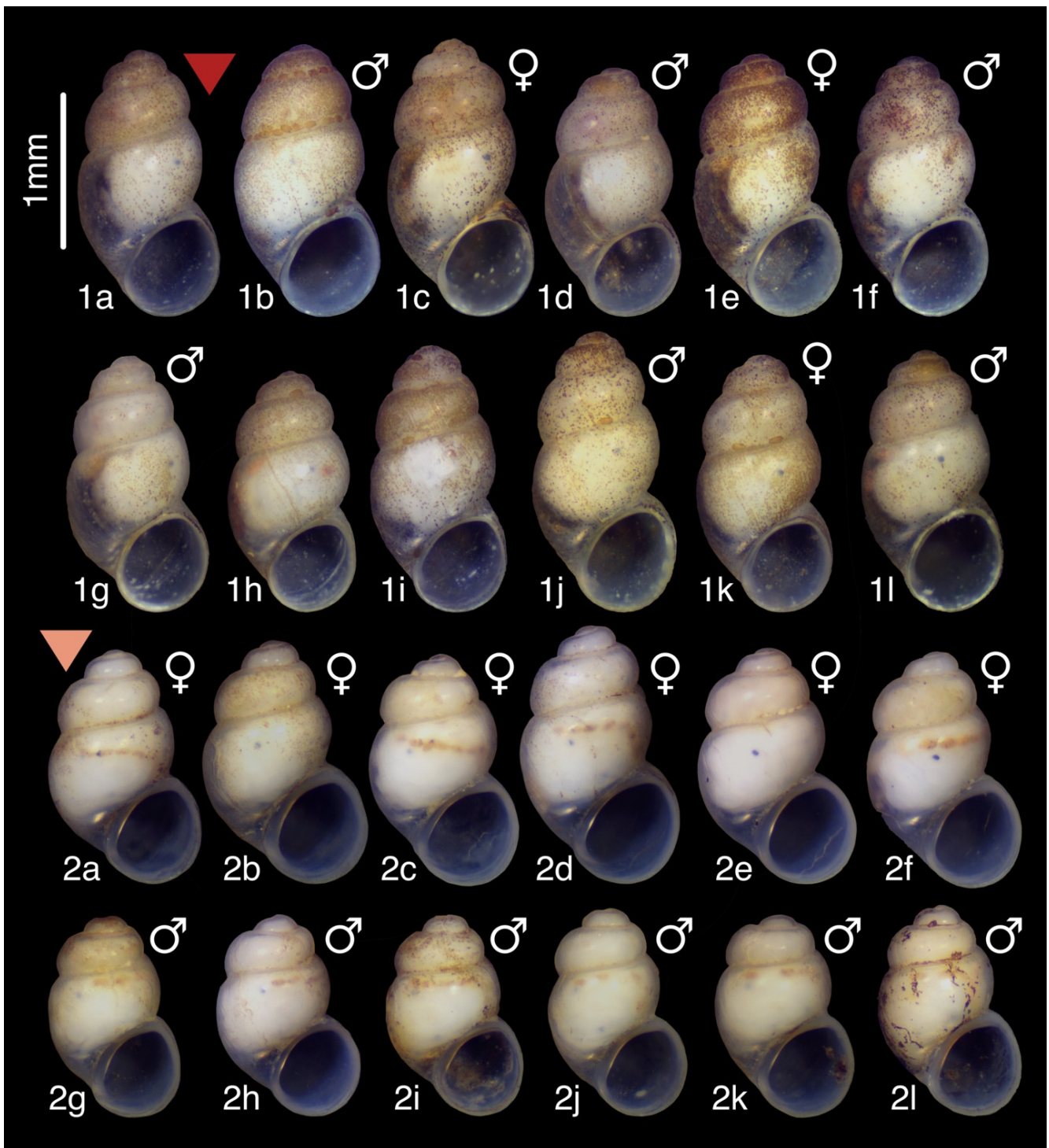


**Figure 9.** (1a–1l) *Tschernomorica kopidophora* sp. nov. Imereti, Motsameta, Gelati spring (red inverted triangle): 1a–holotype; (2a–2l) *Tschernomorica kimmeria* Vinarski & Palatov, 2019 (coral inverted triangle). The numbers represent the different species, and the letters correspond to individuals. Graphic labels refer to Figure 8 (with LDA graph) and Figure 20 (with the map).



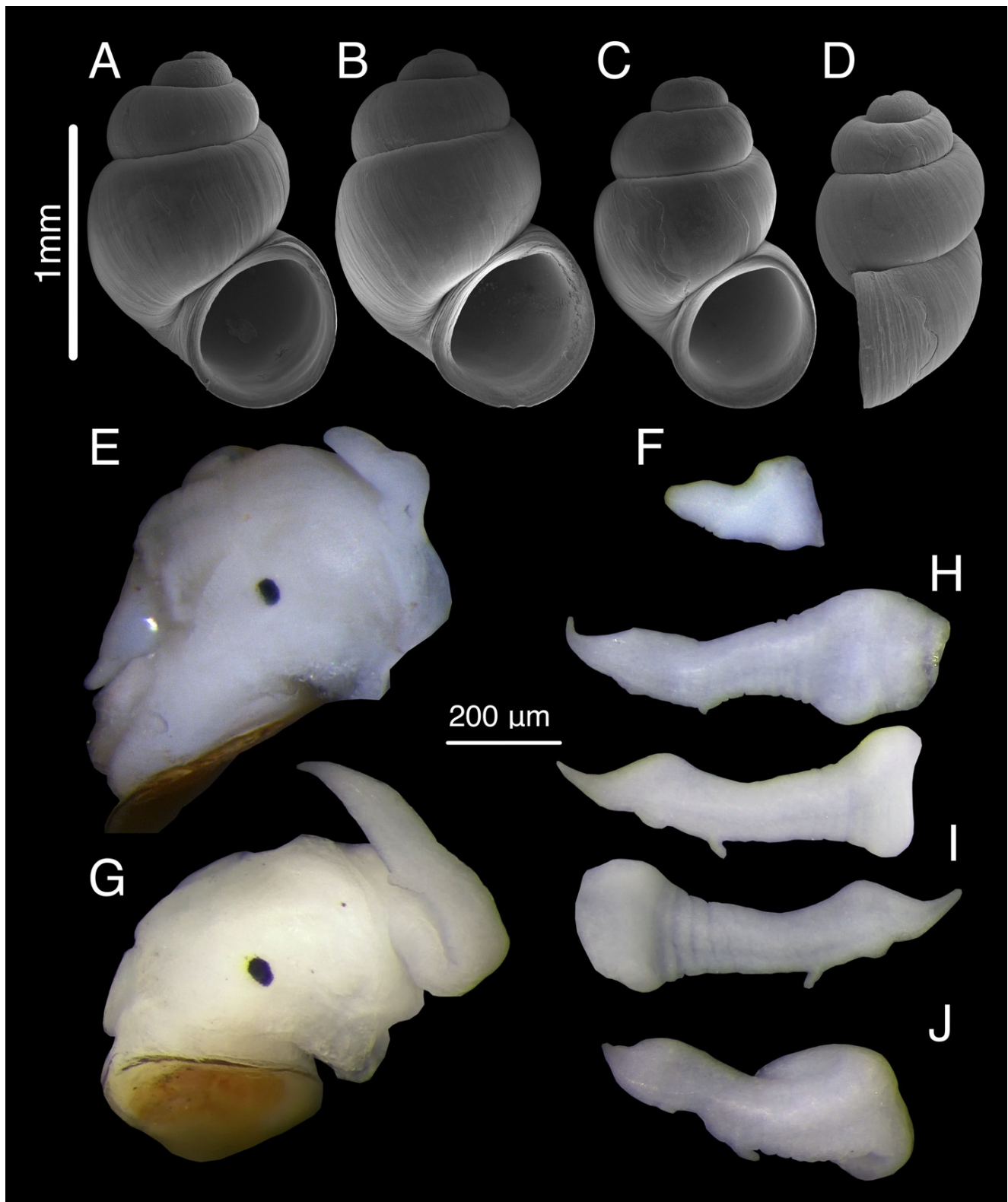


**Figure 10.** *Tschernomorica kinmeria* Vinarski & Palatov, 2019. (A–D)—shell; (E,G)—mollusk head with the penis, lateral view; (F,H–J)—penis habitus: (F)—deviant form, (H–J)—normal form.



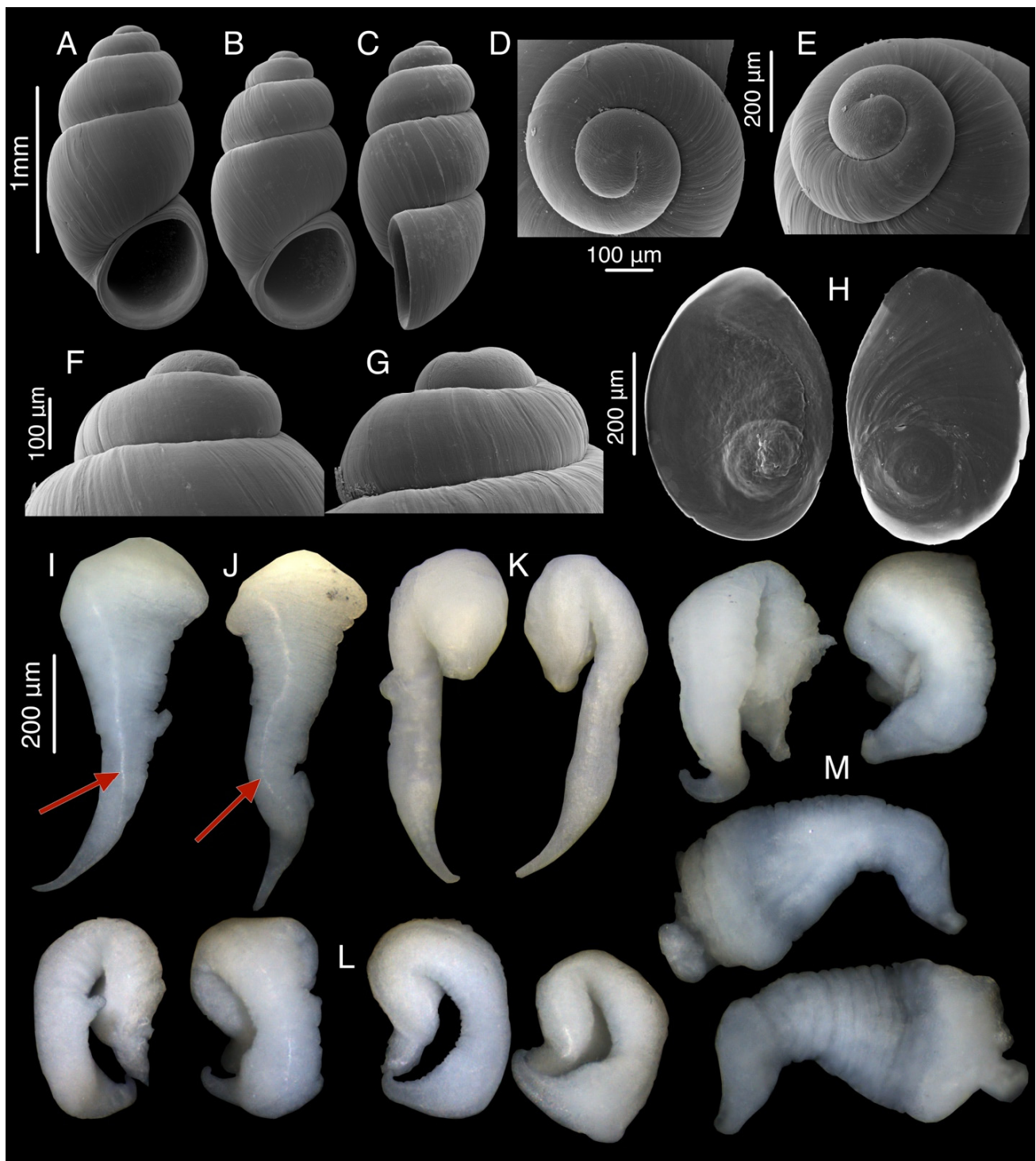


**Figure 11.** *Tschernomorica kopidophora* sp. nov. (A–C)—shell; (D)—protoconch, apical view; (E)—protoconch, latero-apical view; (F,G)—protoconch, lateral view; (H)—operculum; (I–M)—penis habitus: (I)—Imereti, Motsameta, Gelati spring; (J)—Zemo Imereti, Chiatura Municipality, Skindori village, Sakodria spring; (K)—Imereti, Tkibuli-Nikortsminda road left side, spring with travertine waterfall and small cave; (L)—Zemo Imereti, Chiatura Municipality, small cave spring on the left bank of Jruchula river, western outskirts of the Sareki village; (M)—Zemo Imereti, Chiatura Municipality, Shvilobisa Cave. Red arrow points to the vas of the penis.

### 3.8. Genus *Colchiella* Chertoprud, Grego & Mumladze, gen. nov.

LSIDurn:lsid:zoobank.org:act:44AE0561-C4EE-41AC-87CD-B9896AA827F3

**Type species.** *Colchiella dadiani* Chertoprud, Grego & Mumladze, sp. nov.

**Diagnosis.** Conchologically, this genus is hardly distinguishable from some other crenobiotic genera from Western South Caucasus (*Tschernomorica* Vinarski & Palatov, 2019; *Sataplia* Chertoprud, Grego & Mumladze, gen. nov.; *Aetis* Chertoprud, Grego & Mumladze, gen. nov.), except for being smaller and having a slightly broader shell (Table 2, Figures 8, 12 and 15(3a–3f,4a–4f)). However, the new genus can be easily distinguished based on penial morphology. The penis always with a well-pronounced single lateral outgrowth on the left side, which is displaced towards the terminal part of the penis. The shape of the outgrowth varied between species; however, within the genus, there is a tendency to form a process that is bent backward in the shape of a hook (Figures 13K,M,N,U,V and 19(F1,G1,H1)). Its relative size and position remain constant within the genus. The terminal part of the penis also has a similar general outline, usually elongated-triangular with some degree of tapering; the penial tip looks blunt at first glance, but usually with a rather delicate, thin, and more or less curved ending, whose shape and size varied. The COI+H3 tree also confirms the generic distinction from the related genera. COI sequences: OQ396606–OQ396619; H3 sequences: OQ401656–OQ401669. MDCs for *Colchiella* in comparison with other Georgian genera: COI: 94: C; 174: G; 195: G; 294: G; 357: C; 360: A; H3: 222: A.

**Etymology.** The name is derived from Colchis (Κολχίς)—a historical region located along the eastern coast of the Black Sea, which is the modern Colchis lowland and adjacent areas. According to ancient Greek mythology, Colchis was represented as the “land of the rising sun”, that is, a country located on the mysterious periphery of the existing world.

**Species composition.** *Colchiella dadiani* Chertoprud, Grego & Mumladze, sp. nov., *Colchiella lugella* Chertoprud, Grego & Mumladze, sp. nov., *Colchiella nazodelavo* Chertoprud, Grego & Mumladze, sp. nov., *Colchiella shiksha* Chertoprud, Grego & Mumladze, sp. nov.

### 3.8.1. Distribution

Southern slopes of the western Great Caucasus. Found in Samegrelo and adjacent Imereti regions in Georgia. Known from the conglomerate karst of Chkhorotsku up to the Southern Askhi Plateau with the Turchu Gamosadivari Basin and the Okatse Canyon.

### 3.8.2. Remarks

The wide distribution of the genus in the south-western Great Caucasus suggests that some of the *Tschernomorica* populations from southern Abkhazeti likely also belong to this new genus.

### 3.9. *Colchiella dadiani* Chertoprud, Grego & Mumladze, sp. nov.

LSIDurn:lsid:zoobank.org:act:5DD19D22-B2B8-401E-B282-B78C8D4CE6EE

Figure 12(1a–1j), Figure 13A–N, Figure 18F, Figure 19(G1).

**Type locality:** GEORGIA • Imereti (იმერეთი), Zeda Gordi (ზედა გორდი) region, spring in Dadiani forest park (დადაიანის პარკი) above the Okatse (ოკაცე) Canyon (Figure 2B); 42.455460° N, 42.529589° E; 640 m alt.

**Type material:** Holotype: (Figure 12(1a)) 1 adult, alcohol specimen from type locality, 15.10.2021, collected by J. Grego & M. Szekeres, ISU FM-T025-H. Paratypes: 12 dry shells, same data as for holotype, ISU FM-T025-P1/2; 17 dry shells, same data as for holotype, JGS F1943; 2 dry shells, Turchu Gamosadivari (თურჩუს გამოსადივარი) Basin, Nakhriduri (ნახრიდური) 4, travertine spring, NHMW-MO-113733; 2 dry shells, same data as for preceding, NMBE 577009; 2 dry shells, same data as for preceding, MNHN-IM-2012-25411; 2 dry shells, same data as for preceding NHMUK 20220457; 2 dry shells, same data as for preceding UF-580903; 30 wet specimens, same data as for preceding ISU FM-T025-P2/2; 2 dry shells, same data as for holotype, ZMH 141461; 2 dry shells, same data as for preceding, ANSP 493827, 34 dry shells, same data as for preceding, JGS F1067.

### 3.9.1. Material Examined

GEORGIA • 2♂♂, 7♀♀, 5 wet and 23 empty specimens; Imereti (იმერეთი), Turchu Gamosadivari (თურჩუს გამოსადივარი) Basin, Nakriduri (ნახრიდური) 3 spring at path to cave; 42.478030° N, 42.512797° E; alt. 875 m; 03.05.2018; J. Grego, L. Mumladze, M. Olšavský leg.; GEORGIA • 2 dry specimens; Imereti (იმერეთი), Kinchkhaperdi (კინჩხავერდი) about 1.5 km NE of the Kinchkha (კინჩხა) Waterfall; 42.513206° N, 42.558801° E; alt. 923 m; 15.10.2021; J. Grego, M. Szekeres leg.; GEORGIA • 3 wet and 6 dry specimens; Imereti (იმერეთი), Kinchkhaperdi (კინჩხავერდი) about 1.8 km NE of the Kinchkha (კინჩხა) Waterfall; 42.517252° N, 42.559959° E; alt. 978 m; 15.10.2021; J. Grego, M. Szekeres leg.; GEORGIA • 2 dry specimens; Imereti (იმერეთი), Kinchkhaperdi (კინჩხავერდი) about 2 km NE of the Kinchkha (კინჩხა) Waterfall; 42.518485° N, 42.557299° E; alt. 960 m; 15.10.2021; J. Grego, M. Szekeres leg.; GEORGIA • 4 wet and 8 dry specimens; Imereti (იმერეთი), Kinchkhaperdi (კინჩხავერდი), Spring at the right tributary of Satsiskvilo (საწისქვილო) River; 42.519975° N, 42.556215° E; alt. 976 m; 15.10.2021; J. Grego, M. Szekeres leg.; GEORGIA • 6 dry specimens; Imereti (იმერეთი), Kinchkhaperdi (კინჩხავერდი), about 1 km NE of the Kinchkha (კინჩხა) Waterfall; 42.502183° N, 42.559525° E; alt. 874 m; 02.05.2018; J. Grego, L. Mumladze, M. Olšavský leg.; • 3 wet and 5 dry specimens; same data as for preceding; 02.05.2018; J. Grego, L. Mumladze, M. Olšavský leg.; • 2 dry specimens; same data as for preceding; 42.502183° N, 42.559525° E; alt. 1006 m; 15.10.2021; J. Grego, M. Szekeres leg.; GEORGIA • 6 dry specimens; Imereti (იმერეთი), Satsiskvilo (საწისქვილო), Thurchismtha (თურჩისმთა), spring of Okatse (ოკაცე) and cave above the waterfall; 42.497017° N, 42.547122° E; alt. 1044 m; 02.05.2018; J. Grego, L. Mumladze, M. Olšavský leg.; GEORGIA • 2 dry specimens; Imereti (იმერეთი), Turchu Gamosadivari (თურჩუს გამოსადივარი) Basin, Nakhriduri (ნახრიდური) 2 spring above a small ford; 42.477581° N, 42.512194° E; alt. 866 m; 03.05.2018; J. Grego, L. Mumladze, M. Olšavský leg.; GEORGIA • 8 dry and 15 wet specimens; Imereti (იმერეთი), Turchu Gamosadivari (თურჩუს გამოსადივარი) Basin, Upskero (უფსკერო/უძირო) spring lake; 42.463150° N, 42.500967° N; alt. 886 m; 03.05.2018; J. Grego, L. Mumladze, M. Olšavský leg.; GEORGIA • 30 wet and 36 dry specimens; Imereti (იმერეთი), Turchu Gamosadivari (თურჩუს გამოსადივარი) Basin, Nakhriduri (ნახრიდური) 4 spring with travertine cascade; 42.478030° N, 42.512797° E; alt. 875 m; 03.05.2018; J. Grego, L. Mumladze, M. Olšavský leg.; GEORGIA • 12♂♂, 14♀♀, 6 wet and 9 dry specimens; Imereti (იმერეთი), Zeda Gordi (ზედა გორდი), spring in Dadiani forest park (დადაიანის პარკი) above Okatse (ოკაცე) Canyon; 42.456286° N, 42.5291528° E; alt. 642 m; 01.05.2018; J. Grego, L. Mumladze, M. Olšavský leg.; • 27 dry and 4 wet specimens; same data as for preceding; 42.455472° N, 42.529583° E; alt. 637 m; 15.10.2021; J. Grego, M. Szekeres leg.; • 3 wet and 6 dry specimens; same data as for preceding; 42.455460° N, 42.529589° E; alt. 640 m; 11.08.2017; J. Grego leg.

### 3.9.2. Other Material

GEORGIA • 2 dry specimens; Samegrelo (სამეგრელო), Pirveli Balda (პირველი ბალდა), spring at the right bank of Toba (ტობა) River under the waterfall; 42.476505° N, 42.458445° E; alt. 677 m; 14.10.2019; J. Grego leg. leg.; GEORGIA • 2 dry specimens; Samegrelo (სამეგრელო), Pirveli Balda (პირველი ბალდა), spring in the village above the road; 42.484039° N, 42.398128° E; alt. 296 m; 09.05.2018; J. Grego, L. Mumladze, M. Olšavský leg.

### 3.9.3. Diagnosis

The new species differs from other geographically close representatives of the genus (*C. lugella* sp. nov., *C. nazodelavo* sp. nov.) by its higher and rather larger shell as well as a rather characteristic shape of the lateral penial outgrowth: hook-shaped, curved back. Although *C. dadiani* sp. nov. shows a great resemblance to *C. shiksha* sp. nov., both in conchology and the structure of the penial lateral outgrowth, the new species generally has a shorter, triangular, and straighter distal part of the penis and on average a smaller shell. COI sequences: OQ396613-OQ396619; H3 sequences: OQ401663-OQ401669. MDCs

for *C. dadiani* in comparison with other *Colchiella* species: COI: 177: C; 204: G; 228: C; 435: C.

#### 3.9.4. Description

**Shell:** small (SH 1.65 mm on average), varies from elongate-ovoid to almost ovoid or barrel-shaped, up to 4 inflated whorls with noticeable sutures (Figure 13A–F). Umbilicus closed. Shell surface smooth or with irregular growth lines, whitish, translucent. Shell relatively broad, SW/SH ratio about 0.68. Spire height is 0.46–0.56 of shell height. Body whorl high and moderately inflated. Aperture broad-ovoid, quite expanded, parietal margin tightly adjoined to body whorl wall or separated by a barely noticeable slit. Protoconch relatively large, dome-like, consisting of 1.1–1.25 whorls, with a maximum diameter of 320  $\mu\text{m}$  (Figure 13G,H). Protoconch surface covered by a dense net of minute pits (Figure 13I). Border between protoconch and teleoconch not clear, guessed by the termination of embryonic shell sculptural pattern.

**Sexual dimorphism:** There was a pronounced sexual dimorphism in the shell morphology of *Colchiella dadiani* sp. nov. The sexes differed noticeably in shell size: males were usually smaller than females, and the average shell height (SH) was  $1.55 \pm 0.04$  mm for males and  $1.73 \pm 0.08$  mm for females (Figure 12(1a–1j)). These differences were highly significant (Mann–Whitney test for equal SH medians,  $p < 0.0001$ ). Moreover, all other conchological parameters were highly and significantly correlated with SH (all Pearson'  $r = 0.7$ – $0.9$ ; all  $p$ -values  $< 0.001$ ).

Earlier, we [12,76] emphasized the significance of shell height on intraspecific differences in hydrobiids. Therefore, we tried to partition the size-dependent and size-independent components of sexual dimorphism in the shell morphology. For that purpose, we performed separate PERMANOVA analyses based on raw and SH-standardized data (“size-free” data analysis, see Methods). Differences between the sexes accounted for as much as 78.2% of differences in shell height ( $p = 0.001$ ) and 50.8% of total differences in 11 conchological variables, measured as distances in the whole morphospace ( $p = 0.001$ ). After decreasing the size effect (allometric standardization), the intersex differences almost disappeared, only explaining 0.62% of the total variance ( $p = 0.369$ ). Thus, the sexes in *C. dadiani* sp. nov. differed not in any linear shell measurements significantly but in the absolute shell size.

**Operculum:** thin, irregularly-ovoid, orange, translucent, paucispiral with a submarginal nucleus. Muscle attachment area well recognizable by rough sculpture and irregular relief in the nucleus area (Figure 13L).

**Soft parts:** whitish or slightly yellowish with well-developed eyes (Figure 13N).

**Holotype measurements:** SH-1.76 mm; SW-1.16 mm; SpH-0.89 mm; BWH-1.40 mm; BWHap-0.52 mm; BWW-0.94 mm; PWH-0.31 mm; PWW-0.74 mm; AH-0.81 mm; AW-0.68 mm.

**Penial morphology:** Penis large, flattened and folded, elongate triangular, gradually tapering towards the end. Its base situated behind the right eye; the proximal part relatively dilated and plicated. Penis with single lateral outgrowth on its left side. Outgrowth hook-shaped with a relatively broad base and thin ending, curved toward the penial base. Size and shape of outgrowth stable and not varying in the population. Distal penial part, in general, triangular, 150–200  $\mu\text{m}$  in length. Tip pointed, its shape varied from quite broad and straight (Figure 13M,N) to more elongated, narrowed, and curved into a delicate hook (Figure 13J,K). Vas deferens straight, running approximately in the center of the penis or slightly closer to its right edge (Figure 19(G1)).

**Radula:** Rhachis with two basal cusps and four cusps on each side of the median cusp. Median cusp slightly longer and broader than the adjacent ones; cusps elongate triangular, rather short and broad. Basal tongue relatively broad. Lateral tooth with five cusps on the outer side of the largest cusp and four on the inner side; all cusps relatively longer and broader than those of rhachidian. The inner marginal tooth with 29 cusps, outer marginal tooth with 24 cusps (Figure 18F).



### 3.9.5. Etymology

The name was derived from the type locality in the Dadiani forest park, which was built around the Dadiani Family residence and named after the House of Dadiani, which was a Georgian family of nobles, dukes, and princes, a ruling dynasty of the Western Georgian province of Samegrelo during 1046–1867.

### 3.9.6. Habitat

Live specimens were found at the spring head, at the border of stygobiotic and crenobiotic habitats as well as in the primary spring sedimentation zone. Likely inhabiting shallow stygobiotic habitats. Springs are draining the stone screes and bedrock fissures among sub-horizontal limestone beds. Some of the small springs are captured as tap water for the nearby houses. Water parameters at the type locality: temperature 13.6 °C, conductivity 308 µS, pH 7.161; at locality 38: temperature 10.9 °C, conductivity 433 µS, pH 7.626; at locality 39: temperature 9.8 °C, conductivity 336 µS, pH 7.891.

### 3.9.7. Distribution

Known from the Turchu Gamosadivari Basin at Pakhe Plateau (South Aaskhi Plateau) and from springs emerging at and under its eastern slope from Zeda Gordi, through Kinchkaperdi along the rivers Okatse and Saskitsvilo. Findings under Toba waterfall draining the Turchu Basin and Pirveli Balda most likely belong to the same species.

### 3.9.8. Conservation Status

The number of known locations is above 10, and the EOO is 40 km<sup>2</sup>. The AOO is represented by only several underground karst conduits with a much smaller total area compared with the EOO. Each spring represents a diminutive area exposed to anthropogenic and environmental events, as human-driven pollution or habitat destruction could lead to rapid species decline or extinction. Therefore, it is assessed as being Vulnerable (VU) D2. The main threats are climatic changes coupled with droughts and floods and excavation works or road extensions with a waste deposit at the localities.

### 3.10. *Colchiella nazodelavo* Chertoprud, Grego & Mumladze, sp. nov.

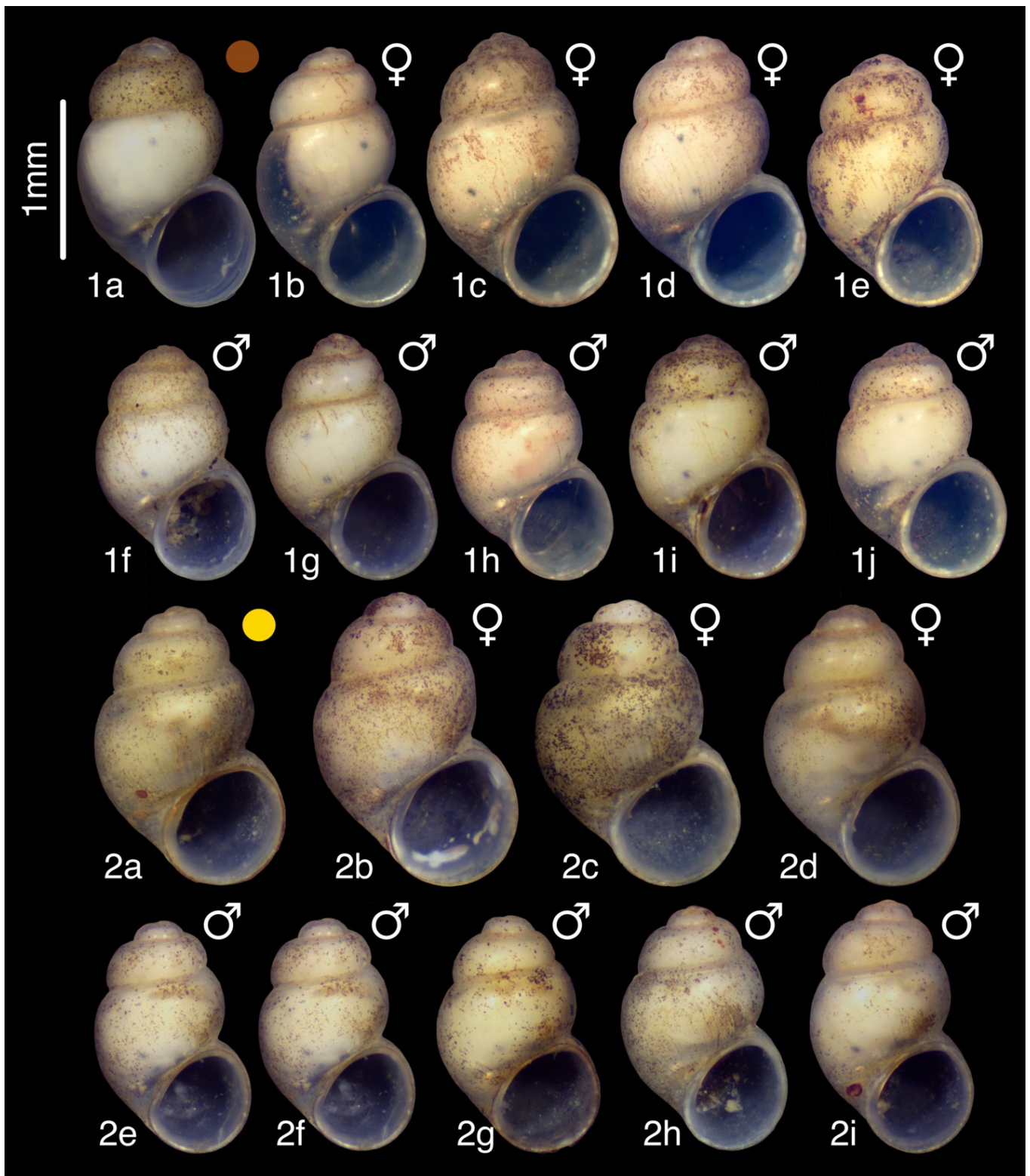
LSIDurn:lsid:zoobank.org:act:1729E817-AEE4-4922-9A0E-B79755897819

Figure 14A–L, Figure 15(4a–4f), Figure 18E.

**Type locality:** GEORGIA • Samegrelo (სამეგრელო), Chkhorotsku (ჩხოროწყუ), Nazodelavo (ნაზოდელავო) cave (Figure 2H); 42.505189° N, 42.220847° E; 275 m alt.

**Type material:** Holotype: (Figure 15(4a)) 1 adult, alcohol specimen from type locality, 11.05.2018, collected by J. Grego, M. Olšovský & L. Mumladze, ISU FM-T028-H. Paratypes: 7 dry shells, same data as for holotype, ISU FM-T028-P1/7; 2 dry shells, same data as for holotype, NHMUK 20220458; 2 dry shells, same data as for holotype, ZMH 141462; 23 dry shells, same data as for holotype, JG F1054.





**Figure 12.** (1a–1j) *Colchiella dadiani* sp. nov. Imereti, Zeda Gordi, spring in Dadiani Forest Park (brown dot): (1a)–holotype; (2a–2i) *Colchiella shiksha* sp. nov. Samegrelo-Zemo Svaneti, Mukhuri, Shiksha spring (yellow dot): (2a)–holotype. The numbers represent the different species, and the letters correspond to individuals. Graphic labels refer to Figure 8 (with LDA graph) and Figure 20 (with the map).

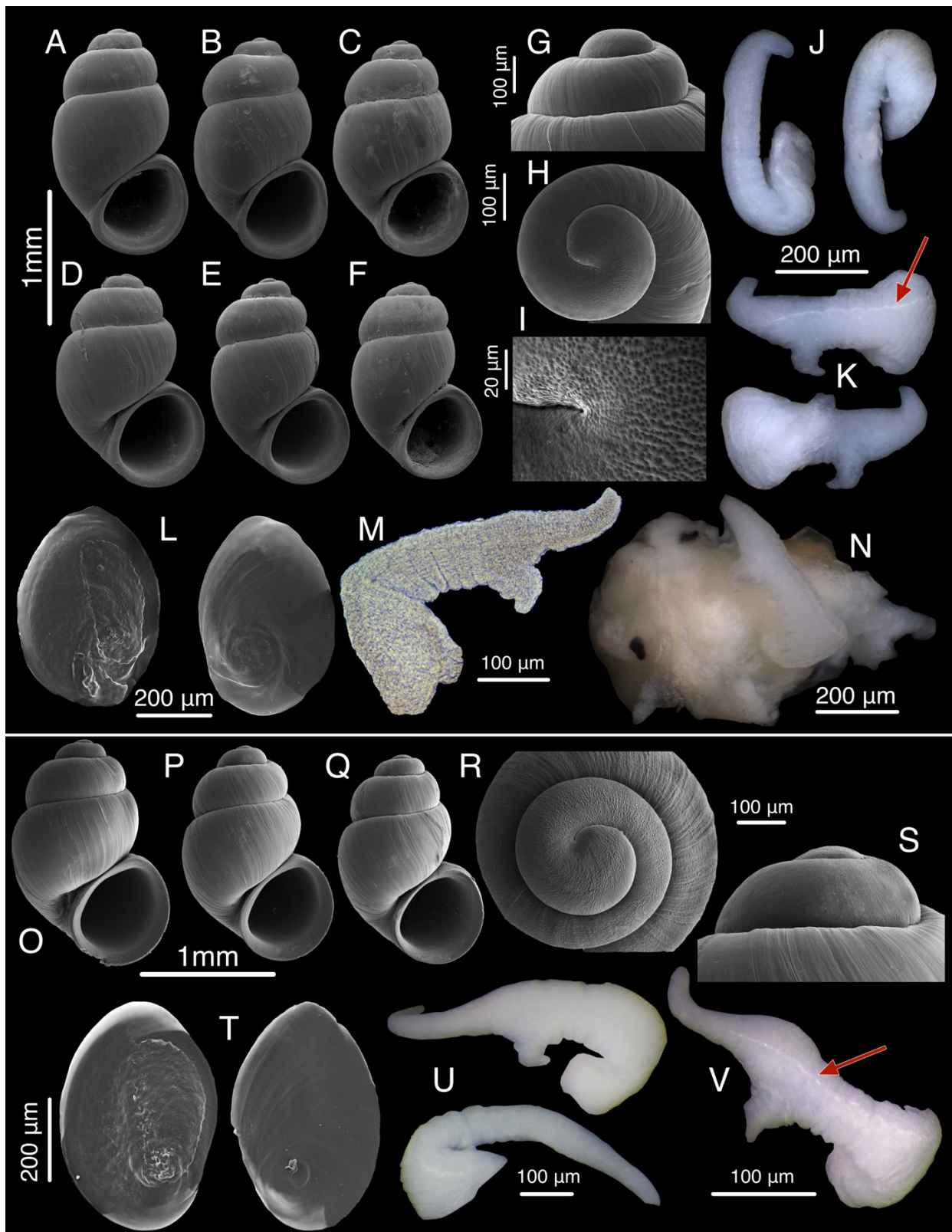


**Figure 13.** *Colchiella dadiani* sp. nov. (A–N) and *Colchiella shiksha* sp. nov. (O–V). (A–C, O–Q)—shell; (G, S)—protoconch, lateral view; (H, R)—protoconch, apical view; (I)—protoconch surface sculpture; (L, T)—operculum; (J, K, M, U, V)—penis habitus; (N)—mollusk head with the penis, dorsal view. Red arrow points to the vas deference inside the penis.



### 3.10.1. Material Examined

GEORGIA • 3♀♀, 4 wet and 43 dry specimens; Samegrelo (სამეგრელო), Chkhorotsku (ჩხოროწყუ), Nazodelavo (ნაზოდელავო) Cave, conglomerates; GEORGIA • 5♂♂, 4♀♀, 1 wet and 1 dry specimen; Samegrelo (სამეგრელო), Kotianeti (კოტიანეთი), Nakhuri (ნახური) stream; 42.322830° N, 42.154000° E; alt. 73 m; 05.08.2019; L. Mumladze; GEORGIA • 6 wet and 43 dry specimens; Samegrelo (სამეგრელო), Cave Onzile (ონზილე) with the spring at the left bank of Chanitskali (ჭანისწყალი) River; 42.529654° N, 42.046006° E; alt. 180 m; 17.09.2022.

### 3.10.2. Other Material

GEORGIA • 3 dry specimens; Samegrelo (სამეგრელო), Chkhorotsku (ჩხოროწყუ), Letsurtsume (ლეთურტუმე) Cave; 42.539228° N, 42.113400° E; alt. 176 m; 10.05.2018; J. Grego, L. Mumladze, M. Olšavský; 42.505189° N, 42.220847° E; alt. 277 m; 11.05.2018; J. Grego, L. Mumladze, M. Olšavský; GEORGIA • 2 dry specimens; Samegrelo (სამეგრელო), Garakha (გარახა), Garakha Cave, conglomerates; 42.177567° N, 42.529869° E; alt. 56 m; 17.09.2021; J. Grego, M. Szekeres; GEORGIA • 8 dry specimens; Samegrelo (სამეგრელო), Nakiani (ნაკიანი), spring near road to Abano (აბანო) Cave; 42.518472° N, 42.202833° E; alt. 216 m; 18.10.2021; J. Grego, M. Szekeres; E. Chertoprud, M. Olšavský; GEORGIA • 2 wet and 6 dry specimens; Samegrelo (სამეგრელო), small cave Hupina with the spring and reservoir; 42.554095° N, 42.036681° E; alt. 232 m; 17.09.2022; E. Chertoprud, J. Grego; GEORGIA • 2 wet and 4 dry specimens; Chkvaleri, Kvatskalara spring; 42.721250° N, 42.091639° E; alt. 383 m; 19.10.2021; J. Grego, M. Szekeres; • 6 wet and 43 dry specimens; same data as for preceding; 17.09.2022; J. Grego, E. Chertoprud.

### 3.10.3. Diagnosis

The shell of the new species is the smallest one within the genus (SH is 1.45 mm on average), with the smallest number of whorls (whorl number varies from 3.1 to 3.8). The new species also differs by its longer penis with a narrower and curved terminal part. COI sequences: OQ396608-OQ396612; H3 sequences: OQ401658-OQ401662x. MDCs for *C. nazodelavo* in comparison with other *Colchiella* species: COI: 225: A; 240: C.

### 3.10.4. Description

**Shell:** SH 1.34–1.6 mm high, ovoid, relatively broad (SW/SH ratio 0.6–0.7 mm), whitish and translucent, with a small number (up to 3.8) of inflated whorls separated by a relatively deep suture (Figure 14A–C). Body whorl quite high (about 0.8 of SH) and inflated. Spire moderately high, on average equaling 0.51 of the shell height. Aperture irregularly tear-shaped, inner lip separated from the body's whorl wall by a barely noticeable slit. Umbilicus slit-like or even absent. Lateral profile of the labral margin almost straight. Protoconch moderately broad (up to 300 µm in diameter), low dome-shaped, on average consisting of 1.2 whorls (Figure 14G–J). Sculpture pitted. Protoconch border indistinct.

**Operculum:** thin, irregularly-ovoid, orange, translucent, paucispiral with a submarginal nucleus. Inner surface with a recognizable muscle attachment area with a rough, irregular sculpture (Figure 14K).

**Soft parts:** white with well-developed eyes (Figure 14L).

**Holotype measurements:** SH-1.57 mm; SW-0.99 mm; SpH-0.83 mm; BWH-1.26 mm; BWHap-0.52 mm; BW-0.85 mm; PWH-0.29 mm; PWW-0.68 mm; AH-0.71 mm; AW-0.56 mm.

**Penial morphology:** Penis large, flattened, and folded, quite broad and plicated in proximal and medial parts, with a single lateral outgrowth on its left side (Figure 14D–F). Outgrowth moderately short, broad, blunt, or slightly tapered and always directed forward. Terminal part of the penis quite long, 200–250 µm in length, gradually tapering towards its end, usually with one or two gentle curves. Penial tip thin and pointed. Vas deferens straight, running approximately in the center of the penis or slightly closer to its right edge.

**Radula:** Rachis with two acute basal cusps and four cusps on each side of the median cusp. Median cusp only longer than adjacent ones, cusps relatively long and narrow, their length becomes shorter towards the edges. The basal tongue has a relatively acute angle. Lateral tooth bears five cusps on the outer side of the largest cusp and three on the inner side. The inner marginal tooth with 23 cusps, outer marginal tooth with 21 cusps (Figure 18E).

### 3.10.5. Etymology

Named after the type locality: the conglomerate cave Nazodelavo near Chkhorotsku city.

### 3.10.6. Habitat

Stygophilic species. Species inhabits permanent cave streams, mostly under stones and on sandy bottoms, occasionally found washed out in the spring head. The species is sympatric in some localities to *Caucasopsis letsurtsume* Grego and Mumladze, 2020, and *Pontohoratia vinarskii* Grego and Mumladze, 2020. Occasionally found in the permanent surface springs. Water parameters at the type locality during the sampling: temperature 15 °C, conductivity 275 µS, pH 7.408.

### 3.10.7. Distribution

Western South Caucasus: confirmed from the Nakhuri stream in Kotianeti and from the type locality in Nazodelavo Cave, but empty shells indicate its presence in the neighboring conglomerate caves such as Letsurtsume, Garakha, and Abano Caves, with several small spring outlets in Nakiani and Kotianteti. Most likely, the species inhabits the whole conglomerate karst region around Chkhorotsku.

### 3.10.8. Conservation Status

The number of known locations is five, and they are spread over an EOO of about 80 km<sup>2</sup>. The AOO is represented by only several underground karst conduits and springs in vulnerable shallow limestone conglomerates, with a much smaller total area compared with the EOO. Each shallow karst conduit is supplied by direct surface water through swallow holes, where stochastic events, such as anthropogenic pollution or habitat destruction, could lead to rapid species decline or extinction. Therefore, it is assessed as being Vulnerable (VU) D2. The main threats are climatic changes coupled with droughts and floods with surface and underground water pollution.

### 3.11. *Colchiella shiksha* Chertoprud, Grego & Mumladze, sp. nov.

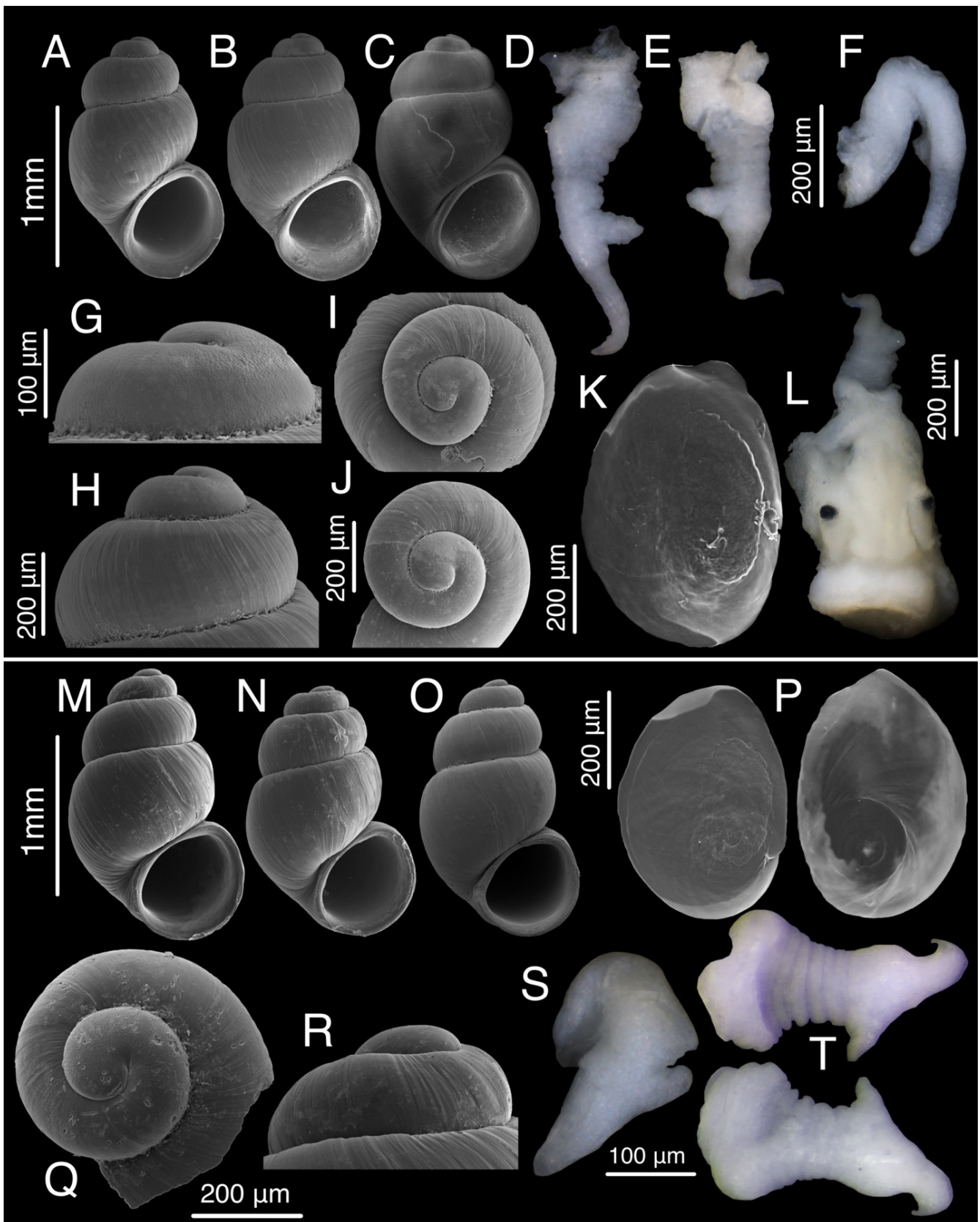
LSIDurn:lsid:zoobank.org:act:BE784866-0790-43FE-9D28-725096B2CB51

Figure 12(2a–2i), Figure 13O–V, Figure 18H, Figure 19(F1,F2).

**Type locality:** GEORGIA • Samegrelo-ZemoSvaneti (სამეგრელო-ზემო სვანეთი) Region, Mukhuri (მუხური), Shiksha (შიქშა) spring (Figure 2F); 42.629884° N, 42.190516° E; 255 m alt.

**Type material:** Holotype (Figure 12(2a)) 1 adult, alcohol specimen from type locality, 16.09.2022, collected by E. Chertoprud & J. Grego, ISU FM-T026-H. Paratypes: 33 dry shells from type locality, 10.05.2018, collected by J. Grego, M. Olšovský & L. Mumladze, ISU FM-T026-P1/33; 26 dry shells from type locality, same data as for preceding, JGS; 430 wet and 430 dry shells, same data as for preceding, 12.10.2019, collected by J. Grego, L.





**Figure 14.** *Colchiella nazodelavo* sp. nov (A–L) and *Colchiella lugella* sp. nov. (M–T). (A–C, M–O)—shell; (G, H, R)—protoconch, lateral view; (I, J, Q)—protoconch, apical view; (K, P)—operculum; (D, E, F, S, T)—penis habitus; (L)—mollusk head with the penis, frontal view.

Mumladze and G. Bananashvili, ISU FM-T026-P2/827; 827 wet specimens, same data as for preceding, JG F1421; 508 wet specimen, same data as for preceding, 10.05.2018, collected by J. Grego, L. Mumladze and M. Olšavský, ISU FM-T026-P3/10; 10 wet specimens, same data as for holotype, NHMW-MO-113734; 10 wet specimens, same data as for holotype, NMBE 577010; 10 wet specimens, same data as for holotype, MNHN-IM-2012-25410; 10 wet specimens, same data as for holotype, NHMUK 20220459; 10 wet specimens, same data as for holotype, UF-580904; 10 wet specimens, same data as for holotype, ZMH 141463; 10 wet specimens, same data as for holotype, ANSP 493828; 194 dry 390 wet specimens, same data as for preceding, JG F1043.

### 3.11.1. Diagnosis

The new species is closer to *C. dadiani* sp. nov. in external and internal morphology and differs from other representatives of the genus (*C. lugella* sp. nov., *C. nazodelavo* sp. nov.) by its higher and rather large shell. The penis presents an intermediate form between *C. dadiani* sp. nov. and *C. nazodelavo* sp. nov. The lateral outgrowth with a hook-like shape, almost similar to that in *C. dadiani* sp. nov., whereas the distal part is rather thinner, elongated, and slightly curved, as that in *C. nazodelavo* sp. nov. Also, the new species differs from *C. dadiani* sp. nov. in the presence of an extension of the right edge of the penis located opposite the left lateral outgrowth. The new species is characterized by the presence of a distinct muscular densification of the tissues of the lateral penial outgrowth, structurally similar to the penial gland and similar to that in *Aetis* gen. nov. and *Sataplia* gen. nov. COI sequences OQ396606-OQ396607; H3 sequences: OQ401656-OQ401657.

### 3.11.2. Description

**Shell:** relatively large for genus (SH 1.71 mm on average), shape varied from elongate-ovoid to almost ovoid or barrel-shaped (Figure 13O–Q). Whorls rounded and moderately convex, separated by deep suture, whorl number 3.37–4.2. Umbilicus slit-like. Shell surface smooth or with irregular growth lines, relatively hard-walled, whitish or yellowish, translucent. Shell relatively broad, SW 1.16 mm on average, SW/SH ratio about 0.68. Spire height equaling 0.48–0.56 of SH. Body whorl high and moderately inflated. Aperture broad-ovoid, quite expanded, and parietal margin tightly adjoined to body's whorl wall or separated by a barely noticeable slit. Protoconch relatively large, dome-like, with an indistinguishable border. Protoconch surface covered by a dense net of minute pits (Figure 3R).

**Sexual dimorphism:** There is a pronounced sexual dimorphism in the shell size of *Colchiella shiksha* sp. nov. (Figure 12(2a–2i)). Males were on average smaller than females (shell height:  $1.56 \pm 0.06$  and  $1.82 \pm 0.08$  mm, width:  $1.08 \pm 0.05$  and  $1.21 \pm 0.08$  mm for males and females, respectively); they also have fewer whorls ( $3.54 \pm 0.08$  against  $3.86 \pm 0.12$  for females). These differences were highly significant (Mann–Whitney test for equal SH medians,  $p < 0.0001$ ). All other conchological parameters were highly and significantly correlated with SH (all Pearson's  $r > 0.77$ ; all  $p$ -values  $< 0.00001$ ), indicating the strong size dependency. The PERMANOVA analyses showed that differences between the sexes accounted for as much as 86.7% of shell height variability ( $p = 0.001$ ). After removing the effect of size (allometric standardization, SH excluded from analysis as reference size measurement), the intersex differences almost disappeared, explaining 1.4% of variations only ( $p = 0.706$ ). Thus, the sexual dimorphism of *C. dadiani* sp. nov., as with *C. dadiani* sp. nov., appeared as differences in absolute size but not in shell forms and proportions.

**Operculum:** thin, irregularly-ovoid, orange, translucent, paucispiral with a submarginal nucleus. Outer surface flat with axial growth lines (Figure 13T).

**Soft parts:** whitish or slightly yellowish. Eyes well-developed.

**Holotype measurements:** SH-1.82 mm; SW-1.25 mm; SpH-0.93 mm; BWH-1.44 mm; BWHap-0.56 mm; BW-1.05 mm; PWH-0.31 mm; PWW-0.75 mm; AH-0.83 mm; AW-0.68 mm.

**Penial morphology:** Penis large, flattened and folded, elongated, plicated in proximal and medial parts. Penis with single lateral outgrowth on its left side. Outgrowth medium

in size, hook-shaped with a relatively broad base and a relatively thin ending, which is curved toward the penial base. Size and shape of outgrowth slightly varied in degree of tip backward-curvature: from being slightly directed towards the penial base to bent at a right angle (Figure 13U,V). Outgrowth containing a small gland discharging through the outgrowth tip (Figure 19(F1,F2)). General penial shape with several extensions along its length: an expanded proximal part, slightly thinner medial part, outgrowth usually expanded, thin, and with a curved distal part. The distal part of the penis rather long, 150–200  $\mu\text{m}$  in length, gradually tapering towards its end, usually with one gentle upward curve. Penial tip rather thin and pointed. Vas deferens straight, running approximately in the center of the penis or slightly closer to its right edge.

**Radula:** Rhachis with two basal cusps and four or five cusps on each side of the median cusp. Median cusp slightly longer and broader than the adjacent ones, cusps elongate triangular, rather short and broad. Basal tongue quite broad. Lateral tooth with five cusps on the outer side of the largest cusp and four on the inner side, all cusps relatively longer and broader than the rhachidian one (Figure 18H).

### 3.11.3. Etymology

The name is derived from the type locality: Shiksha spring near the Mukhuri village.

### 3.11.4. Habitat

The type locality is a karst spring lake connected to a deep, submerged spring cave, about 80 m long and 20 m deep. The water is emerging from Cretaceous shaly limestones, which cause a faint permanent opalescence in the water. The new species inhabits the whole spring zone and the adjacent creek emerging from the spring and can be found under stones in the creek bed. The water parameters in the type locality are 13.7 °C, pH 7.683, and conductivity 325  $\mu\text{S}$ .

### 3.11.5. Distribution

Known only from the type locality.

### 3.11.6. Conservation Status

The species is known from the single locality. The surrounding area is relatively well-investigated for spring snail fauna, and the absence of this species could be considered a sign of its localized distribution. The main threats are climatic changes coupled with droughts and the excavation works in the locality. The AOO might not exceed 20  $\text{km}^2$ , and the species is restricted to a single spring system. Thus, the status of the species should be considered as being Vulnerable (VU) D2.

### 3.11.7. Remarks

The function of the small bulb-shaped gland we observed in the left lateral outgrowth of the penis is uncertain and, therefore, cannot be terminologically specified. According to Hershler and Ponder [29], this structure could be referred to as “glandular papilla”, but others refer to this structure in Truncatelloidea quite differently [76–79]. Having no data on the fine histological structure at our disposal, we did not attribute a special name to it and designated it as a “gland”. Clarification of the structure and functional purpose of this gland is the subject of further studies.



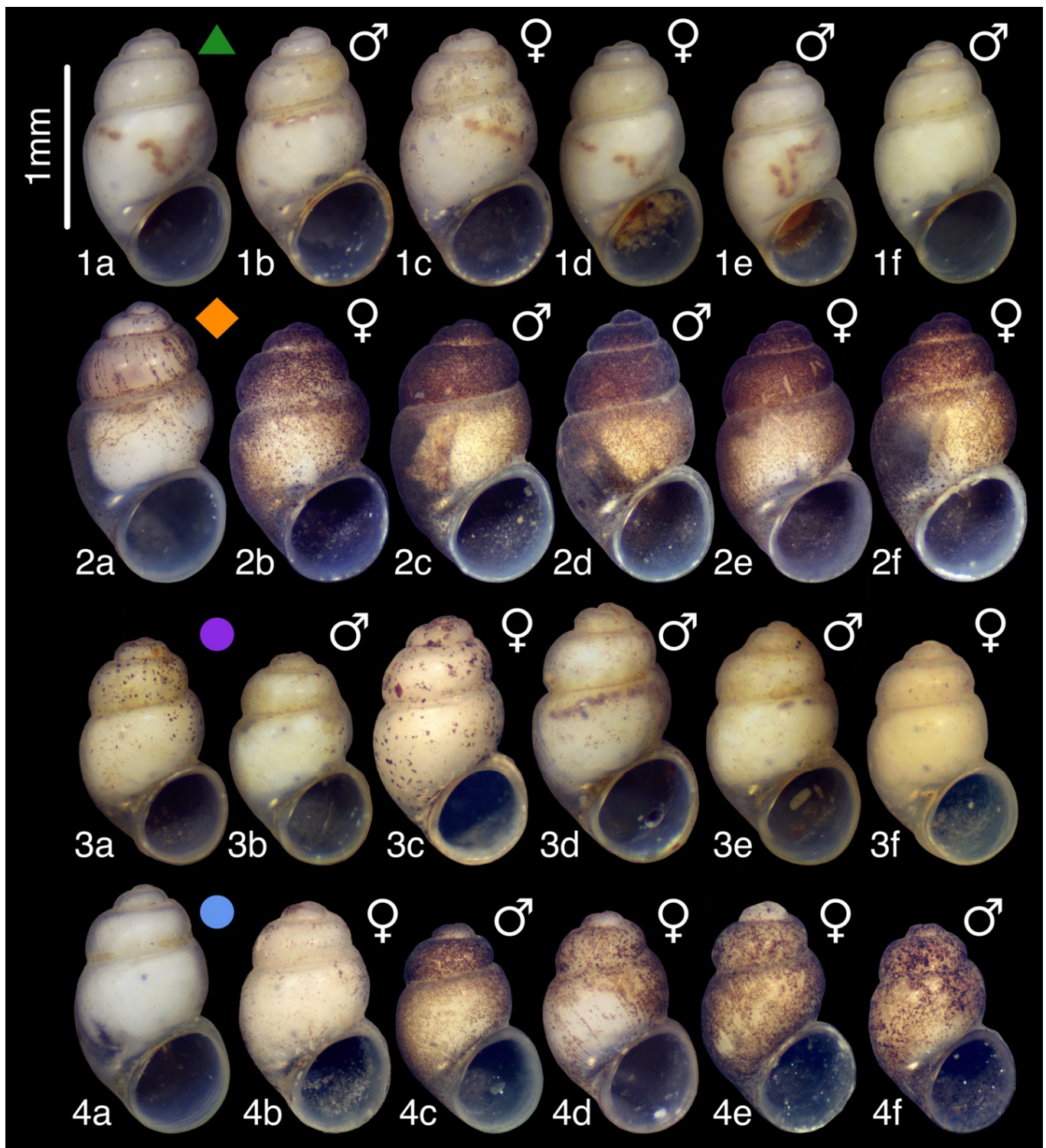


**Figure 15.** (1a–1f) *Aetis starobogotovi* sp. nov. Imereti, Zemaogha, Berdnis Tskaro spring (green triangle): (1a)–holotype; (2a–2f) *Sataplia cavernicola* sp. nov. Imereti, Banoja, Sataplia Cave (orange diamond): (2a)–holotype; (3a–3f) *Colchiella lugella* sp. nov. Samegrelo-Zemo Svaneti, Mukhuri, Lugella spring (purple dot): (3a)–holotype; (4a–4f) *Colchiella nazodelavo* sp. nov. Samegrelo, Chkhorotsku, Nazodelavo Cave (blue dot): (4a)–holotype. The numbers represent the different species, and the letters correspond to individuals. Graphic labels refer to Figure 8 (with LDA graph) and Figure 20 (with the map).



### 3.12. *Colchiella lugella* Chertoprud, Grego & Mumladze, sp. nov.

LSIDurn:lsid:zoobank.org:act:31A039DA-36BC-470B-ACBF-1CFD1CF1BD34

Figure 14M–T, Figure 15(3a–3f), Figure 18G, Figure 19(H1).

**Type locality:** GEORGIA • Samegrelo-ZemoSvaneti (სამეგრელო-ზემო სვანეთი) Region, Mukhuri (მუხური), spring at the right side of Khobistskali (ხობისწყალი) River near the magnesia mineral spring Lugella (ლუგელა) (Figure 2G); 42.654758° N, 42.224125° E; 350 m alt.

**Type material:** Holotype: (Figure 15(3a)) 1 adult, alcohol specimen from type locality, 16.09.2022, collected by E. Chertoprud and J. Grego, ISU FM-T027-H. Paratypes: 1 adult♀, alcohol specimen from type locality, 13.08.2017, collected by J. Grego, ISU FM-T027-P1/1; 3 alcohol specimens, same data as for holotype, ISU FM-T027-P2/3; 18 dry specimens, same data as for holotype, JG F2183; 10 wet specimens, same data as for holotype, ZMH 141464; 30 wet specimens, same data as for preceding, 10.05.2018, collected by J. Grego, L. Mumadze and M. Olšavský, ISU FM-T027-P3/1200; 1200 wet specimens, same data as for preceding, 16.09.2022, collected by J. Grego, and E. Chertoprud, ISU FM-T027-P4/1100; 1100 wet and 10 dry specimens, same data as for preceding, JG F2183; 10 wet specimens, same data as for preceding, NHMW-MO-113735; 10 wet specimens, same data as for preceding NMBE 577011; 10 wet specimens, same data as for preceding, MNHN-IM-2012-25409; 10 wet specimens, same data as for preceding, NHMUK 20220460; 10 wet specimens, same data as for preceding UF-580905; 10 wet specimens, same data as for preceding, ANSP 493829.

#### 3.12.1. Diagnosis

The new species is intermediate in its shell size within the genus (Figure 8). As an example, the height is lower than that of *C. dadiani* sp. nov. but higher than that of *C. nazodelavo* sp. nov. Also, the shell of *C. lugella* sp. nov. has the most convex and rounded whorls in the genus. Another difference is the penial structure. The penis is the shortest among close members of the genus, as well as other Belgrandiellinae genera known from the region. The lateral outgrowth differs in shape and orientation from that of *C. dadiani* sp. nov. and *C. shiksha* sp. nov. The distal part of the penis is shorter and broader, with a rather curved tip. COI COI MG543150-51; H3 sequences: MG543153-54 [25]. MDCs for *C. lugella* in comparison with other *Colchiella* species: COI: 111: G; 137: A; 180: A; 219: C; 225: T; 252: A; 306: A; 345: C; H3: 30: T, 129: C.

#### 3.12.2. Description

**Shell:** minute (SH 1.59 mm on average), elongate-ovoid, thin-walled, fragile, whitish and transparent (Figures 14M–O, 15(4a–4f)). Whorl number up to 4.1. Whorls rounded and moderately convex, separated by a deep suture. Shell quite wide, SW/SH ratio between 0.60 and 0.68. Spire height constitutes 0.50–0.59 of SH. Aperture shape triangular-ovoid, slightly expanded, narrowed in its upper part and separated from the body whorl by a barely noticeable slit. Umbilicus very narrow, slit-like, or absent. Protoconch low-domed, pitted with an indistinct border (Figure 14Q,R).

**Operculum:** flat, thin, orange or yellowish, translucent, ovoid, and paucispiral with a submarginal nucleus. Outer surface flat with axial growth lines. Muscle attachment area edges are clearly differentiated. Nucleus area with rough, slightly tuberos reliefs (Figure 14P).

**Soft parts:** milky white with well-developed eyes.

**Holotype measurements:** SH-1.44 mm; SW-0.94 mm; SpH-0.78 mm; BWH-1.11 mm; BWHap-0.46 mm; BWW-0.79 mm; PWH-0.30 mm; PWW-0.63 mm; AH-0.65 mm; AW-0.54 mm.

**Penial morphology:** Penis smallest in the genus (about 500 µm in length), flattened and folded, quite broad, elongate-triangular, slowly tapering towards its end, with single lateral outgrowth on its left side. Its base situated behind the right eye; proximal part relatively dilated, medial part plicated. Lateral outgrowth medium in size, with the shape of

a short cylindrical protrusion with a blunt or quite pointed end (Figure 14S,T). Penis often with bulbous dilation opposite to the left lateral outgrowth. Distal part elongate-triangular, gradually tapering towards its end and quite short as for the genus, 150 µm on average. Penial tip relatively broad with a slightly curved up-pointed ending (Figures 14T, 19(H1)). Vas deferens slightly convoluted in its proximal and medial parts, straight distally, running approximately in the center of the penis or slightly closer to its right edge, terminating at the left edge of the terminal penial lobe, not reaching the tip (Figure 19(H1)).

**Radula:** Rhachis with two basal cusps and four cusps on each side of the median cusp. Median cusp only longer than adjacent ones, cusps relatively long and narrow, triangular in shape, their length becoming shorter towards the edges. Lateral tooth with four cusps on the outer side of the largest one and three on the inner side: all cusps slightly broader than those of the rhachis. Inner marginal tooth with 28 cusps, outer marginal tooth with 22 cusps (Figure 18G).

### 3.12.3. Etymology

Named after the type locality: near the Lugella Spring at the bank of the Khobistskali River.

### 3.12.4. Habitat

Crenobiotic species. Inhabits a small water stream from the spring head down to its junction with the Khobistskhali River. Live specimens are found at the sandy bottom, under small stones and dead leaves in the stream.

### 3.12.5. Distribution

The species is known from only the type locality at the middle part of the Khobistskali River. The single known locality is situated very close to the Khobistskali River, and it could probably be transported and distributed to a few other small springs along the whole Khobistskhali Valley.

### 3.12.6. Conservation Status

The number of known locations (1) is no more than five, and the EOO is smaller than 20 km<sup>2</sup>. There is no reason to suppose that the AOO, EOO, the number of locations, the number of subpopulations, or the number of mature individuals is declining; however, due to its extremely small EOO, we assessed it as being Vulnerable (VU) D2. The main threat is the locality destruction caused by climate change, induced high floods of the Khobistskhali River, and anthropogenic pollution by visitors of the local famous magnesia spring.

## 3.13. Genus *Sataplia* Chertoprud, Grego & Mumladze, gen. nov.

LSIDurn:lsid:zoobank.org:act:263F3855-8DBB-4028-8632-F653DBA7F3F7

**Type species.** *Sataplia cavernicola* Chertoprud, Grego & Mumladze, sp. nov.

### 3.13.1. Diagnosis

The new genus differs from all the other creno- and stygobiotic Hydrobiidae by its specific penial structure. The penis contains a large, translucent, muscularized cylindrical gland extending from the penial base and running along its left side for most of its length, opening as a small cylindrical protrusion on the left edge of the penis. The vas deferens runs along the right edge of the penis and goes to the lobe-shaped distal part. *S. cavernicola* sp. nov. is morphologically the closest to *Aetis starobogatovi* sp. nov. but differs in the shape of the distal end of the penis. The terminal part of the penial gland almost does not form a pronounced lobe and only slightly protrudes beyond the contour of the penis. Taenioglossate radula also differs in rhachidian structure and size: rachis bears five cusps on each side of the median cusp; the basal tongue is quite broad and V-shaped, with one pair of basal cusps. The animal is whitish with well-developed eyes. COI sequences OQ396631-OQ396632; H3 sequences: OQ401681-OQ401682. MDCs for *Sataplia* in compar-

ison with other Georgian genera: COI: 231: G; 363: G; 384: G; 393: G; 396: C; 399: G; 408: C; 417: G; H3: 255: T.

### 3.13.2. Etymology

Named after the type locality inside of the Sataplia Cave (სათაფლიის მღვიმე). The word “tapli” (თაფლი) in Georgian means “honey”, and the name of the mountain and the cave within it is called “Sataplia” – “the place where there is honey.” Previously, wild bees were numerous in this place and made their hives in the crevices of limestone rocks.

Species composition. A monotypic genus.

**Distribution.** Endemic to western Georgia. Known only from the type locality.

### 3.14. *Sataplia cavernicola* Chertoprud, Grego & Mumladze, sp. nov.

LSIDurn:lsid:zoobank.org:act:B3CD32D0-41C2-4E24-8F96-5459B50BFFA4

Figure 15(2a–2f), Figure 16, Figure 18A, Figure 19(A1,A2).

**Type locality:** GEORGIA • Imereti (იმერეთი), Banoja (ბანოჯა), Sataplia (სათაფლია) Cave (Figure 2A); 42.311641° N, 42.675151° E; 438 m alt.

**Type material:** Holotype: (Figure 15(2a)) 1 adult, alcohol specimen from type locality, 01.05.2018, collected by J. Grego, M. Olšovský & L. Mumladze, ISU FM-T030-H. Paratypes: 10 wet and 4 dry shells, same data as for holotype, ISU FM-T030-P1/10; 30 dry shells, same data as for holotype, JG F0972-76; 11 wet shells, same data as for holotype, 23.03.2014, collected by L. Mumladze, ISU FM-T030-P2/11; 2 dry shells, same data as for holotype, ZMH 141465.

### 3.14.1. Description

**Shell:** small, 1.6–1.79 mm high, elongate-ovoid in shape, relatively broad (SW/SH ratio 0.58–0.66) with four slightly inflated whorls (Figures 15(2a–2f), 16A–C). Body whorl high (about 0.74 of SH), moderately inflated. Height of spire equaling about half of shell height (ratio 0.53–0.61). Aperture triangular-ovoid, slightly expanded and separated from the body whorl by a barely noticeable slit. Lateral profile of labral margin almost straight. Umbilicus slit-like or even absent. Protoconch broad (350 µm in diameter), low domed-shaped, on average consisting of 1.25 whorls (Figure 16E,F). Sculpture pitted. Border between embryonic shell and teleoconch not well defined.

**Operculum:** irregularly-ovoid, repeats shape of the peristome, relatively thin, flat, paucispiral with submarginal nucleus, generally orange. Outer surface flat with axial growth lines (Figure 16D).

**Soft parts:** whitish with well-developed eyes.

**Holotype measurements:** SH-1.79 mm; SW-0.93 mm; SpH-1.01 mm; BWH-1.35 mm; BWHap-0.59 mm; BW-0.92 mm; PWH-0.35 mm; PWW-0.75 mm; AH-0.77 mm; AW-0.60 mm.

**Penial morphology:** Penis elongate, flattened and straight, slightly tapering towards the end. Proximal part slightly dilated. Penis contains a gland that is clearly visible from the outside, having the form of a muscularized, dense, thick, opalescent, cylindrical rod extending from the penial base and ending with an excretory opening on the left edge of the penis. Terminal part of gland protrudes from the left distal penial edge in the form of a small wide-conical protrusion (Figure 19(A2)). Distal part of penis large, about 100–200 µm long and 50–100 µm broad, lobe-shaped, slightly curved to the right from the opening of the penial gland (Figure 16(G1,G2)). The terminal lobe has a thin, curved, delicate tip (Figure 16H). Vas deferens runs along the right edge of the penis, curved in proximal and medial parts and continues into the lobe-shaped distal part, opens at the left edge of the terminal penial lobe, not reaching the curved tip (Figure 19(A1)).

**Radula:** Two basal cusps on each side of the rhachis and five cusps on each side of the median cusp of the rhachis. Median cusp only slightly longer than adjacent ones. Rhachidian tooth broad; the angle of the V-shaped basal tongue is 90° on average. On the lateral tooth, there are three to five cusps on each side of largest cusp (four or five on the outer side,

three on the inner side), all cusps long and narrow as those of the rachis. Inner marginal tooth with 28 cusps, outer marginal tooth with 21 cusps (Figure 18A).

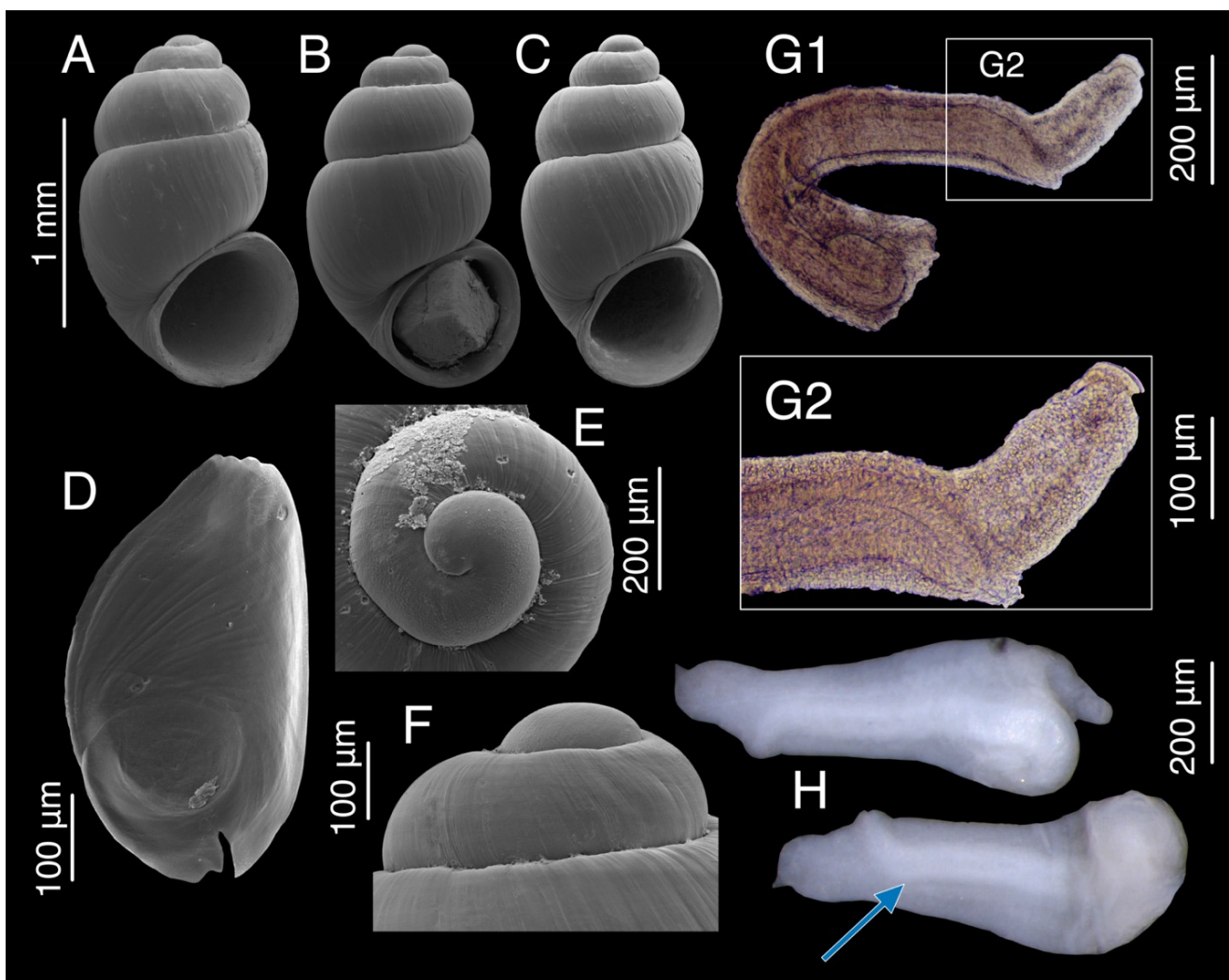


**Figure 16.** *Sataplia cavernicola* sp. nov. (A–C)—shell; (D)—operculum; (E)—protoconch, apical view; (F)—protoconch, lateral view; (G,H)—penis structure: (G1)—penis, general view, (G2)—distal part of the penis, detailed view. Blue arrow points to the penial gland (dorsal and ventral view).

#### 3.14.2. Etymology

The name *cavernicola* (lat.) means “dwelling in cave”, which characterizes the stygophilic preferences of the mollusk, which is not characteristic of other closely related genera that prefer to inhabit surface outlets of groundwater.

#### 3.14.3. Habitat

Stygophilic species. It can be found in all parts of the Sataplia cave where a small permanent water stream is present, namely: (a) a vertical well in the middle of the cave emerging water at its bottom; (b) a cave stream at the end of the cave; (c) several water outlets along the cave stream.

#### 3.14.4. Distribution

The species is found only in its type locality in the Sataplia cave in Banoja village north of Kutaisi. However, similar empty shells are found in a small stream and well in the middle of close Banoja Village, and their relation to the cave species cannot be confirmed so far.



### 3.14.5. Conservation Status

So far, the species is known only from its type locality; the EOO is smaller than 20 km<sup>2</sup>. There is no reason to suppose that the AOO, EOO, the number of locations, the number of subpopulations, or the number of mature individuals is declining. However, due to its extremely small EOO and the fact that Sataplia cave and all of its surrounding habitats are under continuous anthropogenic pressure, we cannot exclude unintended negative impacts on the population. The localities inside the public caves are well protected by the cave directorate and the regulated visitor entrances, although the habitat is subject to high visitor pressure and is regularly disturbed by maintenance works on the cave infrastructure. We assessed the species as being Vulnerable (VU) D2.

### 3.15. Genus *Aetis* Chertoprud, Grego & Mumladze, gen. nov.

LSIDurn:lsid:zoobank.org:act:EE474F38-7C58-447B-B978-AA15E2D7FB61

**Type species:** *Aetis starobogatovi* Chertoprud, Grego & Mumladze, sp. nov.

#### 3.15.1. Diagnosis

The new genus has a shell shape similar to members of the genus *Tschernomorica*, widely distributed in the northern Black Sea region, as well as to *Colchiella* gen. nov. and *Sataplia* gen. nov. representatives, and is actually indistinguishable by the shell. Nonetheless, *Aetis* gen. nov. can be clearly distinguished by the specific structure of its penis, which has a forked distal part (Figure 17I–N). The penial tip is divided into two lobes: the right includes the vas deferens, and the left is a protrusion of the terminal part of the penial gland forming a distinct lobe. The gland is long, clear, opalescent, and covered with a thick layer of muscles. COI sequences: OQ396620–OQ396630; H3 sequences: OQ401670–OQ401680. MDCs for *Aetis* in comparison with other Georgian genera: COI: 90: T; 123: C; 148: C; 156: C; 186: C; 201: G; 396: G; 423: G; 429: T; 432: G; H3: 27: C; 39: T; 231: G.

#### 3.15.2. Etymology

Named after Aeeta (Αἰήτης)—the ancient king of Ea country, which was later identified with Colchis, son of the Sun God Helios and the Oceanid Perseis (in accordance with Ancient Greek mythology).

**Species composition.** Up to date, a monotypic genus.

#### 3.15.3. Distribution

Known from a few localities in eastern Guria and south Imereti around the villages of Vakijvari, Kvabgha, Chkhakoura, and Kvemo Nogha and in the Mitralla N.P. in the Lesser Caucasus.

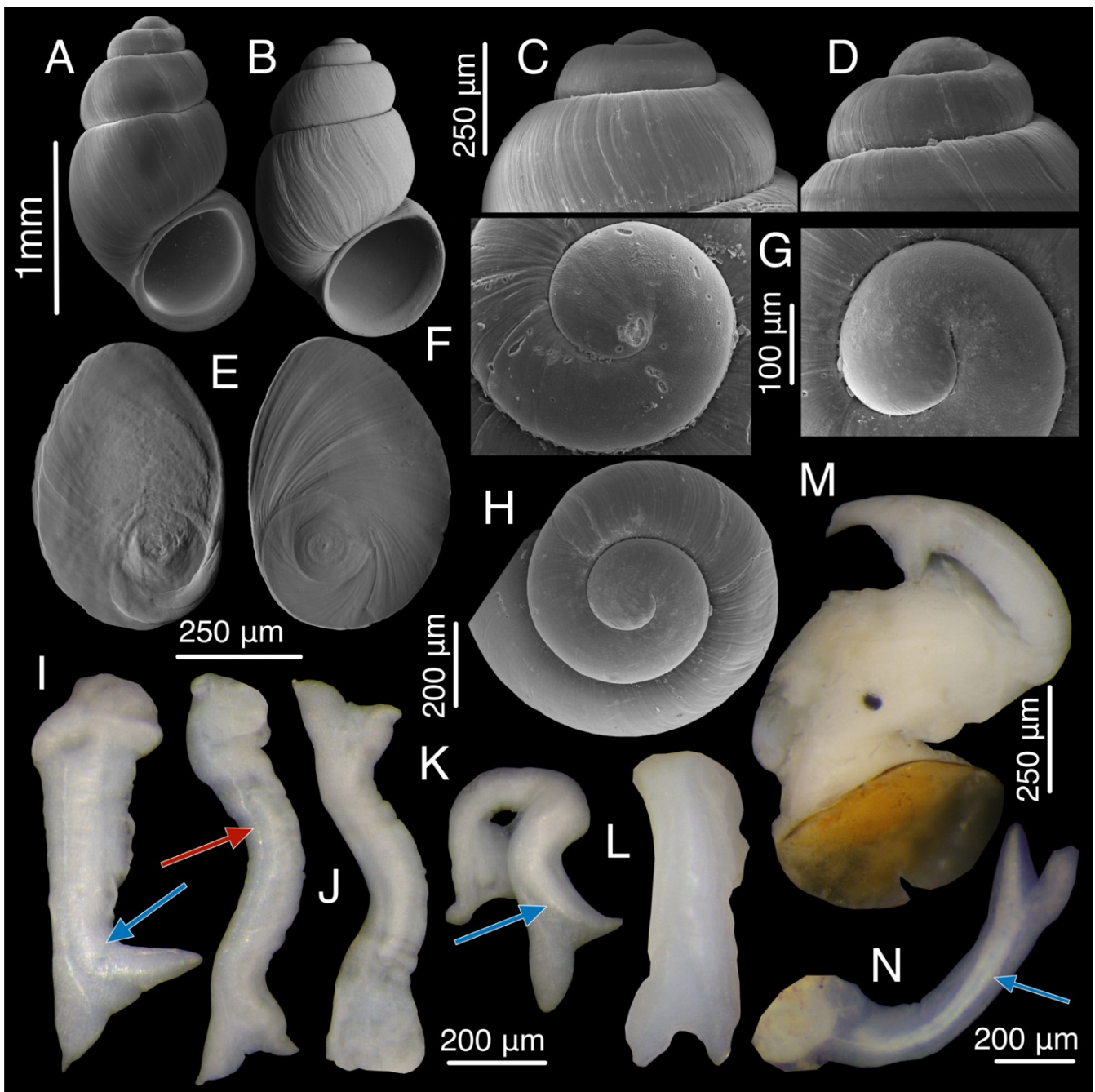


**Figure 17.** *Aetis starobogatovi* sp. nov. (A,B)—shell; (C,D)—protoconch, lateral view; (E)—operculum; (F–H)—protoconch, apical view; (I–L,N)—penis habitus; (M)—mollusk head with the penis, lateral view. Red arrow points to the vas deference visible within the penis. Blue arrow points to the penial gland.

3.16. *Aetis starobogatovi* Chertoprud, Grego & Mumladze, sp. nov.

LSIDurn:lsid:zoobank.org:act:DB4ED2C2-3149-4C69-9DC6-9470F408C38

Figure 15(1a–1f), Figure 17, Figure 18B, Figure 19(B1,C1–C3).

**Type locality:** GEORGIA • Imereti (იმერეთი), Zemo Nogha (ზემო ნოღა) vicinities, Berdinis Tskaro (ბერდინის წყარო) spring (Figure 2C); 42.063539° N, 42.269351° E; 60 m alt.

**Type material:** Holotype (Figure 15(1a)) 1 adult, alcohol specimen from type locality, 14.09.2022, collected by J. Grego & E. Chertoprud, ISU FM-T029-H. Paratypes 2 adults♂, al-

cohol specimen, same data as for holotype, ISU FM-T029-P1/1, ISU FM-T029-P2/1; 2 adults♀, alcohol specimen, same data as for holotype, ISU FM-T029-P3/1, ISU FM-T029-P4/1; 4 alcohol specimens, same data as for holotype, ISU FM-T029-P5/4; 2 dry specimens, same data as for holotype, NHMW-MO-113736; 2 dry specimens, same data as for holotype, NMBE 577012; 2 dry specimens, same data as for holotype, MNHN-IM-2012-25408; 2 dry specimens, same data as for holotype, NHMUK 20220462; 2 dry specimens, same data as for holotype, UF-580906; 2 dry specimens, same data as for holotype, ZMH 141466; 2 dry specimens, same data as for holotype, ANSP 493830; 22 dry specimens, same data as for holotype, JG F2167.

**Material Examined:** GEORGIA • 17♂♂, 17♀♀, 2 dry shells; Guria (გურია), Spring Berdnis Tskaro (ბერდნის წყარო) near Zemo Nogha (ზემო ნოღა), under the pipe; 42.063471° N, 42.269417° E; alt. 50 m; 14.09.2022; E. Chertoprud, J. Grego, M. Olšavský; GEORGIA • 36 dry specimens; Guria (გურია), Spring Berdnis Tskharo (ბერდნის წყარო) near Zemo Nogha (ზემო ნოღა), water stream from spring; 42.063471° N, 42.269417° E; alt. 50 m; 14.09.2022; E. Chertoprud, J. Grego, M. Olšavský; GEORGIA • 12 dry specimens; Guria (გურია), spring by the side of the Chokhatauri-Bakhmaro (ჩოხატაური-ბახმარო) road; 41.891203° N, 42.371960° E; alt. 1368 m; 14.09.2022; E. Chertoprud, J. Grego, M. Olšavský; GEORGIA • 6 specimens; Guria (გურია), spring by the side of the Chokhatauri-Bakhmaro (ჩოხატაური-ბახმარო) road; 41.909662° N, 42.386778° E; alt. 945 m; 14.09.2022. E. Chertoprud, J. Grego, M. Olšavský; GEORGIA • 6 wet specimens; Guria (გურია), Kvabgha (ქვაბღა), at Chokhatauri-Bakhmaro (ჩოხატაური-ბახმარო) road, above Gubazuli (გუბაზული); 41.924991° N, 42.387607° E; alt. 458 m; 01.09.2017; L. Mumladze; GEORGIA • 1♂♂, 6♀♀; Imereti (იმერეთი), Khevistskali (ხევისწყალი) River, south of the village Kvemo Nogha (ქვემო ნოღა); 42.063440° N, 42.269450° E; alt. 53 m; 01.09.2017; L. Mumladze; GEORGIA • 5♂♂; Guria (გურია), Kvabgha (ქვაბღა) spring; 41.925174° N, 42.387773° E; alt. 477 m; 14.09.2022; E. Chertoprud, J. Grego, M. Olšavský; GEORGIA • 2♀♀specimens; Guria (გურია), Small stream near the village Chkhakoura (ჩხაკურა); 41.909827° N, 42.387033° E; alt. 945 m; 30.08.2017; L. Mumladze; GEORGIA • 4 wet specimens; Guria (გურია), Small stream near the village Chkhakoura (ჩხაკურა); 41.947869° N, 41.947869° E; alt.46 m; 24.05.2017; L. Mumladze. Vakijvari (ვაკიჯვარი).

### 3.16.1. Description

**Shell:** small (SH not exceeding 1.76 mm), elongated-oval or barrel-shaped, transparent-whitish (Figures 15(1a–1f), 17A,B). Whorl number up to 4.25. Whorls rounded and quite convex, separated by a weak suture. Shell moderately broad, SW/SH ratio 0.56–0.63. Body whorl relatively high and slightly inflated. Spire constituting 0.50–0.56 of shell height. Aperture triangular-ovoid, slightly expanded, and in tight contact with the body whorl. Lateral profile of the labral margin almost straight. Umbilicus absent. Protoconch moderately broad (up to 270 µm in diameter), low dome-shaped, consisting of 1.2 whorls, pitted surface sculpture (Figure 17C,D,F–H). Protoconch border indistinct.

**Sexual dimorphism:** There is no pronounced sexual dimorphism in the shell morphology of the *Aetis starobogatovi* sp. nov. type population. According to non-parametric multivariate statistical analysis of shell variables, the differences between the sexes account for only 6.7% of all differences (PERMANOVA,  $p > 0.05$ ).

**Operculum:** irregularly-ovoid, relatively thin, paucispiral with a submarginal nucleus, generally orange. Outer surface flat with axial growth lines. Inner surface with roughly sculpted thickening in the nucleus. A curved fold with a subtle pitted sculpture bends the nucleus area around (Figure 17E).

**Soft parts:** white with well-developed eyes (Figure 17M).

**Holotype measurements:** SH-1.63 mm; SW-0.94 mm; SpH-0.89 mm; BWH-1.27 mm; BWHap-0.54 mm; BWW-0.85 mm; PWH-0.29 mm; PWW-0.66 mm; AH-0.72 mm; AW-0.56 mm.

**Penial morphology:** Penis large (up to 1 mm in length), folded, with a bifurcated terminal part (Figure 17I–N). Proximal part slightly dilated, medial part quite long, about



500  $\mu\text{m}$ ). Distal part large, expanded in comparison with the medial part, lies in front of the eye line on the right side, shaped as a broad slingshot or fishtail with two triangular, slightly asymmetrical lobes. Left lobe contains an excretory part of the penial gland with its opening at its cylindrical tip. Right lobe triangular in shape with a delicate narrow curved tip, containing the terminal part of the vas deferens (Figure 19(B1,C1–C3)). Penial gland clearly distinguishable, muscularized, opalescent, in the shape of a thick cylindrical rod, extending from the base of the penis and ending with an excretory opening on the left penial edge. Vas deferens runs along the right edge of the penis and continues into the lobe-shaped distal part, opening at the left edge of the terminal penial lobe and not reaching the curved tip (Figure 19(C3)).

**Radula:** Two basal cusps on each side of the rhachis and four or five cusps on each side of the median cusp. Median cusp only longer than adjacent ones, all cusps relatively long and narrow. Basal tongue with an acute angle. Lateral tooth bears five cusps on the outer side of the largest cusp and three on the inner side, all cusps broader and longer than the rachidian. Inner marginal tooth has 30 cusps, outer marginal tooth has 27 cusps (Figure 18B).

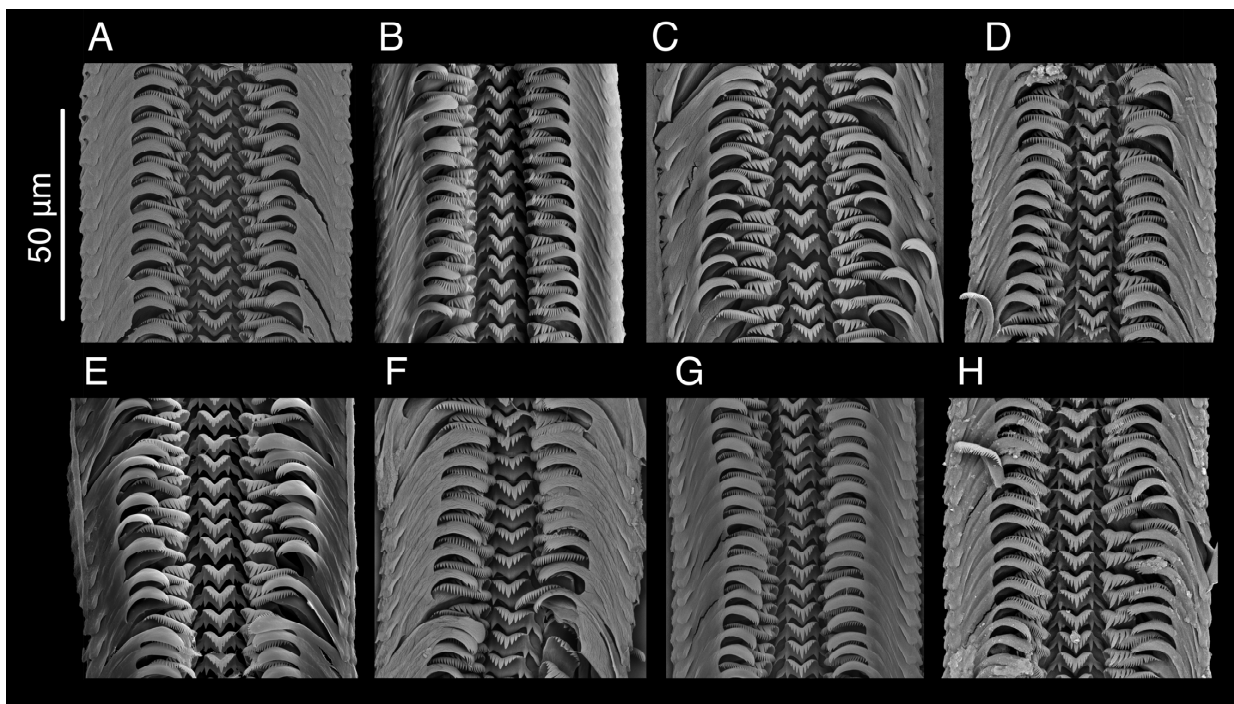


**Figure 18.** Radula. (A)—*Sataplia cavernicola* sp. nov., (B)—*Aetis starobogatovi* sp. nov., (C)—*Tschernomorica kopidophora* sp. nov., (D)—*Tschernomorica kimmeria* Vinarski & Palatov, 2019, (E)—*Colchiella nazodelavo* sp. nov., (F)—*Colchiella dadiani* sp. nov., (G)—*Colchiella lugella* sp. nov., (H)—*Colchiella shiksha* sp. nov.

### 3.16.2. Variation

The shape of the distal penial part of *A. starobogatovi* sp. nov. varies within the type population. The lobes of the penis can be equal or more or less asymmetrical to each other; in this case, either the right or left lobe is predominant in size. The divergence angle of the terminal blades also varies significantly. The left terminal glandular part can be relatively straight or bent to the left, and the angle of this bend may reach  $90^\circ$  or more (Figure 17I). The type of penial folding may also vary from a simple medial fold (Figure 17M) to that of a peculiar, curved shape lying within the mantle cavity (Figure 17L).



### 3.16.3. Etymology

Named after the renowned Russian malacologist Yaroslav Igorevich Starobogatov (13 July 1932–3 December 2004), formerly of the Zoological Institute of the Russian Academy of Sciences, Moscow, who was among the first scientists to bring attention to the stygobiotic mollusks of the Caucasus.

### 3.16.4. Habitat

Crenobiotic species. It can be found on rocks and under fallen leaves in small springs and water seepages from volcanic, mainly andesite bedrock, and in the adjacent small streams over north-facing valleys of the southwest Lesser Caucasus. The type locality is a roadside spring and adjacent moss-covered seepages from several water outlets along the road and a roadside drainage groove containing a small stream. The water parameters on the type locality are 18.6 °C, pH 7.664, and conductivity 242 µS. The same parameters in other localities vary in the range of 6.9–15.7 °C, pH 7.9–8.3, and conductivity 87–126 µ.

### 3.16.5. Distribution

Known from a few localities in eastern Guria and south Imereti around the villages Vakijvari, Kvabgha, Chkhakoura, Zemo Nogha and Kvemo Nogha, together with three localities in the Mitrala National Park in the Lesser Caucasus.

### 3.16.6. Conservation Status

The number of known localities is eight, and they are spread over an EOO of about 200 km<sup>2</sup>. The AOO is represented by only several small, restricted spring outlets draining narrow fissures and faults in volcanic rocks, and thus the real habitat has a much smaller total area compared with the EOO. Each of the spring zones is supplied by direct surface water, where stochastic events, such as human-driven pollution or habitat destruction, could lead to a rapid species decline or extinction. The roadside localities are exposed to pollution, grazing, and potential destruction due to road extension projects. Therefore, it is assessed as being Vulnerable (VU) D2.

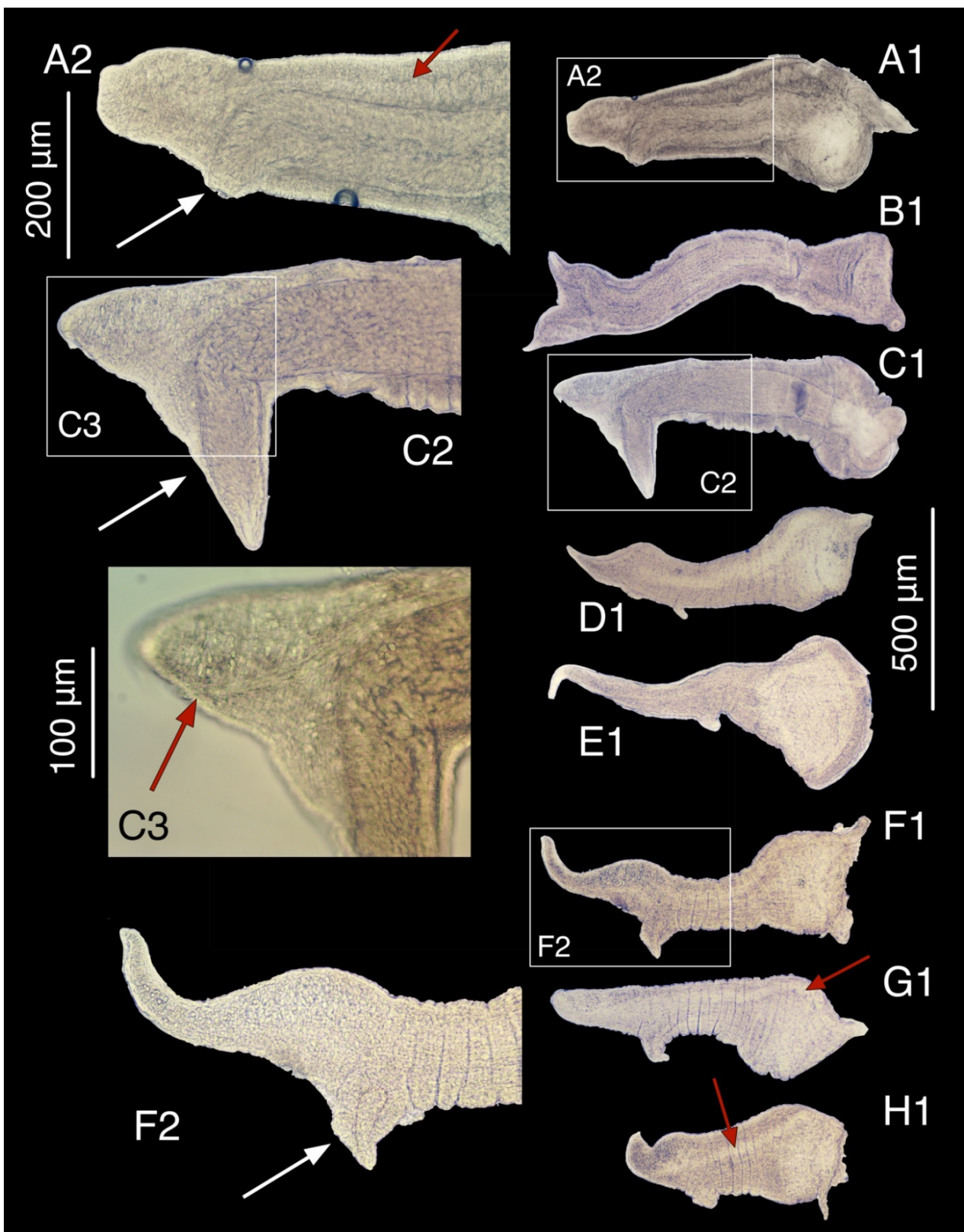


**Figure 19.** The structural features of the male copulatory apparatus. (A1)—*Sataplia cavernicola* sp. nov.; (B1,C1)—*Aetis starobogatovi* sp. nov.; (D1)—*Tschernomorica kimmeria* Vinarski & Palatov, 2019 in dorsal view; (E1)—*Tschernomorica kopidophora* sp. nov.; (F1)—*Colchiella shiksha* sp. nov.; (G1)—*Colchiella dadiani* sp. nov.; (H1)—*Colchiella lugella* sp. nov. (A2,C2,F2)—distal part of the penis, detailed view; (C3)—penial tip, detailed view. The letters correspond to individual penis habitus, and numbers represent the different detailed views of the penis. Red arrow points to the vas deference within the penis. White arrow points to the lateral outgrowth of the penis.

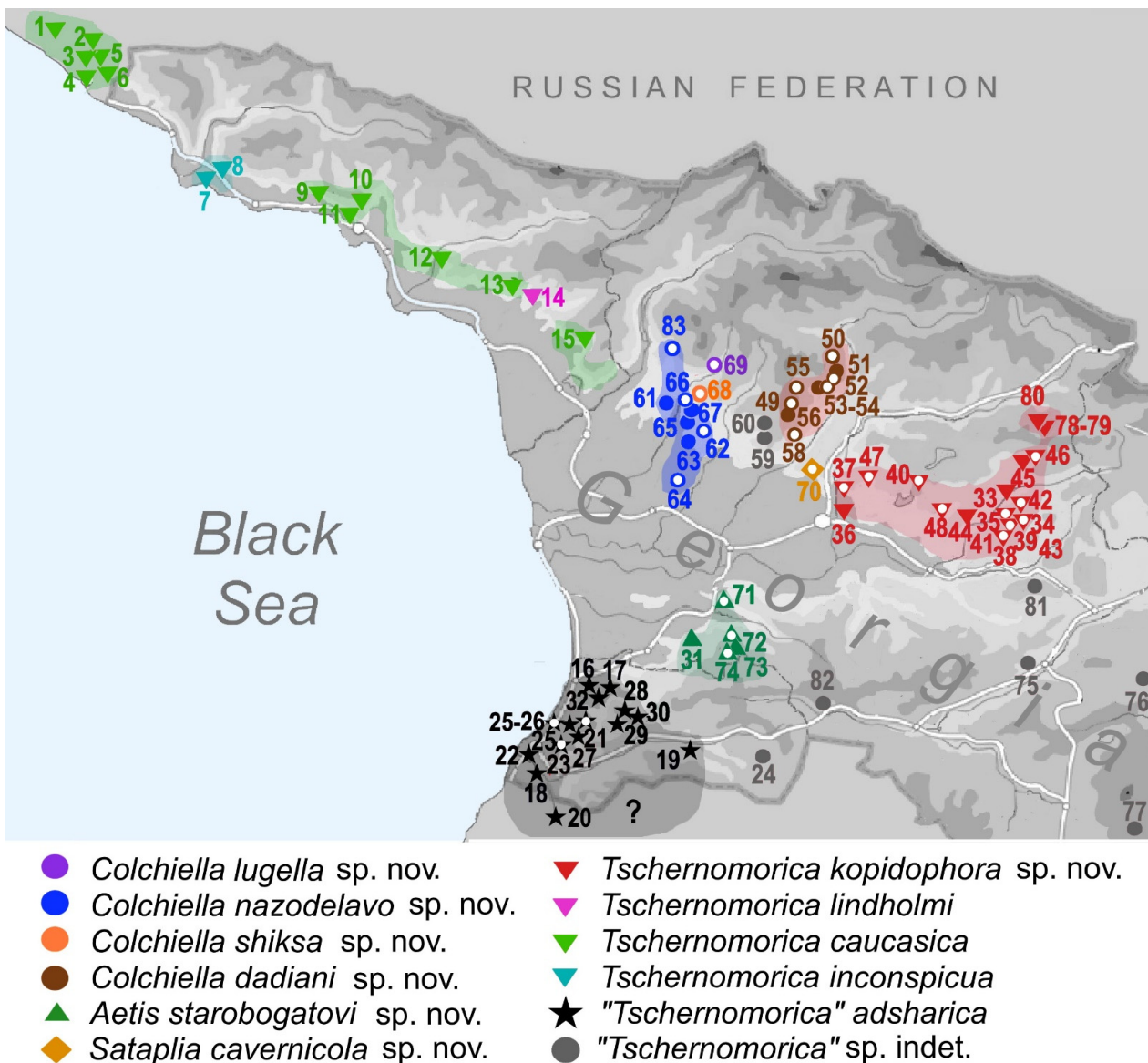


**Figure 20.** Distribution map of crenobiotic Belgrandiellinae species in the south-western Caucasus. Localities with available sequences with white central dot.

#### 4. Discussion

##### 4.1. Habitats of Caucasian Belgandiellinae

The south-western Great Caucasus region is typical in being southward-framed by a belt of Mesozoic carbonates, predominantly limestones, and sandy limestones. The usually sub-horizontal beds are altered by less permeable sandstones, leading to multiple levels of epi-saturation in carbonate massifs, where different perched water tables are situated at different levels of the limestone blocks [10]. The result of such epi-saturation is a high number of karst springs, spring outlets, or water leaks situated at different levels of the hill-slope down to the riverbeds. This type of geology necessitates a higher level of hypogean freshwater aquifer isolation, as is evidenced by the presence of a large number of stygobiotic gastropod species in relatively small areas [10]. The stygobiotic habitats also influence the adjacent epigeal springs and crenobiotic habitats, which do not possess such a high level of isolation, and thus mutual surface connections and gene flow between populations are possible among closer surface localities. Therefore, most of the crenobiotic gastropod genera display a lower level of speciation over a larger area when compared with their hypogean relatives. Similar but even larger distribution areas are expected for the Lesser

Caucasus crenobiotic species adapted to springs emerging from volcanic substrates such as andesite. The isolation of the crenobiotic habitats in the vulcanite region is apparently not so prominent, and the species may be dispersed over the spring habitats within the entire valley or even larger areas. The only Greater Caucasus locality (Lugella) known from crystalline rocks indicates a possible presence in non-karstic springs over large, uninvestigated crystalline bedrock areas north of the Samegrelo-Imeretian limestone belt. The interesting and outstanding geological phenomena of the studied region are the large deposits of Cretaceous/Eocene limestone conglomerates around Chkhorotsku and its shallow wells and karstified conduits abundant in the epigeal substrate, hosting a diverse stygobiotic and crenobiotic fauna. The diversity of the stygobiotic subfamily Horatiinae Taylor 1966, reported in previous papers [10–12], displayed a remarkable specific radiation in the region. A similar high obligate stygobiotic radiation is found in the subfamily Belgrandiellinae Radoman, 1983. They will be the subject of our next study. While the Horatiinae is represented in the region exclusively by stygobiotic taxa, many of the Belgrandiellinae species belong to a crenobiotic species group, occasionally stygophilic, lacking pigmentation but with the eyespots still present (presented in the current study). The crenobiotic Belgrandiellinae species are found in most karst localities of the region, sympatrically with one or four stygobiotic Horatiinae species and occasionally with one stygobiotic Belgrandiellinae species in the Racha region. However, each spring hosts exclusively only one crenobiotic species of Belgrandiellinae (the only known exception to this rule is the Lesser Caucasus spring in Vakijvari with two species “*T*”. cf. *adsharica* and *A. starobogatovi* sp. nov.). Due to the more universal, non-karstic geological substrate preference of Lesser Caucasus crenobiotic Belgrandiellinae, it seems that their distribution will be much wider than it has been previously thought and could be present in the entire western part of the Lesser Caucasus from the Javakheti plateau to the Black Sea seashore and maybe in the non-karstic part of the western Greater Caucasus.

#### 4.2. Shell Morphology

It has been repeatedly noted that the shell morphology of truncatelloid gastropods cannot be used as a main taxonomic character and should be used only as presumptive until relevant molecular and anatomical information is available [80–83]. How useful are standard conchological characters in defining the hydrobiid species studied, and are these characters sufficient for their identification? Our results do not provide an unambiguous answer. On the one hand, analysis of variance indicated that almost all species, considered collectively at the population level, differ significantly from each other in shell morphology. On the other hand, each species showed rather wide individual variability so that the areas they occupied in multidimensional morphospace overlapped widely. According to the LDA analysis, on average, every fifth shell would be assigned to a particular species incorrectly. This is despite the fact that our individuals were collected from the type populations only, while possible interpopulation differences were not evaluated. This preliminary result challenges the ability to discriminate the species reliably if based on the formal geometric morphometry of individuals. More extensive investigation of interpopulation vs interspecific shell shape variation is necessary to reveal and describe the patterns of the morphometric variability of Caucasian Belgrandiellinae.

#### 4.3. Historical Biogeography

The history and evolution of the crenobiotic Belgrandiellinae have remained unresolved so far. The hitherto known distribution of the subfamily displays a fragmented relict occurrence of diverse genera ranging from Middle Europe through the Balkans to the Crimea, Caucasus, Turkey, and Lebanon (Figure 21). The splits in the molecular chronogram (Figure 7) match with the main geological events known from the current distribution area of Belgrandiellinae and suggest their possible dispersal from the Balkans to the Aegean area, towards the south-western Greater Caucasus and the western Lesser Caucasus.



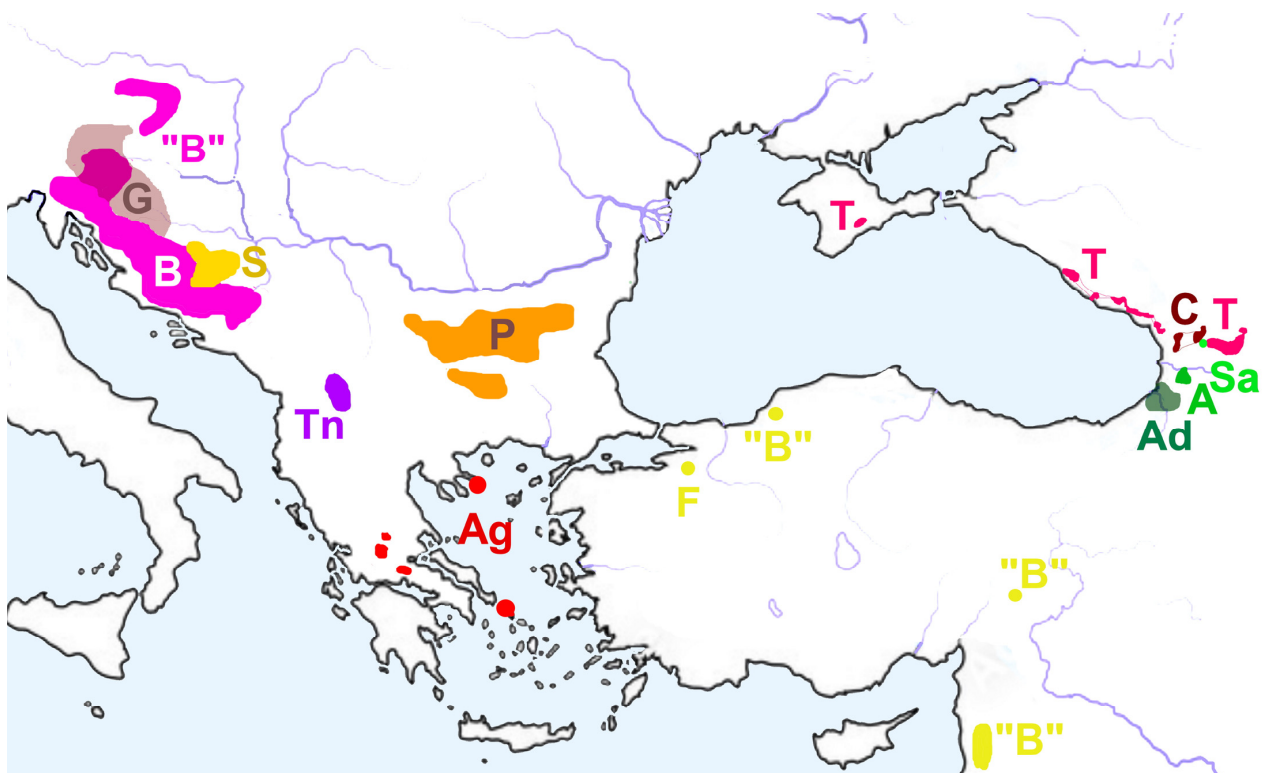


**Figure 21.** Current relict distribution of Belgrandiellinae genera in the studied area: A—*Aetis* gen. nov.; Ag—*Agrafia* Szarowska and Falniowski; Ad—“*Tschernomorica*” *adsharica*; 2011; B—*Belgrandiella* Wagner, 1928; “B”—taxa provisionally lumped under *Belgrandiella*; C—*Colchiella* gen. nov.; F—*Falsibelgrandiella* Radoman, 1973; G—*Graziana* Radoman, 1975; P—*Pontobelgrandiella* Radoman, 1978; S—*Sarajana* Radoman, 1975; Sa—*Sataplia* gen. nov.; T—*Tschernomorica* Vinarski & Palatov, 2019; Tn—*Terranigra* Radoman.

The molecular data indicate that two independent parallel colonization events of the south-western Caucasus by a common ancestor started during the ultimate period of the Messinian Salinity Crisis (5.60 to 5.31 Ma) [74] and took place between the Zanclean flood event (Mediterranean Basin reflooding) [84] and the Euxino-Caspian Basin reflood event (5.31 to 4.60 Ma) [85,86]. Similar separation of European and Crimean-Caucasian clades of stygobiotic amphipod genera *Niphargus* Schiödt [87–90], *Proasellus* Dudich, 1925 [91] and for cave shrimps *Xiphocaridinella* Sadowsky, 1930 [92–94] was dated back to the Messinian Salinity Crisis. The common Belgrandiellinae ancestor(s) of the Caucasian clades had separated from its Balkan relatives about  $3.75 \pm 0.89$  Ma after the end of the Messinian Salinity Crisis and Euxine-Caspian Basin reflooding and the restoration of the pre-Messinian humid climate.

The Messinian Salinity Crisis is characterized by the drying out of the Mediterranean Basin after the orogenic uplift of the Gibraltar arc [74,75], with just several hyper-salinated lakes remaining at the lowest basins and trenches of the Mediterranean Sea during its culminating period 5.5 Ma [95]. The desiccation had been interrupted by three phases of brackish water inflow from the Paratethys Lake, known as “Lago Mare” [96]. At the same time, the Paratethys Sea (Lake) in central and eastern Europe had already been shrunken to just a few freshwater or brackish lakes. The Euxine Lake in the lowest part of the Black Sea Basin was prominent, together with the Caspian Lake in the Ponto-Caspian Basin, with the Dacic Lake and the Slavonian Lake (as a remnant of the former larger Pannonian Lake) remaining in central Europe [97]. This radical shrinking of the water bodies opened large terrestrial and fluvial areas for species dispersal across the region [75,98]. Nevertheless, the period of the culminating crisis was also a period of very low rainfall and local deser-

tification, which was not too favorable for any large dispersal of freshwater species. The further separation of the two Caucasus colonizing clades took place around 5.46 Ma, at the time of the Mediterranean Basin reflooding event after the opening of the Gibraltar Strait, known as the Zanclean Flood [74]. This event took place in several phases, resulting in the geomorphological rearrangement and even elevation of the pre-Messinian Mediterranean Sea level up to the Apennine Foredeep and the Aegean Sea. The Euxino-Caspian Basin still remained isolated and unflooded. The Mediterranean Sea evaporation, however, supported more intense rainfalls in the region and over the Euxine Basin area, and this more humid climate could support more effective migration of freshwater species around the fluvial and paludine habitats of the Euxine Lake. The width of the dispersal path was significantly reduced after the post-Messinian refill of the Euxino-Caspian Basin, which was refilled through a narrow channel opened up from the Aegean Sea through the Balakan Channel, Skopje Basin, and the Dacic Lake [74]. This refill was induced by an additional global seawater level increase caused by the melting of the polar ice cap [99].

The molecular-clock data indicate the dispersal of the Belgrandiellinae ancestors from the western Balkans to the Caucasus during this relatively narrow geological time window between the end of the Zanclean Flood and the end of the refilling of the Euxino-Caspian Basin. It is most likely that the colonization happened by the two genetically well-defined clades (Figure 22) using different dispersal paths. The one could be the northern path, from the foothills of the Great Balkan Mountain range through the northern shoreline of the diminished Euxine Lake through Crimea. With this path, the ancestral lineages had reached the western Great Caucasus foothills within  $2.71 \pm 0.84$  Ma and evolved into two genera—*Colchiella* gen. nov. (in the areas of the Markotkh Range, the Arabika Massif, and the Bzyb Ridge, down to the Samegrelo conglomerate deposits, Aaski Plateau), and *Tschernomorica* (near the Zemo Imereti Plateau). This was then followed by intrageneric radiations in both genera that were estimated to be rather young ( $<0.1$  Ma). Both the current genera of the “northern” clade are specialized dominantly to inhabit karstic springs and caves, which indicates that during their migration from Crimea to Samegrelo, the limestone formations were positioned closer to the seashore and became more easily available for colonization. Later, due to continued orogenesis, the karstic areas were elevated, which resulted in isolations among populations.

The migration of another lineage along the southern path (a second hypothesized dispersal path) started in the South Balkanas and Rodopi Mountains and through Asia Minor and reached the Lesser Caucasus along the southern shoreline of the Euxine Lake at around  $2.94 \pm 0.87$  Ma. The ancestral lineage appeared to have spread fast throughout the modern Adjara-Guria-Kvemo Imereti regions and was split out into modern genera ( $2.53 \pm 0.78$  Ma) (*Sataplia* gen. nov., *Aetis* gen. nov., and so far unnamed genus tentatively represented here as “*Tschernomorica*” *adsharica*). From this scenario, *Sataplia* gen. nov. from Sataplia cave represents a relic lineage, while the more recent genera *Colchiella* gen. nov. and *Tschernomorica* from the Northern lineage are currently more successful in the south-western Great Caucasus. The members of the “southern” clades have non-strict habitat preferences and so adapted to non-karstic rocks with low mineralization and calcium content, inhabiting a network of small permanent water seepages, small water streams and brooks, small ponds with moss, and fallen leaves in humid valleys of the Lesser Caucasus. The lower specialization and low habitat preference of this clade are likely closer to one of the ancestor populations and give it higher chances for effective dispersal. On the contrary, the genus *Sataplia* gen. nov. seemed to be specialized to the cave environment and had not been found in epigeal habitats.

The radiation of the “northern” Clade was culminated by the genus *Tschernomorica* gen. nov. about  $2.71 \pm 0.84$  Ma. This genus developed a very effective colonization strategy by its lower habitat preference and succeeded in populating large and very diverse areas of Imereti to eastern Racha, from altitudes of 130 m to almost 1800 m. Nevertheless, the known populations are still found to have preferences for karstic and calcareous substrates and seem not to inhabit the crystalline rock substrates. The further dispersal of

*Tschernomorica* gen. nov. took place by the end of Pleistocene  $0.39 \pm 0.12$  Ma, most likely supported by Euxine Lake water level fluctuations and by karstic areas situated closer to the seashore. The dispersal was interrupted by the Pleistocene glaciation events, during which the genera had survived in the moderate conditions of the Colchis refugia [100–104]. After the end of the Würm Glacial Stage 11,000 years ago, it took just a few thousand years before the Euxinian Lake was again at its low water level about 8000 years ago (though still higher than its previous level during the Messinian Salinity Crisis: [105]), and the potential migration corridors around the Lake were becoming more open [106]. It is very likely that the pre-Pleistocene populations of the *Colchiella* gen. nov. in the Crimea and in the more glaciated parts of the south-western Greater Caucasus [107] were either entirely diminished or at least reduced to several small refugial populations. The reopened northern migratory path was used to recolonize along the Black Sea's north-eastern coastline at about  $0.39 \pm 0.12$  Ma. This time, the route of recolonization was in the reverse direction, as had happened during the end of the Messinian Salinity Crisis. It is also likely that such a north-westward dispersal could be supported by the Black Sea currents [108]. Thus, the current occurrence of the genus *Tschernomorica* along the Black Sea coastline from the Crimea through the Markotkh Range and Abkhazeti is a relatively young phenomenon that happened far before the ancient Black Sea flood after the opening of the Bosphorus Strait 7600 years ago [109]. It is likely that similar events determined the pre- and post-glacial dispersal of the stygobiont amphipod genus *Niphargus* [110]. Such a dispersal of the Belgrandiellinae gastropods could hardly be explained by the currently known narrow crenobiotic or stygobiotic specialization of their ancestors. It is most likely that the ancestors were adapted to a variety of lotic, rheic, or paludine freshwater habitats, maybe even with brackish water. Thus, they had much broader habitat preferences when compared with the recently known, fragmented populations. Another dispersal option would be the hyporheic and alluvial interstitial habitats opened by the repeatedly diminished Euxine Lake surface. The dispersal among alluvial interstitials had been highlighted for postglacial distribution of genus *Bythiospeum* Bourguignat, 1882 [111] and *Hauffenia* Bourguignat, 1882 [112]. The possible dispersal of Belgrandiellinae is suggested in Figure 22.

Further molecular studies of the Crimean and Abkhazian populations as well as populations from the southern Black Sea coastline in Turkey, would be needed (together with data from other parts of Turkey, Levant (Lebanon), Greece, North Macedonia, Albania, and Kosovo) to confirm the above scenario of dispersal. We hope that by revealing the missing links, we could better reconstruct the historical biogeography of the Belgrandiellinae with much higher certainty and shed light on the origin of the Caucasian Stygobiont mollusks. The same events likely influenced the current brackish water Hydrobiinae evolution [56,60,113]. It is likely that some other operculate terrestrial gastropods might have also used the same or similar dispersal pathway towards the Caucasus and further to the Eborz Mountains, e.g., genera such as *Renea* Nevill, 1880 [114] or *Cochlostoma* Jan, 1830 [115]. Nevertheless, there are strong indications that the current crenobiotic Belgrandiellinae distribution pattern is a result of paleogeographic and paleoclimatic events in the Pontic Realm. In particular, repeated climate oscillations coupled with sharp Black Sea level changes during the Plio-Pleistocene could be considered one of the main reasons for the radiation of the Caucasian Belgrandiellinae.



**Figure 22.** Possible ways of *Belgrandiellinae* dispersal From the Balkans to Caucasus reconstructed according to molecular time tree on background of geological events between the end of Messinian Crisis (Mediterranean Sea reflooding after the opening of Gibraltar Strait), Euxino-Caspian Basin reflood through Dacic Lake, and Black Sea flood (after the opening of Bosphorus Strait). Legend provided within the Figure 21 capture.

#### 4.4. Extinction Threats and Conservation

The geology and hydrogeology of most karstic and non-karstic water conduits and springs determine the quality and quantity of water supply. The springs themselves represent a vulnerable ecosystem determined by the small area of the spring zone. A reliable, even if small, water supply is critical to the survival of the crenobiotic ecosystems. During the short drought seasons, many crenobiotic species have developed an aestivation strategy by moving into the wet parts of the subterranean habitats, caves, fissures interstitial or hyporheic parts of the springs. Nevertheless, after longer droughts and terminations of the subterranean water supply, the refugial habitats then become desiccated, which has a fatal and irreversible impact on the whole of the localities, with the result that the vulnerable crenobiotic or stygobiotic species become extinct. The main reasons for such observed spring-fauna extinctions are the lowering of the water table by mining activity or overexploitation of the water supply, the latter usually for irrigation or industrial purposes [116,117]. Sometimes, the wrong positioning of a well can lead to water loss in an adjacent spring. As an example from Georgia, we can use the spring in Itkhvisi in Zemo Imereti, which lost its water during the last 40 years due to manganese mining exploitation in the area. The spring was not repopulated by the spring fauna even after a small water flow reappearance during the last 10 years. Additionally, in past decades, the spring fauna has been increasingly threatened by repeated and aggravating drought periods without sufficient rainfall. The droughts are a result of human-driven climatic changes and alterations, as are the extremely high rainfall and flood events. The high floods can also irreversibly destroy the vulnerable spring localities situated close to the riverbanks. Among such threatened localities, we can point out the single known occurrence of *C. lugella* sp. nov in a small spring situated just at the bank of the Khobistskali River.



The garbage and waste plastic deposits left by campers enjoying the cold spring water for cooling their beverages or by intentional waste disposal in the belief that the water will take it away are the next major threats to the spring fauna. Such disrespectful behavior usually cannot be addressed just by a prohibition table at the locality but would be more effective by means of intensive ecological education programs throughout the population. Fortunately, many of the small local springs are maintained by the local villages for potable water supplies, but even such localities are under threat of being “upgraded” by a concrete wall, collector, staircase, or other construction, which would negatively alter the original spring habitats.

The conservation of spring snails is globally challenging. Despite a good understanding of freshwater hydrobiid species diversity and distribution, conservation actions targeting a specific species are rarely considered, even in more developed countries. Spring snails are mostly associated with underground habitats for which the human impact is difficult to observe at the very beginning (i.e., until the impact on the animal community of the habitat becomes apparent or other physical signs are visible), and species are typically found at subterranean habitat openings (e.g., cave entrances, spring origins) or deeply, inside caves. Such habitats are usually considered highly vulnerable and are subject to conservation in many countries [118–121]. Thus, the communities within those habitats, including the hydrobiids, are also protected. The situation is different in Georgia and the Caucasus as a whole.

In Georgia, invertebrate species diversity is generally poorly studied except for only a few taxa (such as mites, spiders, and terrestrial mollusks) [122]. Just a few years ago, the diversity and distribution of stygo- and crenobiotic gastropods of the south western Caucasus were virtually unknown. Hence, the evaluation of species conservation statuses or ensuring species protection was impossible.

Recent studies [7,9–12], including the current paper, have revealed a high level of species diversity in these snails, with 37 species already identified. However, during all these studies, only a very small portion of suitable habitats (springs and caves) in the studied area were sampled, and a large karstic and volcanic area of the south-western Caucasus remains unexplored. Given the diverse hydrogeological preconditions and event-abundant geological history of the area, we believe a much greater crenobiotic diversity exists than that presented in this study. Nonetheless, 37 species are known to be endemic to the area, with the majority of them only known from a single location. While the very locally distributed species might, in general, have a larger distribution even in the underground, it is not expected that the rate of endemism will decline. Since freshwater subterranean environments are particularly vulnerable to human impact, we believe that the conservation statuses proposed above cannot be overstated. On the other hand, Georgia (and any Caucasian country) does not have a well-developed conservation policy with regard to invertebrate animals or subterranean habitats or caves. The only means of protection of molluscan taxa are protected areas, which at the time of writing do not exceed 10% of the country’s territory. However, existing protected areas are not sufficient to guarantee the protection of terrestrial mollusks [123] and are even less effective for freshwater mollusks. As a result, hydrobiidae in the region, as well as other endemic freshwater organisms, is facing an increasing threat of extinction and so requires immediate action to develop conservation strategies for both species and their habitats.

## 5. Conclusions

In the present study, based on anatomical and molecular evidence, we are confirming the south-western Caucasus, a hitherto known diversity hotspot for stygobiotic spring snails, as being a diversity hotspot for crenobiotic species. In spite of a large number of localities/specimens investigated, a more intensive field study of the area is necessary to document the species distribution, and most likely, this will also yield a higher number of taxa. The shell morphology of the crenobiotic *Belgrandiellinae* group seems to be quite uniform and does not ensure a reliable taxonomy of the group. The penis morphology

and molecular markers are more decisive, albeit both also having their limitations. The penial morphology and anatomical features have a much higher taxonomical value than the shell morphology but frequently are still not sufficient for the species delimitation, and the molecular data of several markers (hence the integrative taxonomic approach) are needed to establish and justify the systematics of the Caucasian Belgrandiellinae.

As is already known, the high level of species diversity of freshwater hydrobiids in the south-western Caucasus points out the need for special conservation efforts, particularly due to the limited distribution of most of the species and the high vulnerability of their respective habitats. Given the absence of any conservation policy in the region, the small localities are often deliberately exposed to anthropogenic impacts such as ongoing excavations, road and infrastructure constructions, and environmental pollution.

**Supplementary Materials:** The following supporting information can be downloaded at: <https://www.mdpi.com/article/10.3390/d15030450/s1>, Table S1: The quality of classification of individuals by species according to the results of LDA; Table S2. Results of pair-wise PERMANOVA tests. *p* values are significant levels estimated by permutations of residuals (*p* < 0.05 are given in bold).

**Author Contributions:** Conceptualization J.G., L.M. and E.C.; methodology, S.H., E.C. and A.J.; software, S.H., A.J., A.O. and E.C.; formal analysis, A.F.; field investigation, L.M., J.G., E.C. and D.P.; resources, S.H., A.F. and L.M.; molecular analysis, S.H.; statistical analysis, E.C.; morphological study, E.C.; data curation, E.C., A.O. and S.H.; writing—original draft preparation, J.G., E.C. and S.H.; writing—review and editing, L.M. and A.F.; visualization, E.C., S.H., A.O. and J.G.; supervision, A.F. and D.P.; project administration, A.J.; funding acquisition, A.F. and E.C. All authors have read and agreed to the published version of the manuscript.

**Funding:** The molecular part of the research was financed by the Ministry of Education and Science of Poland (Subvention 020013-D017 for A.O.). The molecular part of the study was supported by the National Science Centre under Grant 2017/25/B/NZ8/01372 to A.F. This study was also partially funded by the Russian Scientific Fund, project No. 21-14-04401.

**Institutional Review Board Statement:** Not applicable.

**Informed Consent Statement:** Not applicable.

**Data Availability Statement:** The primary data and materials for this study are placed in some public repositories (zoological museums as refereed in the text); the newly obtained DNA sequences were submitted to GenBank. See the text for more information.

**Acknowledgments:** We would like to express our thanks to Roman A. Rakitov from the Paleontological Institute of the Russian Academy of Sciences, Moscow, for his help with obtaining SEM images of shells, protoconchs, operculums, and radula. The light microscopy studies were conducted using the equipment of the Centre of microscopy WSBS LMSU, PIN RAS, and IEE RAS. We express our gratitude to Andrei I. Azovsky (MSU) for the help with morphometrical data analysis, especially for providing access to the PRIMER 7 statistical software. We are grateful to Miklós Szekeres, Budapest, Hungary, and Mário Olšovský, Banská Bystrica, Slovak Speleological Society, for their active participation in the field trips. Special thanks also go to members of the Georgian Speleological Society: Igor Pichkhaia and Tamar Tolordava from Chkhorotsku and Gogita Chitaia from Khoni. We would like to thank Ani Bikashvili and Bella Japoshvili for their help and patience during the various collecting trips. We would like to express our gratitude to the European Speleological Federation for supporting our project “Biodiversity of Georgian Caves and Karst Areas 2021” under the grant ESP 2021-06, and to members of the 2021 international field trip: Joerg Dreybrodt, Bern, Switzerland and Rainer and Connie Straub, Filderstadt, Germany. We are grateful to Brian Lewarne of “The Proteus Project” and the Devon Karst Research Society, Plymouth, United Kingdom, for proofreading the English. We thank three anonymous reviewers for their valuable comments during the review of the manuscript.

**Conflicts of Interest:** The authors declare no conflict of interest.

## References

1. Lindholm, W.A. Beschreibung neuer Arten und Formen aus dem Kaukasus-Gebiete. *Nachricht. Der Deuts. Malakozool. Gesells.* **1913**, *45*, 17–23, 62–69. Available online: <https://www.biodiversitylibrary.org/page/15107980> (accessed on 22 December 2022).
2. Shadin, V.I. Die Süßwassermollusken aus der Rion-Höhle bei Kutais (Transkaukasien, Georgien). *Arch. Für Mollusk.* **1932**, *64*, 12–14.
3. Tzvetkov, B.N. A note on cave molluscs of South Caucasus. *Byull. Moskovsk. Obshch. Isp. Prir. Otd. Biol.* **1940**, *49*, 57–59.
4. Shadin, V.I. *Mollusks of Fresh and Brackish Waters of the USSR*; Academy of Sciences of the U.S.S.R.: Moscow, Russia, 1952.
5. Starobogatov, Y.I. Contribution to molluscs from subterranean waters of the Caucasus. *Byulleten Mosk. Obs. Ispyt. Prir. Otd. Biol.* **1962**, *67*, 42–54.
6. Schütt, H.; Şeşen, R. *Pseudamnicola* species and other freshwater gastropods (Mollusca, Gastropoda) from East Anatolia (Turkey), the Ukraine and the Lebanon. *Bacteria* **1993**, *57*, 161–171.
7. Vinarski, M.V.; Palatov, D.M.; Glöer, P. Revision of ‘Horatia’ snails (Mollusca: Gastropoda: Hydrobiidaesensulato) from South Caucasus with description of two new genera. *J. Nat. Hist.* **2014**, *48*, 2237–2253. [[CrossRef](#)]
8. Chertoprud, E.S.; Palatov, D.M.; Borisov, R.R.; Marinskiy, V.V.; Bizin, M.S.; Dbar, R.S. Distribution and a comparative analysis of the aquatic invertebrate fauna in caves of the western Caucasus. *Subterr. Biol.* **2016**, *18*, 49–70. [[CrossRef](#)]
9. Vinarski, M.V.; Palatov, D.M. A survey of the *Belgrandiella*-like gastropods of the Northern Black Sea Region (Mollusca, Gastropoda, Hydrobiidae s.l.): Morphological variability and morphospecies. *Zool. Zh.* **2019**, *98*, 988–1002.
10. Grego, J.; Mumladze, L.; Falniowski, A.; Osikowski, A.; Rysiewska, A.; Palatov, D.M.; Hofman, S. Revealing the stygobiotic and crenobiotic molluscan biodiversity hotspot in Caucasus: Part I. The phylogeny of stygobiotic Sadlerianinae Szarowska, 2006 (Mollusca, Gastropoda, Hydrobiidae) from Georgia with descriptions of five new genera and twenty-one new species. *ZooKeys* **2020**, *955*, 1–77.
11. Chertoprud, E.M.; Palatov, D.M.; Vinarski, M.V. Revealing the stygobiont and crenobiont Mollusca biodiversity hotspot in Caucasus: Part II. *Sitnikovia* gen. nov., a new genus of stygobiont microsnails (Gastropoda: Hydrobiidae) from Georgia. *Zoosyst. Rossica* **2020**, *29*, 258–266. [[CrossRef](#)]
12. Chertoprud, E.M.; Palatov, D.M.; Vinarski, M.V. Revealing the stygobiont and crenobiont Mollusca biodiversity hotspot in the Caucasus: Part III. Revision of stygobiont microsnails (Mollusca: Gastropoda: Hydrobiidae) from the Russian part of Western Transcaucasia, with the description of new taxa. *Zootaxa* **2021**, *5005*, 257–275. [[CrossRef](#)] [[PubMed](#)]
13. Arconada, B.; Ramos, M.A. The Iberico-Balearic region: One of the areas of highest Hydrobiidae (Gastropoda, Prosobranchia, Rissooidea) diversity in Europe. *Graellsia* **2003**, *59*, 91–104. [[CrossRef](#)]
14. Arconada, B.; Delicado, B.; Ramos, Á.M. A new genus and two new species of Hydrobiidae (Mollusca, Caenogastropoda) from the Iberian Peninsula. *J. Nat. Hist.* **2007**, *41*, 29–32. [[CrossRef](#)]
15. Haase, M. Differentiation of selected species of *Belgrandiella* and the redefined genus *Graziana* (Gastropoda: Hydrobiidae). *Zool. J. Linn. Soc.* **1994**, *111*, 219–246. [[CrossRef](#)]
16. Haase, M. The radiation of spring snails of the genus *Belgrandiella* in Austria (Mollusca: Caenogastropoda: Hydrobiidae). *Hydrobiologia* **1996**, *319*, 119–129. [[CrossRef](#)]
17. Radoman, P. Nochmals über die Gattung *Pseudamnicola* und schliesslich die Gattung *Orientalia* n. gen. *Arch. Moll.* **1972**, *102*, 195–200.
18. Radoman, P. *Hydrobioidea a Superfamily of Prosobranchia (Gastropoda). I. Systematics*; Serbian Academy of Sciences and Arts: Belgrade, Serbia, 1983.
19. Falniowski, A.; Beran, L.; Belgrandiella, A.J. Wagner, 1928 (Caenogastropoda: Truncatelloidea: Hydrobiidae): How many endemics? *Folia Malacol.* **2015**, *23*, 187–191. [[CrossRef](#)]
20. Radoman, P. New classification of fresh and brackish water Prosobranchia from the Balkans and Asia Minor. *Posebna Izdanja Prirodn. Mus. Beograd.* **1973**, *32*, 1–30.
21. Bole, J.; Velkovrh, F. Mollusca from continental subterranean aquatic habitats. In *Stygofauna mundi*; Botosaneanu, P., Ed.; E.J. Brill: Leiden, The Netherlands, 1986; pp. 177–208.
22. Kantor, Y.I.; Vinarski, M.V.; Schileyko, A.A.; Sysoyev, A.V. Continental Molluscs of Russia and Adjacent Territories [Internet]. Version 2.3.1. 2010. Available online: <http://www.ruthenica.com/categorie-8> (accessed on 20 December 2022).
23. Barjadze, S.; Murvanidze, M.; Arabuli, T.; Mumladze, L.; Pkhakadze, V.; Djanashvili, R.; Salakaia, M. *Annotated List of Invertebrates of the Georgia Karst Caves*; Georgian Academic Book: Tbilisi, Georgia, 2015.
24. Vinarski, M.V.; Kantor, Y.I. *Analytical Catalogue of Fresh and Brackish Water Molluscs of Russia and Adjacent Countries*; Tovarishestvo Nauchnykh Izdaniy KMK: Moscow, Russia, 2016.
25. Grego, J.; Hofman, S.; Mumladze, L.; Falniowski, A. *Agrafia Szarowska et Falniowski*, 2011 (Caenogastropoda: Hydrobiidae) in the Caucasus. *Folia Malacol.* **2017**, *237*–25247. [[CrossRef](#)]
26. Grego, J.; Glöer, P.; Erőss, Z.P.; Fehér, Z. Six new subterranean freshwater gastropod species from northern Albania and some new records from Albania and Kosovo (Mollusca, Gastropoda, Moitessieriidae and Hydrobiidae). *Subterr. Biol.* **2017**, *23*, 85–107. [[CrossRef](#)]
27. Rueden, C.T.; Schindelin, J.; Hiner, M.C.; DeZonia, B.E.; Walter, A.E.; Arena, E.T.; Eliceiri, K.W. ImageJ2: ImageJ for the next generation of scientific image data. *BMC Bioinform.* **2017**, *18*, 529. [[CrossRef](#)] [[PubMed](#)]

28. Davis, G.M.; Chen, C.-E.; Wu, C.; Kuang, T.-F.; Xing, X.-G.; Li, L.; Liu, W.-J.; Yan, Y.-L. The Pomatiopsidae of Hunan, China (Gastropoda: Rissoacea). *Malacologia* **1992**, *34*, 143–342.
29. Hershler, R.; Ponder, W.F. A review of morphological characters of Hydrobioid snails. *Contrib. Zool.* **1998**, *600*, 1–55. [[CrossRef](#)]
30. Hammer, Ø.; Harper, D.A.T.; Ryan, P.D. PAST-palaeontological statistics, ver. 1.89. *Palaeontol. Electron.* **2001**, *4*, 1–9.
31. Anderson, M.J. A new method for non-parametric multivariate analysis of variance. *Austral Ecol.* **2001**, *26*, 32–46.
32. Anderson, M.J.; Gorley, R.N.; Clarke, K.R. *PERMANOVA + for PRIMER: Guide to Software and Statistical Methods*; PRIMER-E Ltd.: Plymouth, UK, 2008.
33. Elliott, J.M.; Hurley, M.A. The functional relationship between body size and growth rate in fish. *Funct. Ecol.* **1995**, *9*, 625–627. [[CrossRef](#)]
34. Szarowska, M.; Osikowski, A.; Hofman, S.; Falniowski, A. *Pseudamnicola* Paulucci, 1878 (Caenogastropoda: Truncatelloidea) from the Aegean Islands: A long or short story? *Org. Divers. Evol.* **2016**, *16*, 121–139. [[CrossRef](#)]
35. Edgar, R.C. MUSCLE: Multiple sequence alignment with high accuracy and high throughput. *Nucleic Acids Res.* **2004**, *32*, 1792–1797. [[CrossRef](#)]
36. Kumar, S.; Stecher, G.; Tamura, K. MEGA7: Molecular Evolutionary Genetics Analysis Version 7.0 for Bigger Datasets. *Mol. Biol. Evol.* **2016**, *33*, 1870–1874. [[CrossRef](#)]
37. Hall, T.A. BioEdit: A user-friendly biological sequence alignment editor and analysis program for Windows 95/98/NT. *Nucleic Acids Symp.* **1999**, *41*, 95–98.
38. Xia, X. *Data Analysis in Molecular Biology and Evolution*; Kluwer Academic Publishers: Boston, MA, USA; Dordrecht, The Netherlands; London, UK, 2000.
39. Xia, X.; Xie, Z.; Salemi, M.; Chen, L.; Wang, Y. An index of substitution saturation and its application. *Mol. Phylogenet. Evol.* **2003**, *26*, 1–7. [[CrossRef](#)] [[PubMed](#)]
40. Xia, X. DAMBE: A comprehensive software package for data analysis in molecular biology and evolution. *Mol. Biol. Evol.* **2013**, *30*, 1720–1728. [[CrossRef](#)]
41. Miller, M.A.; Pfeiffer, W.; Schwartz, T. Creating the CIPRES Science Gateway for inference of large phylogenetic trees. In Proceedings of the Gateway Computing Environments Workshop (GCE), New Orleans, LA, USA, 14 November 2010; pp. 1–8.
42. Kozlov, A.M.; Darriba, D.; Flouri, T.; Morel, B.; Stamatakis, A. RAxML-NG: A fast, scalable and user-friendly tool for maximum likelihood phylogenetic inference. *Bioinformatics* **2019**, *35*, 4453–4455. [[CrossRef](#)]
43. Nylander, J.A.A. *MrModeltest v.2. Program Distributed by the Author*; Evolutionary Biology Centre, Uppsala University: Uppsala, Sweden, 2004.
44. Ronquist, F.; Teslenko, M.; van der Mark, P.; Ayres, D.L.; Darling, A.; Höhna, S.; Larget, B.; Liu, L.; Suchard, M.A.; Huelsenbeck, J.P. Efficient Bayesian phylogenetic inference and model choice across a large model space. *Syst. Biol.* **2012**, *61*, 539–542. [[CrossRef](#)]
45. Rambaut, A.; Drummond, A.J.; Xie, D.; Baele, G.; Suchard, M.A. Posterior summarisation in Bayesian phylogenetics using Tracer 1.7. *System. Biol.* **2018**, *67*, 901–904. [[CrossRef](#)] [[PubMed](#)]
46. Rambaut, A. FigTree v1.3.1. 2010. Available online: <http://tree.bio.ed.ac.uk/software/figtree> (accessed on 26 November 2022).
47. Zhang, J.; Kapli, P.; Pavlidis, P.; Stamatakis, A. A general species delimitation method with applications to phylogenetic placements. *Bioinformatic* **2013**, *29*, 2869–2876. [[CrossRef](#)] [[PubMed](#)]
48. Puillandre, N.; Lambert, A.; Brouillet, S.; Achaz, G. ABGD, Automatic Barcode Gap Discovery for primary species delimitation. *Mol. Ecol.* **2011**, *21*, 1864–1877. [[CrossRef](#)]
49. Merckelbach, L.; Borges, L. Make every species count: FastaChar software for rapid determination of molecular diagnostic characters to describe species. *Mol. Ecol. Res.* **2020**, *20*, 1761–1768. [[CrossRef](#)]
50. Wilke, T. *Salenthydrobia* gen. nov. (Rissooidea: Hydrobiidae): A potential relict of the Messinian Salinity Crisis. *Zool. J. Linn. Soc.* **2003**, *137*, 319–336. [[CrossRef](#)]
51. Wilke, T.; Davis, G.M. Intraspecific mitochondrial sequence diversity in *Hydrobia ulvae* and *Hydrobia ventrosa* (Hydrobiidae: Rissoacea: Gastropoda): Do their different life histories affect biogeographic patterns and gene flow? *Biol. J. Linn. Soc.* **2000**, *70*, 89–105. [[CrossRef](#)]
52. Falniowski, A.; Szarowska, M.; Sirbu, I.; Hillebrand, A.; Baciu, M. *Heleobia dobrogica* (Grossu & Negrea, 1989) (Gastropoda: Rissooidea: Cochliopidae) and the estimated time of its isolation in a continental analogue of hydrothermal vents. *Molluscan Res.* **2008**, *28*, 165–170.
53. Bouckaert, R.; Vaughan, T.G.; Barido-Sottani, J.; Duchêne, S.; Fourment, M.; Gavryushkina, A.; Heled, J.; Jones, G.; Kühnert, D.; De Maio, N.; et al. BEAST 2.5: An advanced software platform for Bayesian evolutionary analysis. *PLoS Comp. Biol.* **2019**, *15*, e1006650. [[CrossRef](#)] [[PubMed](#)]
54. Szarowska, M.; Falniowski, A. An unusual, flagellum-bearing hydrobiid snail (Gastropoda: Rissooidea: Hydrobiidae) from Greece, with descriptions of a new genus and a new species. *J. Nat. Hist.* **2011**, *45*, 2231–2246. [[CrossRef](#)]
55. Wilke, T.; Davis, G.M.; Falniowski, A.; Giusti, F.; Bodon, M.; Szarowska, M. Molecular systematics of Hydrobiidae (Mollusca: Gastropoda: Rissooidea): Testing monophyly and phylogenetic relationships. *Proc. Acad. Nat. Sci. Phila.* **2001**, *151*, 1–21. [[CrossRef](#)]



56. Osikowski, A.; Hofman, S.; Rysiewska, A.; Sket, B.; Prevorčnik, S.; Falniowski, A. A case of biodiversity overestimation in the Balkan *Belgrandiella*, A.J. Wagner, 1927 (Caenogastropoda: Hydrobiidae): Molecular divergence not paralleled by high morphological variation. *J. Nat. Hist.* **2018**, *52*, 323–344. [[CrossRef](#)]
57. Falniowski, A.; Szarowska, M. Phylogenetic relationships of *Dalmanella fluviatilis* Radoman, 1973 (Caenogastropoda: Rissooidea). *Folia Malacol.* **2013**, *21*, 1–7. [[CrossRef](#)]
58. Szarowska, M.; Hofman, S.; Osikowski, A.; Falniowski, A. *Daphniola* Radoman, 1973 (Caenogastropoda: Truncatelloidea) at east Aegean islands. *Folia Malacol.* **2014**, *22*, 269–275. [[CrossRef](#)]
59. Hofman, S.; Grego, J.; Fehér, Z.; Erőss, Z.P.; Rysiewska, A.; Osikowski, A.; Falniowski, A. New data on the valvatiform-shelled Hydrobiidae (Caenogastropoda, Truncatelloidea) from southern Greece. *ZooKeys* **2021**, *1062*, 31–47. [[CrossRef](#)]
60. Osikowski, A.; Hofman, S.; Georgiev, D.; Kalcheva, S.; Falniowski, A. Aquatic snails *Ecrobia maritima* (Milaschewitsch, 1916) and *E. ventrosa* (Montagu, 1803) (Caenogastropoda: Hydrobiidae) in the east Mediterranean and Black Sea. *Annal. Zool.* **2016**, *66*, 477–486. [[CrossRef](#)]
61. Falniowski, A.; Szarowska, M. A new genus and new species of valvatiform hydrobiid (Rissooidea; Caenogastropoda) from Greece. *Moll. Res.* **2011**, *31*, 189–199.
62. Falniowski, A.; Georgiev, D.; Osikowski, A.; Hofman, S. Radiation of *Grossuana* Radoman, 1973 (Caenogastropoda: Truncatelloidea) in the Balkans. *J. Moll. Stud.* **2016**, *82*, 305–313. [[CrossRef](#)]
63. Rysiewska, A.; Prevorčnik, S.; Osikowski, A.; Hofman, S.; Beran, L.; Falniowski, A. Phylogenetic relationships in *Kerkia* and introgression between *Hauffenia* and *Kerkia* (Caenogastropoda: Hydrobiidae). *J. Zool. Syst. Evol. Res.* **2017**, *55*, 106–117. [[CrossRef](#)]
64. Szarowska, M.; Falniowski, A. *Horatia* Bourguignat, 1887: Is this genus really phylogenetically very close to *Radomaniola* Szarowska, 2006 (Caenogastropoda: Truncatelloidea)? *Folia Malacol.* **2014**, *22*, 31–39. [[CrossRef](#)]
65. Hofman, S.; Rysiewska, A.; Osikowski, A.; Grego, J.; Sket, B.; Prevorčnik, S.; Zagmajster, M.; Falniowski, A. Phylogenetic relationships of the Balkan Moitesseriidae (Caenogastropoda: Truncatelloidea). *Zootaxa* **2018**, *4486*, 311–339. [[CrossRef](#)]
66. Beran, L.; Osikowski, A.; Hofman, S.; Falniowski, A. *Islamia zermanica* (Radoman, 1973) (Caenogastropoda: Hydrobiidae): Morphological and molecular distinctness. *Folia Malacol.* **2016**, *24*, 25–30. [[CrossRef](#)]
67. Falniowski, A.; Pešić, V.; Glöer, P. *Montenegrospeum* Pešić et Glöer, 2013: A representative of Moitesseriidae? *Folia Malacol.* **2014**, *22*, 263–268. [[CrossRef](#)]
68. Grego, J.; Glöer, P.; Rysiewska, A.; Hofman, S.; Falniowski, A. A new *Montenegrospeum* species from south Croatia (Mollusca: Gastropoda: Hydrobiidae). *Folia Malacol.* **2018**, *26*, 25–34. [[CrossRef](#)]
69. Rysiewska, A.; Georgiev, D.; Osikowski, A.; Hofman, S.; Falniowski, A. *Pontobelgrandiella* Radoman, 1973 (Caenogastropoda: Hydrobiidae): A recent invader of subterranean waters? *J. Conch.* **2016**, *42*, 193–203.
70. Szarowska, M.; Falniowski, A. Species distinctness of *Sadleriana robici* (Clessin, 1890) (Gastropoda: Rissooidea). *Folia Malacol.* **2013**, *21*, 127–133. [[CrossRef](#)]
71. Hofman, S.; Osikowski, A.; Rysiewska, A.; Grego, J.; Glöer, P.; Dmitrović, D.; Falniowski, A. *Sarajana* Radoman, 1975 (Caenogastropoda: Truncatelloidea): Premature invalidation of a genus. *J. Conch.* **2019**, *43*, 407–418.
72. Jaszczyńska, A.; Hofman, S.; Erőss, Z.P.; Fehér, Z.; Grego, J. Phylogenetic relationships of *Terranigra* Radoman, 1978 (Truncatelloidea: Hydrobiidae). *Folia Malacol.* **2023**; in press.
73. Cardoso, P.; Borges, P.A.; Triantis, K.A.; Ferrández, M.A.; Martín, J.L. Adapting the IUCN Red List criteria for invertebrates. *Biol. Conserv.* **2011**, *144*, 2432–2440. [[CrossRef](#)]
74. Bache, F.; Popescu, S.M.; Rabineau, M.; Gorini, C.; Suc, J.P.; Clauzon, G.; Olivet, J.L.; Rubino, J.L.; Melinte-Dobrinescu, M.C.; Estrada, F.; et al. A two-step process for the reflooding of the Mediterranean after the Messinian Salinity Crisis. *Basin Res.* **2011**, *24*, 125–153. [[CrossRef](#)]
75. Krijgsman, W.; Tesakov, A.; Yanina, T.; Lazarev, S.; Danukalova, G.; Van Baak, C.G.C.; Agustí, J.; Alçiçek, M.C.; Aliyeva, E.; Bista, D.; et al. Quaternary time scales for the Pontocaspian domain: Interbasinal connectivity and faunal evolution. *Earth-Sci. Rev.* **2019**, *188*, 1–40. [[CrossRef](#)]
76. Glöer, P.; Slavevska-Stamenković, V. *Bythinella melovskii* n. sp., a new species from R. Macedonia (Gastropoda: Hydrobiidae). *Ecol. Montenegr.* **2015**, *2*, 150–154. [[CrossRef](#)]
77. Georgiev, D.; Glöer, P. A new species of *Bythinella* from Strandzha mountain, SE Bulgaria (Gastropoda: Rissooidea). *Ecol. Montenegr.* **2014**, *1*, 78–81. [[CrossRef](#)]
78. Glöer, P.; Hirschfelder, H.J. New Freshwater molluscs from Crete, Greece (Gastropoda: Hydrobiidae, Bythinellidae, Valvatidae). *Ecol. Montenegr.* **2019**, *20*, 1023. [[CrossRef](#)]
79. Falniowski, A.; Lewarne, B.; Rysiewska, A.; Osikowski, A.; Hofman, S. Crenobiont, stygophile and stygobiont molluscs in the hydrographic area of the Trebišnjica River Basin. *ZooKeys* **2021**, *1047*, 61–89. [[CrossRef](#)]
80. Kabat, A.R.; Hershler, R. The prosobranch snail family Hydrobiidae (Gastropoda: Rissooidea): Review of classification and supraspecific taxa. *Smiths. Contrib. Zool.* **1993**, *547*, 1–94. [[CrossRef](#)]
81. Szarowska, M. Molecular phylogeny, systematics and morphological character evolution in the Balkan Rissooidea (Caenogastropoda). *Folia Malacol.* **2006**, *14*, 99–168. [[CrossRef](#)]
82. Szarowska, M.; Falniowski, A. There is no philosopher's stone: Coup de grace for the morphology-based systematics in the rissooidean gastropods? In Proceedings of the 5th Congress of the European Malacological Societies, Ponta Delgada, Portugal, 2–6 September 2008; p. 28.

83. Falniowski, A. Species Distinction and Speciation in Hydrobioid Gastropods (Mollusca: Caenogastropoda: Truncatelloidea). *Archiv Zool. Stud.* **2018**, *1*, 1–6. [CrossRef]
84. Garcia-Castellanos, D.; Micallef, A.; Estrada, F.; Camerlenghie, A.; Ercilla, G.; Periáñez, R.; Abrill, J.M. The Zanclean megaflood of the Mediterranean—Searching for independent evidence. *Earth-Sci. Rev.* **2020**, *201*, 103061. [CrossRef]
85. Krezsek, C.; Schleder, Z.; Bega, Z.; Ionescu, G.; Tari, G. The Messinian sea-level fall in the western Black Sea: Small or large? Insights from offshore Romania. *Petroleum Geosci.* **2016**, *22*, 392–399. [CrossRef]
86. Grothe, A.; Andreetto, F.; Reichart, G.J.; Wolthers, M.; Van Baak, C.G.C.; Vasiliev, I.; Stoica, M.; Sangiorgi, F.; Middelburg, J.J.; Davies, G.R.; et al. Paratethys pacing of the Messinian Salinity Crisis: Low salinity waters contributing to gypsum precipitation? *Earth Planet. Sci. Lett.* **2020**, *532*, 116029. [CrossRef]
87. Marin, I.N. The Quaternary speciation in the Caucasus: A new cryptic species of stygobiotic amphipod of the genus *Niphargus* (Crustacea: Amphipoda: Niphargidae) from the Kumistavi (Prometheus) Cave, Western Georgia. *Arthropoda Sel.* **2020**, *29*, 419–432. [CrossRef]
88. Marin, I.N.; Krylenko, S.; Palatov, D. The Caucasian relicts: A new species of the genus *Niphargus* (Crustacea: Amphipoda: Niphargidae) from the Gelendzhik-Tuapse area of the Russian southwestern Caucasus. *Zootaxa* **2021**, *4963*, zootaxa.4963.3.5. [CrossRef] [PubMed]
89. Marin, I.N.; Palatov, D. Cryptic refugee on the northern slope of the Greater Caucasian Ridge: Discovery of *Niphargus* (Crustacea: Amphipoda: Niphargidae) in the North Ossetia–Alania, North Caucasus, separated from its relatives in the late Miocene. *Zool. Anz.* **2021**, *292*, 163–183. [CrossRef]
90. Marin, I.N.; Turbanov, I.S.; Prokopov, G.A.; Palatov, D.M. A New Species of the Genus *Niphargus* Schiødt, 1849 (Crustacea: Amphipoda: Niphargidae) from Groundwater Habitats of the Tarkhankut Upland, Crimean Peninsula. *Diversity* **2022**, *14*, 1010. [CrossRef]
91. Palatov, D.M.; Sokolova, A.M. Two new stygobiotic species of the genus *Proasellus* (Crustacea: Isopoda: Asellidae) from the North Caucasus. *Invert. Zool.* **2021**, *18*, 481–501. [CrossRef]
92. Marin, I.N.; Barjadze, S. A new species of stygobiotic atyid shrimps of the genus *Xiphocaridinella* (Crustacea: Decapoda: Atyidae) from the Racha-Lechkhumi and Kvemo Svaneti, with a new record of *X. kumistavi* from the Imereti, Western Georgia. *Invert. Zool.* **2022**, *19*, 24–34. [CrossRef]
93. Zakšek, V.; Sket, B.; Trontelj, P. Phylogeny of the cave shrimp *Troglocaris*: Evidence of a young connection between Balkans and Caucasus. *Mol. Phylogenet. Evol.* **2007**, *42*, 223–235. [CrossRef]
94. Marin, I.N.; Krylenko, S.V.; Palatov, D.M. Euxinian relict amphipods of the Eastern Paratethys in the subterranean fauna of coastal habitats of the Northern Black Sea region. *Invertebr. Zool.* **2021**, *18*, 247–320. [CrossRef]
95. Rouchy, J.M.; Caruso, A. The Messinian salinity crisis in the Mediterranean basin: A reassessment of the data and an integrated scenario. *Sedimentary Geol.* **2006**, *188–189*, 35–67. [CrossRef]
96. Couto, D.D.; Popescu, S.; Suc, J.; Melinte-Dobrinescu, M.C.; Barhoun, N.; Gorini, C.; Jolivet, L.; Poort, J.; Jouannic, G.; Auxietre, J.L. Lago Mare and the Messinian Salinity Crisis: Evidence from the Alboran Sea (S. Spain). *Mar. Pet. Geol.* **2014**, *52*, 57–76. [CrossRef]
97. Bartol, J.; Govers, R. Flexure due to the Messinian-Pontian sea level drop in the Black Sea. *Geochem. Geophys. Geosyst.* **2009**, *10*, 1–14. [CrossRef]
98. Garcia-Alix, A.; Minwer-Barakat, R.; Suarez, E.M.; Freudenthal, M.; Aguirre, J.; Kaya, F. Updating the Europe–Africa small mammal exchange during the late Messinian. *J. Biogeogr.* **2016**, *43*, 1336–1348. [CrossRef]
99. Krijgsman, W.; Capella, W.; Simon, D.; Hilgen, F.J.; Kouwenhoven, T.J.; Meijer, P.T.; Sierro, F.J.; Tulbure, M.A.; van den Berg, B.C.J.; van der Schee, M.; et al. The Gibraltar Corridor: Watergate of the Messinian Salinity Crisis. *Marine Geol.* **2018**, *403*, 238–246. [CrossRef]
100. Kikvidze, Z.; Ohsawa, M. Richness of Colchic vegetation: Comparison between refugia of south-western and East Asia. *BMC Ecology* **2001**, *1*, 1–10. Available online: <http://www.biomedcentral.com/1472-6785/1/6> (accessed on 20 December 2022). [CrossRef] [PubMed]
101. Connor, S.E.; Kvavadze, E.V. Modelling late quaternary changes in plant distribution, vegetation and climate using pollen data from Georgia, Caucasus. *J. Biogeogr.* **2009**, *36*, 529–545. [CrossRef]
102. Tarkhnishvili, D.; Gavashelishvili, A.; Mumladze, L. Palaeoclimatic models help to understand current distribution of Caucasian forest species. *Biol. J. Linn. Soc.* **2012**, *105*, 231–248. [CrossRef]
103. Nieber, M.T.; Hausdorf, B. Phylogeography of the land snail genus *Circassina* (Gastropoda: Hygromiidae) implies multiple Pleistocene refugia in the western Caucasus region. *Mol. Phylogenet. Evol.* **2015**, *93*, 129–142. [CrossRef]
104. Sękiewicz, K.; Danelia, I.; Farzaliyev, V.; Gholizadeh, H.; Iszkuło, G.; Naqinezhad, A.; Ramezani, E.; Thomas, P.A.; Tomaszewski, D.; Walas, Ł.; et al. Past climatic refugia and landscape resistance explain spatial genetic structure in Oriental beech in the South Caucasus. *Ecol. Evol.* **2022**, *12*, e9320. [CrossRef] [PubMed]
105. Krijgsman, W.; Hilgen, F.; Raffi, I.; Sierro, F.J.; Wilson, D.S. Chronology, causes and progression of the Messinian salinity crisis. *Nature* **1999**, *400*, 652–655. [CrossRef]
106. Laermanns, H.; Kelterbaum, D.; May, S.M.; Elashvili, M.; Opitz, S.; Hülle, D.; Rölkens, J.; Verheul, J.; Riedesel, S.; Brückner, H. Mid-to Late Holocene landscape changes in the Rioni Delta area (Kolkheti lowlands, W Georgia). *Quat. Int.* **2018**, *465 Part A*, 85–98. [CrossRef]

107. Gobejishvili, R.; Lomidze, N.; Tielidze, L. Chapter 12—Late Pleistocene (Würmian) Glaciations of the Caucasus. *Dev. Quarter. Sci.* **2011**, *15*, 141–147.
108. Birkun, A.; Atudorei, A.; Gamgebeli, T.; Dedeoglu, S.G.; Movchan, N.; Nikolova, A.; Okus, E.; Yurenko, Y. *Marine Litter in the Black Sea Region: A Review of the Problem*; Black Sea Commission Publications 2007-1, BSC Report 2007; Black Sea Commission Publications: Istanbul, Turkey, 2007; p. 160. ISBN 978-9944-245-32-6.
109. Ryan, W.B.F.; Major, C.O.; Lericolais, G.; Goldstein, S.L. Catastrophic Flooding of the Black Sea. *Ann. Rev. Earth Planet Sci.* **2003**, *31*, 525–554. [[CrossRef](#)]
110. Rendoš, M.; Delić, T.; Copilaş-Ciocianuc, D.; Fišer, C. First insight into cryptic diversity of a Caucasian subterranean amphipod of the genus *Niphargus* (Crustacea: Amphipoda: Niphargidae). *Zool. Anz.* **2021**, *290*, 1–11. [[CrossRef](#)]
111. Richling, I.; Malkowsky, Y.; Kuhn, Y.; Niederhöfer, H.-J.; Boeters, H.D. A vanishing hotspot—impact of molecular insights on the diversity of Central European *Bythiospeum* Bourguignat, 1882 (Mollusca: Gastropoda: Truncatelloidea). *Org. Divers. Evol.* **2016**, *17*, 67–85. [[CrossRef](#)]
112. Haase, M.; Grego, J.; Erőss, Z.P.; Farkas, R.; Fehér, Z. On the origin and diversification of the stygobiotic freshwater snail genus *Hauffenia* (Caenogastropoda: Hydrobiidae) with special focus on the northern species and the description of two new species. *Europ. J. Taxon.* **2021**, *775*, 143–184. [[CrossRef](#)]
113. Anistratenko, V.V.; Palatov, D.M.; Chertoprud, E.M.; Sitnikova, T.Y.; Anistratenko, O.Y.; Clewing, C.; Vinarski, M.V. Keyhole into a Lost World: The First Purely Freshwater Species of the Ponto-Caspian Genus *Clathrocaspia* (Caenogastropoda: Hydrobiidae). *Diversity* **2022**, *14*, 232. [[CrossRef](#)]
114. Páll-Gergely, B.; Grego, J. A Georgian and an Iranian new species of *Renea*, G. Nevill, 1880 enormously extend the genus's distribution (Gastropoda: Caenogastropoda: Aciculidae). *Zootaxa* **2022**, *5188*, 596–600. [[CrossRef](#)]
115. Zallot, E.; Fehér, Z.; Bamberger, S.; Gittenberger, E. *Cochlostoma* revised: The subgenus *Lovcenia* Zallot et al., 2015 (Caenogastropoda, Cochlostomatidae). *Europ. J. Tax.* **2018**, *464*, 1–25. [[CrossRef](#)]
116. Czaja, A.; Cardoza-Martínez, G.F.; Meza-Sánchez, I.; Estrada-Rodríguez, J.L.; Saenz-Mata, J.; Becerra-López, J.; Romero-Méndez, U.; Estrada-Arellano, J.R.; Garza-Martínez, M.Á.; Dávila Paulín, J.A. New genus, two new species and new records of subterranean freshwater snails (Caenogastropoda; Cochliopidae and Lithoglyphidae) from Coahuila and Durango, Northern Mexico. *Subterr. Biol.* **2019**, *29*, 89–102. [[CrossRef](#)]
117. Mammola, S.; Cardoso, P.; Culver, D.C.; Deharveng, L.; Ferreira, R.L.; Fišer, C.; Galassi, D.M.P.; Griebler, C.; Halse, S.; Humphreys, W.F.; et al. Scientists' Warning on the Conservation of Subterranean Ecosystems. *BioScience* **2019**, *69*, 641–650. [[CrossRef](#)]
118. Souza Silva, M.; Martins, R.P.; Ferreira, R.L. Cave Conservation Priority Index to Adopt a rapid protection strategy: A case study in Brazilian Atlantic rain forest. *Environ. Manag.* **2015**, *55*, 279–295. [[CrossRef](#)]
119. Polak, S.; Pipan, T. The Subterranean Fauna of Križna Jama, Slovenia. *Diversity* **2021**, *13*, 210. [[CrossRef](#)]
120. Gillieson, D.S.; Gunn, J.; Auler, A.; Bolger, T. (Eds.) *Guidelines for Cave and Karst Protection*, 2nd ed.; International Union of Speleology and Gland, Switzerland, IUCN: Postojna, Slovenia, 2022; 112p, ISBN 978-0-646-84911-9.
121. Eusébio, R.P.; Taiti, S. Species conservation profiles of cave-adapted terrestrial isopods from Portugal. *Biodiver. Data J.* **2022**, *10*, e78796.
122. Mumladze, L.; Japoshvili, B.; Anderson, E.P. Faunal biodiversity research in the Republic of Georgia: A short review of trends, gaps, and needs in the Caucasus biodiversity hotspot. *Biologia* **2020**, *75*, 1385–1397. [[CrossRef](#)]
123. Mumladze, L.; Cameron, R.A.; Pokryszko, B.M. Endemic land molluscs in Georgia (Caucasus): How well are they protected by existing reserves and national parks? *J. Molluscan Stud.* **2014**, *80*, 67–73. [[CrossRef](#)]

**Disclaimer/Publisher's Note:** The statements, opinions and data contained in all publications are solely those of the individual author(s) and contributor(s) and not of MDPI and/or the editor(s). MDPI and/or the editor(s) disclaim responsibility for any injury to people or property resulting from any ideas, methods, instructions or products referred to in the content.